AN ANALYSIS OF FLASH FLOODS IN THE PEYNE CATCHMENT SOUTHERN FRANCE

WRITTEN BY:
C.A. BACKWELL & T.G.J.BIJKERK

SUPERVISED BY:
PROF. DR. S. M. DE JONG & DR. L.P.H. VAN BEEK

MASTER RESEARCH IN ORDER OF:

Universiteit Utrecht

UTRECHT UNIVERSITY
NATURAL HAZARDS AND EARTH OBSERVATION,
PHYSICAL GEOGRAPHY
EARTH SURFACE HYDROLOGY, HYDROLOGY

Preface

This report is the final product of the Master thesis project to finalize the Master Physical Geography and the Master Hydrology. The report contains the interpretation and the implementation of the data and experiences acquired during a fieldwork campaign which took place in September and October 2009 in the Peyne catchment, Languedoc Roussillon, France.
The research was supervised by Prof. Dr. de Jong and Dr. L.P.H. van Beek

The report is the result of a team effort. We have worked on the same issues at the same time in order to learn from each other and give opportunity for the team strategies to evolve. In some cases one of use took the lead but within reasonable time the other was on the same level of understanding and more then able to finish that particular part of the research. The following table contains an overview of the steps taken to come up with the final results.

	C.A. Backwell	**T.G.J. Bijkerk**
Task	Share in %	Share in %
Fieldwork preparation	50	50
Fieldwork	50	50
Field data preparation and analyzes	40	60
Laboratory work	50	50
Initial map making	50	50
Model set up	50	50
Model calibration	40	60
Model validation	60	40
Modeling scenarios	50	50
Addition calculations and statistical analyzes on model output	50	50
Communication with external contacts	60	40
Report writing	60	40
Layout and appendix	40	60
Database management	50	50

Abstract

Highlighted by the recent event at Draguignan, France on June 15th 2010, in which 25 people lost their lives, there is insufficient knowledge of the processes involved in flash flood occurrence. Despite centuries of effort to understand and mitigate these natural hazards, predictive strategies are still not reliable enough.

The main objective of this study is to define the source areas and gain insight into the processes involved generating large quantities of surface runoff in such short periods of time which forms the basis of flash floods. The study was performed in the catchment of the river Peyne. A 120km^2 catchment situated 60km northwest of Montpellier Languedoc Roussillon, Southern France. This region was, despite prevention measures, struck 5 times by flash floods over the past 25 years. The main land cover consists of viniculture which was seen as a predominant runoff source.

A field study was carried out to gain primary data on the catchment hydrological characteristics. This data was further used in the LISFLOOD, a model which forms the arithmetic basis of the European Flood Alert System (EFAS). The model is originally designed for simulating larger (Pan European) catchments, however, its ability to represent flash flood occurrence within smaller catchments is investigated based on the case study of the Peyne catchment Southern France

Keywords: LISFLOOD, VINEYARDS, FLASH FLOODS, PEYNE

Samenvatting

Uit de recente gebeurtenissen in de Draguignan regio in Zuid Frankrijk, waar 25 mensen om het leven kwamen door flash floods (18 juni 2010) blijkt hoe kwetsbaar deze regio is en hoe ontoereikend de kennis met betrekking tot de initiërende processen van Flash floods. Hieruit blijkt eveneens dat, ondanks jarenlang onderzoek in het begrijpen en doorgronden van deze processen, waarschuwingsmechanismen, voorspellingen en genomen maatregelen niet toerijkend zijn.
Het hoofddoel van dit onderzoek is het definiëren van brongebieden van de grote hoeveelheden runoff en het verkrijgen van inzicht in de processen die verantwoordelijk zijn voor het genereren van dergelijk grote hoeveelheden runoff die de basis vormen voor flash floods. Het onderzoek heeft plaatsgevonden in het stroomgebied van de rivier de Peyne een 120km^2 groot gebied 60km ten noordwesten van Montpellier, Languedoc Roussillon, Zuid Frankrijk. Een gebied dat ondanks ingrijpende maatregelen meer dan 5 maal getroffen is door flash floods in de afgelopen 25 jaar. Het gebied is hoofdzakelijk in gebruik voor wijnbouw, een sector die gezien werd als een belangrijke bron van runoff.
Veldwerk is uitgevoerd om meer inzicht te verkrijgen in het hydrologisch functioneren van het gebied. De hierbij verzamelde data is bewerkt en gebruikt als input voor het LISFLOOD model. Dit model vormt het rekenkundige hart van het European Flood Alert System (EFAS). Het LISFLOOD model is ontworpen voor het modeleren van de grotere Pan Europese stroomgebieden, echter in geval van voorliggend onderzoek is LISFLOOD gebruikt voor het modeleren van flash floods in een relatief klein stroomgebied.

Trefwoorden: LISFLOOD, WIJNGAARDEN, FLASH FLOODS, PEYNE

Résume

Les événements récents survenus à Draguignan, en France, le 15 juin dernier ont mis en évidence le manque certain de connaissances concernant la maîtrise des inondations. Malgré des siècles d'efforts pour comprendre et maîtriser ces catastrophes naturelles, les stratégies mises en place pour les prévenir ne sont toujours pas efficaces.

L'objectif principal de cette étude est de définir les lieux propices aux inondations et d'avoir un aperçu des procédés impliqués dans le phénomène et qui génèrent une si grande quantité d'eau dans un laps de temps aussi court – c'est la définition même de l'inondation. L'étude a été menée dans le bassin de la Peyne, une rivière du département de l'Hérault. Le bassin s'étend sur plus d'un kilomètre carré et est situé au Nord-Ouest de Montpellier dans la région du Languedoc-Roussillon dans le sud de la France. Malgré toutes les précautions mises en place, cette région s'est vue surprendre 5 fois par des inondations durant les 25 dernières années. Une grande partie des terres est cultivée pour son vin ce qui a été perçu comme l'origine principale des inondations.

Une étude de terrain a été menée dans le bassin de la Peyne afin de connaître les données de base des propriétés hydrologiques du bassin. Ces informations ont été traitées en profondeur au sein du LISFLOOD, un modèle qui crée les bases arithmétiques du Système Européen d'Alerte aux Inondations. Ce modèle est construit pour simuler des bassins de plus grande étendue. Néanmoins, sa capacité à représenter les inondations au sein de bassins plus petits est basée sur le cas d'étude du bassin de la Peyne, au sud de la France.

Mots-clés: LISDFLOOD, VIGNOBLES, CRUES, PEYNE

Acknowledgements

We would like to take the opportunity to thank those people who spent their time and shared their knowledge to help to complete this thesis with the best possible result.

At first, a big *thank you* to Steven de Jong, Rens van Beek and Elisabeth Addink for their ultimate support and dedication to sharing their expertise with us. The door was always open! We wish to express appreciation to Ad de Roo, Peter Burek and Bart Pannemans at the JRC for the modelling opportunities and data provided and for their exceptional software support. We would also like to take the opportunity to thank Dr. R. Moussa at the University of Montpellier for his generosity in providing us with papers of his research and access to required datasets. Thank you to Chris Roosendaal for his laboratory apparatus and technical support, to dr. F. Grasso who spoke French on our behalf to organisations in the Languedoc Region and to Prof Dr. Marc. Bierkens and prof. Dr. Hans Middelkoop for their resourceful innovations. We would also like to thank Sarah Débatisse for some high speed translation.

And cheers (Santé!) to Ruud Vink, Renee Oerlemans, Kevin Gortmaker Anne Karlijn de Rijcke and Simone Hoogeveen for their companionship throughout our expedition in France and to Emma van der Zanden for her friendship and support throughout the desk research phase. Finally we wish to thank our families for their undivided support throughout this project.

This report was established in the same way as we conducted the field campaign.
By old-fashioned teamwork!!

Table of Contents:

List of Figures, Tables & Graphs 9

List of Parameters 11

1. Introduction 13

2. Flood formation in the Peyne Catchment 16
2.1 The study area 16
2.1.1 Topography 16
2.1.2 Geology 17
2.1.3 Hydrology 18
2.2 Climate at the Peyne catchment 18
2.3 The reservoir – Lac des Olivettes 19
2.4 Pézenas – A high flood risk 20
2.2. Flash flood Formation and Characteristics 22
2.2.1 Direct runoff fraction (DRF) 22
2.2.2 Hydraulic conductivity (k) 23
2.2.3 Manning's Roughness (n) 23
2.2.4 Sorptivity (s) 23
2.2.5 Reservoirs 24
2.2.6 Subsurface flow 24

3. Data and Method description 25
3.1 Introduction to the LISFLOOD Model 25
3.1.1 Model processes and theoretical background 25
3.1.2 Model Input 28
3.1.3 Model restrictions 29
3.1.4 Modelling Scenarios 29
3.2. Input Data Acquisition 30
3.2.1 The fieldwork campaign 31
3.2.2 External sources 34
3.3 Input data preparation 34
3.4.1 Sensitivity analysis 35
3.4.2 Nimbus & the SCEUA algorithm 36
3.4.3 Calibration and validation data 37
3.4.4 Calibration and validation runs 37

4. Results 39
4.1 Database analysis 39
4.1.1 Lake Mass Balance 39
4.1.2 Precipitation and discharge data analysis 40
4.1.3 Normalized Difference Vegetation Index 41
4.2 Fieldwork data 41
4.2.1 Infiltration 41
4.2.2 Surface roughness 42
4.2.3 Sorptivity 43
4.2.4 Direct runoff fraction 43
4.3 Scenario modelling 44
4.3.1 Tributaries 44

4.3.2 The influence of crusted vineyards 45
4.3.3 Soil textures classes 46
4.3.4 Land cover classes 47
4.3.5 The flash flood of 1996 49
4.4 Model behaviour 51
4.4.1 Preferential flow versus Infiltration 51
4.4.2 Equifinality 53

5. Discussion 54
5.1 The catchment response to Mediterranean precipitation 54
5.2 Factors influencing model outcomes 55
5.3 The model 58

6. Conclusion 60

7. Further Research 62

8. References 63

9. Appendices 68

List of Figures, Tables & Graphs

Chapter 1

Figure 1.1: Bridge at Vaison la Romaine during the devestating 1992 crues and under normal conditions
Figure 1.2: a) Pezenas bridge acting as a debris obstacle during the 1907 crues
b) the concrete floodplain at Pezenas

Chapter 2

Figure 2.1: a) location of the Peyne catchment; b) the Peyne catchment with the Pezenas located at point D.
Figure 2.2: Soil texture map of the Peyne catchment (Risson, 1995)
Figure 2.3: A schematic representation of Lac des Olivettes and thresholds of outflow.
Figure 2.4: a) birds eye view of the narrow canalised river in Pézenas, b) front view of the canal
Figure 2.5: The bridges at Pézénas contributing to flood risk in the town (Diren Languedoc Roussillon (2007)
Figure 2.6: Schematic display of subsurface flow and resurfacing of the shallow groundwater

Graph 2.1: Northwest to Southeast orientated cross section through the Peyne catchment (transect drawn from C to D in figure 2.1)
Graph 2.2: Average precipitation and temperature distribution over the year (Risson, 1995)
Graph 2.3: Influence of antecedent conditions on the Sorptivity and Infiltration rate as a function of time

Table 2.1: Peyne river and tributary lengths in kilometres (SANDRE, 2010)
Table2.2: Examples of extreme events occurring over the last 55 years.
Table 2.3: Lac des Olivettes in numbers (Conseil general de Herault, 2010)
Table 2.4: Proportion of events in each reduced peak discharge category (%). (HYDRATE, 2010)

Chapter 3

Figure 3.1: Schematic representation of the LISFLOOD model (based on Everhardus et al., 2002)
Figure 3.2: a) Locations of the infield observations b) Infiltration location after 20min of water supplying c) Measuring the wetted perimeter
Figure 3.3: Schematic representation of the single ring falling head method applied in the field to determine the sorptivity values of the different soil texture classes
Figure 3.4: The infield installed typing bucket at the reservoir location (Gortmaker, 2010)

Graph 3.2: The above graphs show the sensitivity to a changing CCM.
Graph 3.3: The observed discharges plotted against the by LISFLOOF calculated discharge. From left to right: a) calibration run b) calibrations run 2 c) validation run 1 d) validation run 2

Table 3.1: List of the required input maps and tables (van der Knijf et al. 2008)
Table 3.2: Peyne catchment database features
Table 3.3: the calibration parameters
Table3.4: The range of the calibration parameters within the most successive calibration run
Table 3.5: The original and optimized CCM parameter values

Chapter 4

Figure 4.1: The water level before October 11th 2009 and the expected (manipulated) water level on February 10th 2010 relative to the22m^3/s spill (yellow cube).
Figure: 4.2 The NDVI for June 2002 and February 2003 and the related land cover classes

Figure 4 3: Examples of visual data used to validate the infield observed direct runoff fractions for a vineyard area (5%) and the schlerophyllous vegetation (25%) (Geoportail, 2010)
Figure 4.4: The simulated propagation of discharges through the stream network during the 1996 event

Graph 4.1: Precipitation intensity versus the total precipitation based on 13 years of data (Omere, 2009)
Graph 4.2: Discharge and precipitation data ranging from 01/01/10 to 22/03/10 showing the irregular behavior of the catchment (vigicrues 2010)
Graph 4.3: a) Boxplot diagrams of the infield measured hydraulic conductivity classified on crusting appearance b) Mean and standard deviation values related to the boxplot Diagrams.
Graph 4.4: The influence of an increasing direct runoff fraction in the downstream vineyards on the hydrograph in Pezenas
Graph 4.5: An illustration of the most extreme response is shown in spider diagram format relative to the modelled discharge under normal parameterization(equal to 100%).
Graph 4.6: a) preferential as a function of time during the 1996 event; b) infiltration as a function of time during the 1996 event; c) moisture conditions as function of time during the 1996 event; d) the location of the points of interests
Graph 4.7: The waterlevel in the Pézenas floodplain during the 1996 event
Graph 4.8: The interaction between preferential flow and infiltration rate under different initial moisture conditions which highly influences and balances the total discharge

Table 4.1: Mass balance of Lac des Olivettes for 11/10/09 to 10/02/10
Table 4.2: The statistics related to the infield observed infiltration values.
Table 4.3: Statistical analysis of infield measured Manning's N displaying the mean median and variance values
Table 4.4: The five direct runoff fraction classes
Table 4.5: Tributaries ranked from largest to smallest total discharges
Table 4.6: Three sub catchments covered by one particular land cover type and the related runoff generation
Table 4.7: The summed discharges and generated runoff of the three main land cover classes
Table 4.8: The influence of a changing soil type on the tributary and total discharge(s)
Table 4.9: Land cover classes ranked from largest to smallest total discharges (table continued on following page).
Table 4.10: Infiltration rate and preferential flow behaviour of the LISFLOOD model and the infield observed situation
Table 4.11: The interaction between preferential flow and infiltration rate under different initial moisture conditions which highly influences and balances the total discharge
Table 4.12: The frequency of Nash Sutcliffe values generated by NIMBUS

Chapter 5

Figure 5.1: a) A flooded vineyard observed on the 21st of October during the fieldwork (X: 525048; Y: 4820707) b) Runoff flowing into the Peyne where no water was discharged through the drainpipe
Figure 5.2: a) The concrete floodplain with the Peyne centered in a 25cm wide ditch under normal conditions (18 September 2009); b) The concrete floodplain during a minor flash flood (21st October 2009); c) One of the bridges in the Pézenas floodplain acting as an obstacle for flooding debris during a minor flash flood (21st October 2009)
Figure 5.3: Pont du Peyne crossing the concrete floodplain in Pézenas

List of Parameters

A	Wetted area (cm^2)
A_s	Saturated fraction of the cell
bXinj	empirical/calibration parameter part of the VIC/ARNO Scheme used to update the moisture states of each modeled cell and determine the saturated fraction (-)
C	Chézy roughness (-)
CCM	Cal Chan Man (-)
C_{rr}	Saleh roughness (-)
Dirrf	Direct runoff fraction (impervious fraction) (%)
$D_{pref\ gw}$	the water flow that follows preferential pathways leading it directly to the ground water without infiltrating the soil matrix (mm)
E_s	Evapotranspiration from the soil (mm)
E_t	Evapotranspiration of a reference crop (mm)
E_w	Evaporation from open water (mm)
F	Darcy-Weisbach friction (-)
F_{dr}	direct runoff fraction related to impervious areas such as concrete landscapes and frozen land) in which infiltration is considered 0 (-)
G_{wpf}	Groundwater percolation rate (mm/day)
I	Infiltration under steady state conditions (cm/s^{-1}
Inf_{act}	Actual infiltration (mm)
Int	Interception per time step (mm)
K	Conversion factor (1.49 from feet to m)
k	factor accounting for vegetation density in the interception formula (-)
K_{sat}	Saturated Hydraulic conductivity (cm/h^{-1})
L_1	Length total chain (cm)
L_2	Length draped chain (cm)
LAI	Leaf Area Index (m^2/m^2)
LAI_{re}	Leaf area index compensation factor per month
LAI_g	Leaf area index during the growing season (m^2/m^2)
LAI_d	Leaf area index during dormancy (m^2/m^2)
Lztc	Lowerzonetimezone constant residence time of water in the upper zone (days)
N	mannings N Value related to the surface roughness of the terrain (-)
NDVI	Normalized Difference Vegetation Index
NS	Nash Sutcliff, objective function which gives an indication of the goodness of fit between model output and observed values
Pr	Precipitation (mm)
Pwpf	Power calibration value assigned to the preferential flow equation (-)
q	Discharge ($volume^3$/unit of $time^{-1}$)
Q	Discharge ($volume^3$/unit of $time^{-1}$)
Q_{uz}	Outflow upperzone to streamnetwork (mm)
R	Rainfallintensity (mm/day)
R_d	direct runoff which is generated using a direct runoff fraction (F_{dr}) in each pixel (mm)
R_s	Surface runoff which is generated as a result of excess overland flow (mm)
RMSE	Root Means Square Error
RR	Random roughness (cm)
rRMSE	relative Root Mean Square Error
S	Sorptivity ($cm/h^{-0,5}$)
S_{max}	Maximum interception of vegetation (mm)

STDEV	Standard deviation
t	Timestep (min)
T_a	Average temperature (^{0}C)
$Theta_{ini}$	Initial soil moisture status of the soil
T_{uz}	Timezone constant (days)
Upztc	Uppertimezone constant residence time of water in the upper zone (days)
$UZ_{\Delta t}$	Watercontent in upperzone (mm)
W_{av}	the actual water available for infiltration (mm)
W_{s1}	Saturated watercontent (mm)
W_1	Actual watercontent (mm)

1. Introduction

Flash floods, are categorised as one of the largest natural hazards in the world (Gaume et al., 2004). These events are known to cause extensive damage and numerous casualties in many cases (Gaume et al., 2009), in America such events have been recorded to result in a higher mortality rate than hurricanes, tornados and winter storms together over the last thirty years. (Gruntfest et al., 2001). In Europe, it is one of the most damaging hazards experienced. Economical damage over the last two decades by flashfoods in France alone where estimated on one billion Euro (Younis, 2008).

Flash floods, sometimes referred to as storm driven floods (JRC, 2010), are the result of a combination of numerous parameters. A definition of flash floods is given bellow:

'Sudden floods with high peak discharges, produced by severe thunderstorms that are generally of limited areal extent'. (International Association of Hydrological Sciences, 1974)

Within Europe the Mediterranean region is known for its flash floods which are in this region known as one of the most devastating hazards based on economical damage and loss of human lives (Younis 2008). During the last seven centuries sixty seven flash floods causing casualties (more than a 1000 human lives) were reported in the Languedoc Roussillon region (Antoinne et al., 2001).

The Mediterranean part of France is renowned for its unstable synoptic conditions and warm moist winds in autumn (more specifically September – October) which result in intense precipitation events that occur over a short period of time (most often less than a day). The majority of these flash flood events are caused by mesoscale convective storm systems (MCS) which are relatively short lived and remain in an area for several hours. Mesoscale convective systems are a combination of smaller convective systems (i.e. thunderstorms) that reach a size of between 2km – 2000km. They occur in the Mediterranean due to the evaporation of Mediterranean sea water (synchronised with seasonal high sea surface temperature peak in late summer to autumn) which remains in the lower atmosphere until reaction with colder jet streams sourcing from the north. Such jet streams that affect the south – South-west of France in this way include the colder drier northern winds called la Bise (originating from the Northeast of france), le Mistral (originating from the North-Northwest) and La Tramontane (originating from the North) which would mix with the warmer and very moist Marin jet stream which originates over the Mediterranean sea. The area's orography which consists of the Pennines and the Massif Central depression create a funnel for these winds to travel and eventually become stationary causing intense down pouring of precipitation over a short period of time (Drobinsky et al., 2008).

Figure 1.1: *bridge at Vaison la Romaine during the devastating crues (Leerwiki 2010), 1992, and under normal conditions (Wikipedia, 2010)*

Two well known examples of these events include the Vaison La Romaine flood of September 1992 in which 179mm of rain fell in 2 hours and 220mm fell in 3 hours taking 58 lives (Senesi et al., 1996) and the 8–9 September 2002 event in the C´evennes–Vivarais region with more then 600mm accumulated

rainfall in 24 hours causing 25 casualties (figure 1.1) (Younis et al. 2008, JRC 2010 & Hydrate 2010). It was noted that the rainfall over the catchment containing Vaison La Romaine is not the sole cause of flash flooding but the catchments hydrological configuration of all subcatchments contained within the larger sub catchment is what made Vaison La Romaine vulnerable to flash flooding (Senesi et al., 1996).

Despite the devastating effects of flash floods and abundance of intensive research, many questions remain unanswered. The majority of conducted research can be subdivided into two categories (Gaume et al., 2006):

- Post disastrous event research to satisfy queries/concerns raised by public opinion.
- Research in order to document extreme events.

Such research is highly influenced by the availability of data and detailed information, which is unfortunately not always accessible. For instance, observation devices damaged or destroyed during flash flooding are to blame for a lack of discharge data all too often. This lack of information limits the amount of detailed rainfall runoff analyses are that are carried out (Gaume et al., 2006).

Flash floods often happen in small ungauged catchments (Borga et al 2008). One of these small Mediterranean watersheds known to suffer from flash floods is the Peyne catchment. The river Peyne with an average discharge of only 0,2m^3/s can suddenly increase to over a 100m^3/s in just a few hours after a Mediterranean shower of localy more than 200mm within 24h (28 january 1996 (Lac des Olivettes reports, Meteofrance, 2010)).These extreme discharges causes flash floods in the city of Pézenas. Pézenas, an ancient town in the Hérault region of Southern France which is built upon the mature to old-age phase of the river Peyne, has a prominent history of flash flooding. The region was struck by 5 noteworthy events (due to Peyne catchment flood waves) over the last 25 years (PRIM, 2010). Historical records show that the flash flood hazard has existed for centuries and inhabitants have been continuously influencing the rivers path in order to try to order and structure the river. Consequently, today much of the aggravation experienced by the river is thought to be due to these and other anthropogenic interferences. This includes drastically narrowing and cementing of the river bed at Pézenas, placement of bridges over the river (figure 1.2), and areas in use for agricultural purposes further north within the catchment, supplying large amounts of runoff during extreme events (Valarie et al., 2004).

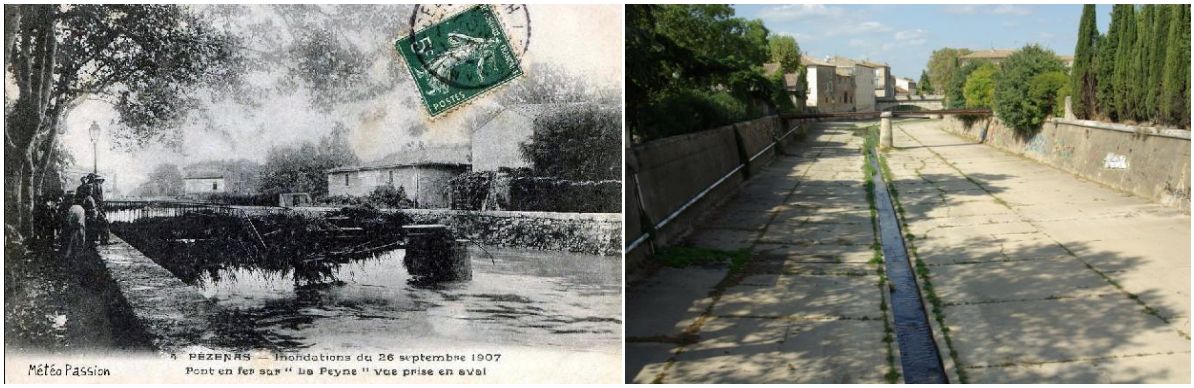

Figure 1.2: a) *Pézenas bridge acting as a debris obstacle during the 1907 crues, (meteopassion, 2010) b) the concrete floodplain at Pézenas*

The objective of this research is to locate the source areas of highest runoff within the Peyne catchment and to determine the underlying causal mechanisms resulting in flooding of Pézenas and determine the influence of management on these parameters by applying a LISFLOOD modelling approach and an infield study of the hydrological processes influencing flood generation as soil crusting, infiltration and surface roughness.

Based on previous literature study and a quick scan using the Curve Number method (Backwell & Bijkerk, 2009 a & b) the following hypotheses were formulated for this research:

- It is expected that most runoff will be generated in regions with a high fraction of impervious area. This implies that crusted vineyards and urban area will contribute most to flash floods
- It is expected that the applied management in vineyards highly influences the amounts of runoff generation
- Due to interception and higher infiltration capacities it is expected that the forested areas will contribute less than vineyards and urban areas
- Large differences will be found between the discharges of different tributaries of the river Peyne.
- The reservoir location and dimensions are not sufficient to carry out its purpose efficiently.
- It is expected that Hortonian overland flow will be the most important runoff generating process seen the short high intensity precipitation events.
- It is expected that the anthropogenic influences at Pézenas (the concrete flood plain, bridges) increase the peak discharges.

LISFLOOD is the chosen hydrological model to research the validity of these hypotheses. The development of LISFLOOD has proven itself highly beneficial to the analysis of water balances and flooding within Europe. It is used in flood forecasting operations and is currently incorporated within the European wide flood early warning system, the European Flood Alert System (EFAS) (JRC, 2010). The LISFLOOD model is furthermore successfully applied in Flash flood research in Southern France (Younis, 2008 & Real 2002) and is exploited from numerous angles and viewpoints. It is used for simulations post flood, to understand the mechanisms and dynamics involved in the flood and the afflicted catchment. It is further used to analyse specific mechanisms within a catchment such as urban sprawl (land use) or flood prevention techniques, in order to quantify the implications of these on the catchments vulnerability to flooding. The Oder river basin, Germany, has been analyzed extensively from both viewpoints mentioned. LISFLOOD and other techniques were employed to investigate how the affect of land use change over the course of the basins history has influenced the severe floods experienced in 1977, 1985, and 1997 (De Roo et al., 2002). Furthermore, it is used in comparative studies aiming to gain more understanding of model behaviour and uncertainty (Feyen et al., 2007).

TheLISFLOOD model and the related calibration software used for this research where provided by the Joint Research Centre Institute for Environment and Sustainability part of the European Commission .

2. Flood formation in the Peyne Catchment

2.1 The study area

The study area involves the entire catchment of the river Peyne, situated in the Hérault department of the Languedoc Roussillon region of southern France. The Peyne is one of the larger tributaries of the Hérault River (Sandre, 2010). The catchment covers 120km^2 7 small villages are spread over the catchment from upstream to the outlet: Pézenès les mines, Vailhan, Neffiès, Roujan, Caux and Alignan-du-vent. Its largest human settlement is Pézenas (8925 inhabitants); a town located at the outlet, south of the catchment, approximately 60 km to the west of Montpellier and 30 km north of the Mediterranean Sea (figure 2.1).

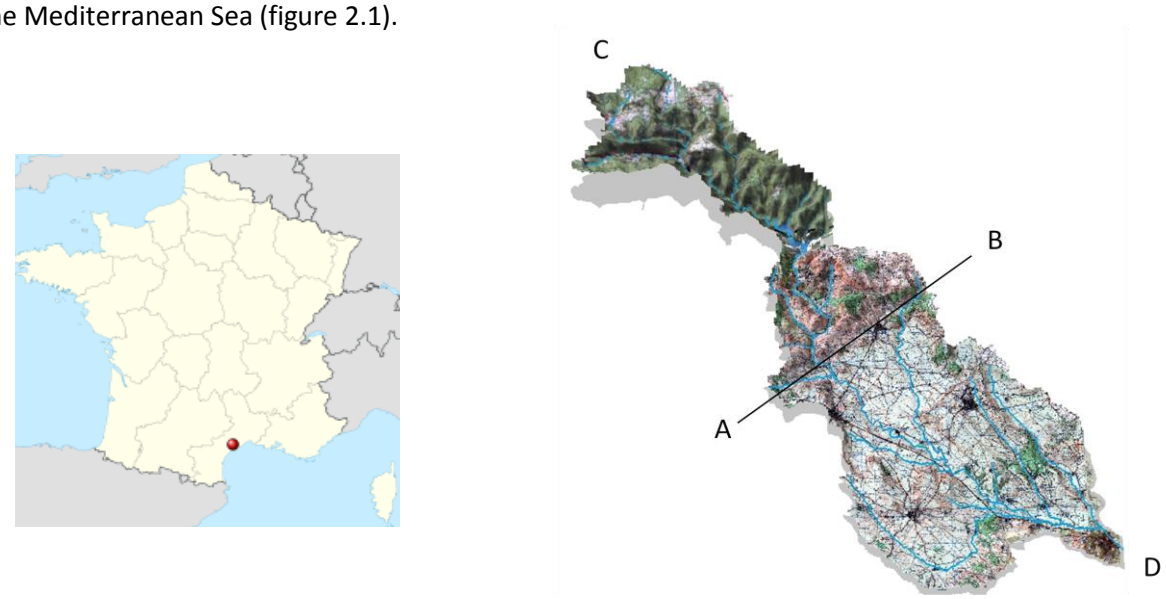

Figure 2.1: *a) location of the Peyne catchment; b) the Peyne catchment with the Pezenas located at point D.*

2.1.1 Topography

The two main land cover types are broadleaved forest and vineyards (23% and 53% respectively (CORINE, 2006)). These two cover classes can be assigned to two distinct topographical classes, with a division that can be drawn coarsely between Neffiès and Lac des Olivettes (figure 2.1b, graph 2.1 and appendices I & II). Topography to the North of this divide is dominated by accentuated relief covered by forests (green oak, white oak, chestnut and arbutus). To the south, man has a heightened influence on the topography resulting in dominant agricultural land cover with vineyards as the most important class, but also includes other general agricultural activity. (Risson, 1995).

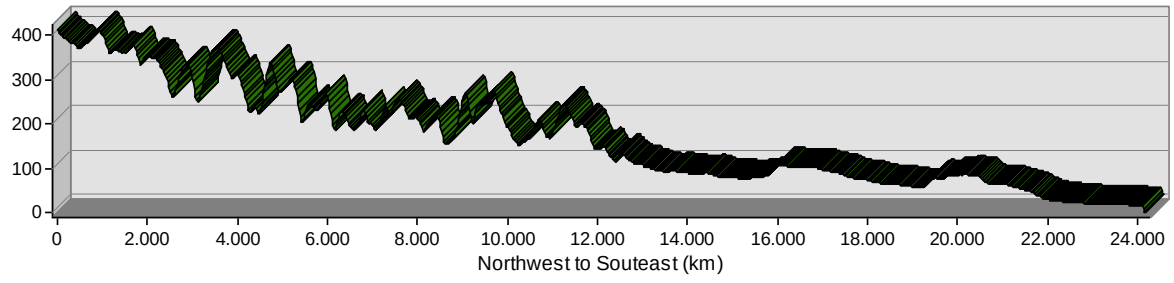

Graph 2.1: *Northwest to Southeast orientated cross section through the Peyne catchment (transect drawn from C to D in figure 2.1)*

2.1.2 Geology

The geology differs north and south of the divide line. The Montagne Noire runs northwest of the Peyne catchment with the northern part of the catchment lying at the foothills of this mountainous range. (Risson, 1995). At the end of the paleozoic era between 330 to 300ma the Montagne Noire were formed during the Hercynian Orogeny, a geological mountain forming event caused by a collision of continents.

To the north lies schist, basalt and calcareous sandstone. Bauxite is also found within Pézènes les Mines in the northwest of the catchment and was formed during the middle of the cretaceous 100ma, in which the emersion of horsts and anticlines contributed to additional surface area, extending the continental plate. (Risson, 1995).

To the south the flatlands with sandy/silty marine deposits dominate. This was formed when the sea retreated after a short period of transgression during the teriary period 65a to 40 Ma giving way to erosion and the subduction of the Pyrenees. The sea transgressed once again during the Miocene 23 Ma and ceased depositing marine aggregates after regression around 12ma. This activity formed the base of the Peyne valley until upstream of Roujan. Such large scale continental alterations slowed after the Pliocene 12 to 3 Ma and much evidence of such activity is found in the region of Alignan du Vent. (Risson, 1995).

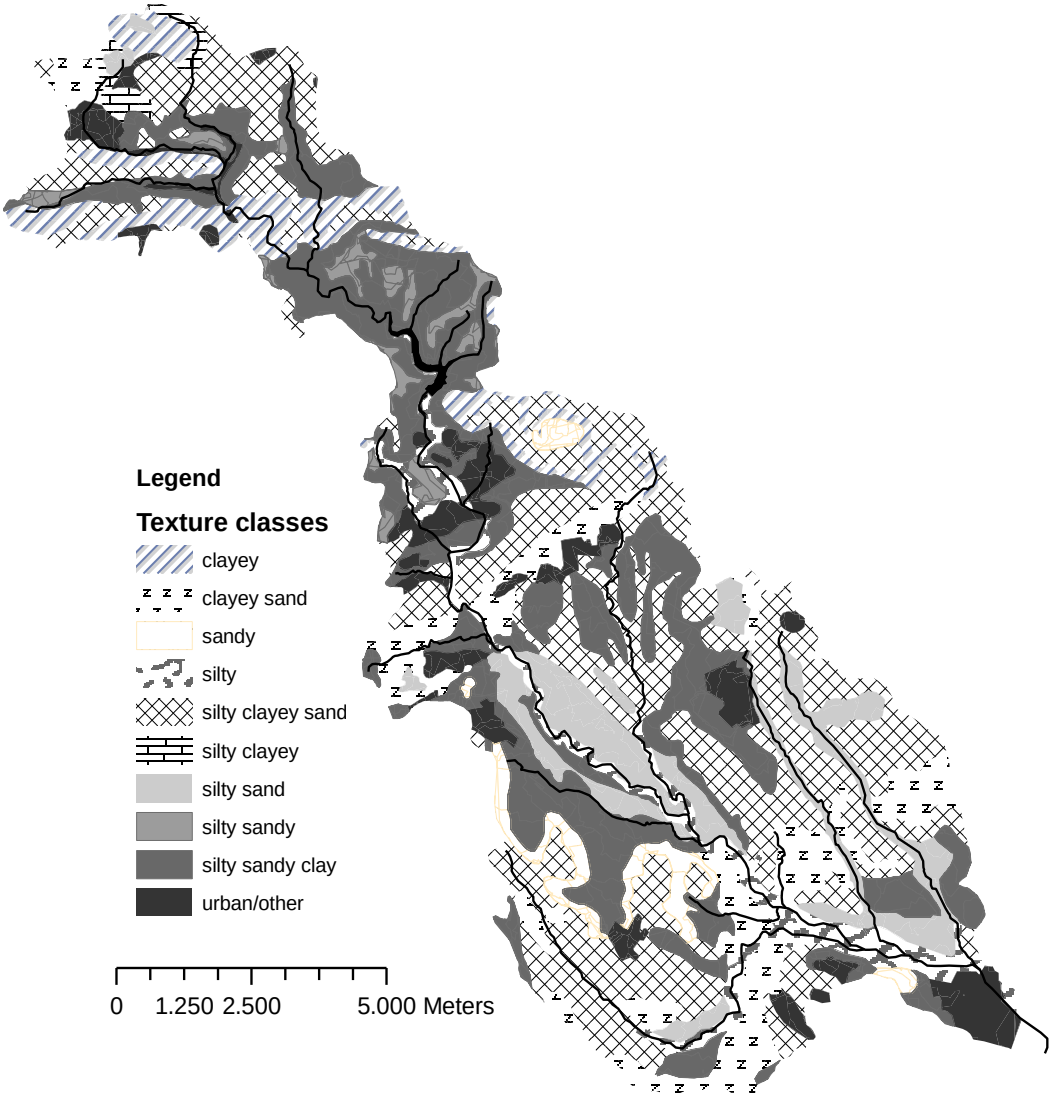

Figure 2.2: *Soil texture map of the Peyne catchment (Risson, 1995)*

2.1.3 Hydrology

Due to the differing topography north and south of the catchment, the hydrological network in the south is comprised of a longer and flatter pattern in the south, and less dense than the northern area. (Risson, 1995).

The Peyne is a 32km long river which is fed by 18 tributaries (appendix III). Each of these tributaries drain small subcatchments and show large heterogeneity in landcover (appendix VI).

Table 2.1:Peyne river and tributary lengths in kilometres (SANDRE, 2010)

Name	Length (km)
Peyne	32.9
saint martial	10.5
Bayelle	8.4
de tartuguier	7.6
rieutord	6.7
de levers	4.7
de pouzes	4.4
la margaride	4.2
Boudic	4.2
mourissou	3.7
de ribouyrel	3
Rounel	2.7
de la charette	2.1
le vallat	2.1
de la bayse	1.8
de font rarens	1.8
de maro	1.5
de fer	1.3
de roquemaliere	1.2

In the northern part, smaller steep sub catchments covered with forest can be found (Tributary le Vallat) whereas larger less steep sub catchments lie in the southern area which are mainly covered by vineyards (tributary de St. Martial). A large anthropogenic construction interrupts the natural flow of the river Peyne - Lac des Olivettes which is a reservoir situated near the transition of the two topographical regions (near the village of Vailhan) (Risson, 1995).
Keeping in mind that both the northern and southern sections of the catchment have different morphological characteristics, it must be remembered that the two areas are in reality inseparable and each interact and contribute to the hydrological network that describes the River Peyne (Risson, 1995).

2.2 Climate at the Peyne catchment

Flash flooding is a prominent hazard in France causing 1 billion Euros worth of damage in the last 20 years (Huet et al., 2003 in Younis et al., 2008). The Mediterranean area is most at risk of flash flooding due to the typical Mediterranean climate, consisting of hot summers dominated by subtropical high pressure cells and dry air that descends over the Mediterranean Sea inhibiting cloud formation. Mild winters follow with preceding autumnal convective rain storms which are often severe and unstable. These intense storms occur due to interaction between warm moist air flow (Le vent Marin) over the Mediterranean sea and polar jet streams which carry much precipitation

(including Le vent Cers & Le vent Tramontane), and such fronts are destabilised by local trigger mechanisms including mountainous topography such as the Montagne Noir southwest of the Languedoc Roussillon department (Midi-France, 2010).
The catchment specific to this study receives approximately 880mm of rain on the annual basis of which most on average is received in the October/November months (graph 1.2). Deviation from this mean value is observed across the catchment and can be explained partly by the elevation range (20m.a.sl. at Pézenas versus >400m.a.s.l. at the Northwestern part) (Bonfils, 1993).

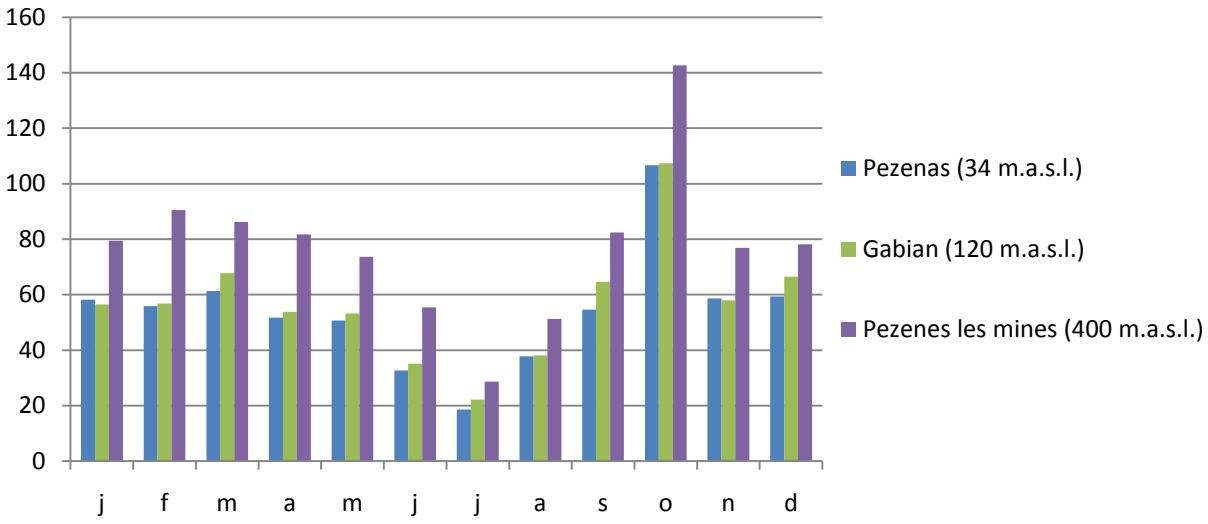

Graph 2.2: *Average precipitation and temperature distribution over the year (Risson, 1995)*

Table2.2*: Examples of extreme events occurring over the last 55 years.*

Date	Duration (h)	Gabian	Caux	Pezenes les mines
30 Sept - 2 Oct 1964	24	180	-	200
04-Dec-87	24	-	-	159
6 Nov - 8 Nov 1982	48	194	152	235
28-June-96	48	180	-	193

2.3 The reservoir – Lac des Olivettes

Lac des Olivettes is an artificial reservoir that commenced service in 1985 (appendix III and X). The main function of the reservoir is to act as a buffer for discharge, absorbing water coming from the forested upstream area and hence moderate the magnitude of discharges released into the downstream catchment. This reduces potential flood risk in the lower part of the catchment. The second function of the reservoir is to provide irrigation water in times of drought (approximately 0,1Mm^3 on an annual basis). (Conseil Géneral d'Hérault, 2010)

Under normal hydrological/meteorological conditions the reservoir stores approximately 2,6Mm^3 (equating to a water level of +/-158 m.a.s.l). During extreme hydrological conditions the maximum storage is a total of 7.1million/m^3 (equating to a water level of 169.5m.a.s.l.) or equivalent to 59 mm of runoff spread over the entire catchment. The reservoir is built as a passive system thus regulating discharge based on water height (appendix X). Besides the baseflow which is regulated through tubes, two spills facilitate a discharge of respectively 22m^3/s (located at 163 m.a.sl.) and 290 m^3/s (166,5 m.a.s.l). (Conseil Géneral d'Hérault, 2010)

Table 2.3: *Lac des Olivettes in numbers (Conseil general de Hérault, 2010)*

Lac des Olivettes	
Area normal conditions	40 hectares
Volume normal conditions	2,6 Mm^3
Bottom level	136 m.a.s.l
Storage during events	Ranging from 1,8 to 4,6 Mm^3 max
Yearly evaporation	1,35m
Barrage des Olivettes	
Height	35 m
Volume of concrete	85000 m^3
Extreme event	28 January 1996 inflow 106m^3/s
Max discharge	330m^3/s
Catchment	
Peyne Catchment	120km2
Subcatchment of the Lac	29,5km2

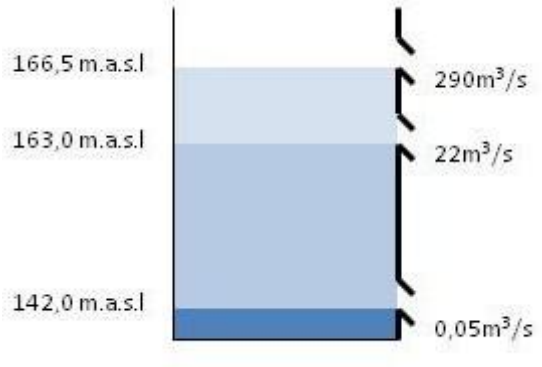

Figure 2.3: *A schematic representation of Lac des Olivettes and thresholds of outflow.*

Another cause of flash flooding which is considered in the catchments protection plan is a breach of the Lac des Olivettes (Conseil general de Hérault, 2010). However, such a hazard is considered different from the definition of a flash flood as it involves alternative water sources and driving mechanisms. Therefore this will not be considered in this research project.

2.4 Pézenas – A high flood risk

Pézenas is a location vulnerable to flash flooding for many reasons. Firstly it lies upon the river Peyne and near to three tributaries to the North (Appendices III); tributaries St. Martial, de Rieutord and de Tartuguier. In fact, the latter tributary joins the Peyne meters to the North of Pézenas and is the third longest tributary (7.6km) while the St. Martial is the longest tributary at 10.6km in length (SANDRE, 2010), thus these tributaries are considered to be large contributors to the Peyne. During times of intense rainfall these tributaries similar in length can have similar travel times of their peak discharges. This could coincide spatially and temporally at the river Peyne, consequently exceeding the water volume capacity of the river and its flood plains in the vicinity of Pézenas. River inundation combined with Dunnian and Hortonian overland flow are sources of runoff contributing to the flash flooding of the location.

Secondly, the river Peyne is entering the village from a north western direction. Beginning at the entrance of the village, the river is canalised manually and the river channel is reduced to a width of a mere 25cm with a concrete floodplain of approximately 30 metres wide. During peak discharges the river Peyne can make use of this artificial floodplain (figure 2.4), however it is constructed using

concrete with an infiltration rate approaching zero and a low surface roughness, blocking the buffering interactions of the soil below, and promotes faster water flow.

Figure 2.4: *a) birds eye view of the narrow canalised river in Pézenas, b) front view of the canal*

Other anthropogenic constructions include the bridges in the town of Pézenas. From photographic evidence (figure 2.5 below) it can be concluded that the pillars of the middle bridge rising from the centre of the river bed encourage debris collection, obstructing smooth water flow. The bridges themselves lie across the river at a height that will make contact with the flowing water upon the water level reaching a sufficient height. For the river to reach such a height implies that the water flow is in a dynamic state and the power behind such waves will likely breach the floodplain banks if flow is obstructed, such as by these bridges.

Figure 2.5 *The bridges at Pézenas contributing to flood risk in the town.*

According to information provided by Diren Languedoc Roussillon, the Regional Directorate of Environment, Physical Planning and Housing (2007), about Pézenas, the left bank of the Peyne is heavily modified by human activity. No further details are given about the actual constructions, however it is mentioned that such aggravation caused by urban infrastructure is somewhat buffered by water pipes leading water from the area to the plains of the Hérault river. It is important to further note that the Tartiguier tributary joins the Peyne on the left side at the northwest of Pézenas, causing a widening of the river bed of La Peyne at that location. This implies that the narrow canalisation within Pézenas acts as a bottleneck for smooth flow, and that this combined with the anthropogenic aggravations on the left river bank leave the town at an increased risk of flooding. Areas at higher exposure to flooding are indicated by the presence of cofferdams and flood markers. It is also mentioned that the lower part of the city suffers from floods due to outbursts of the Peyne combined with urban runoff.

As the Peyne itself relies on its connection to the Hérault for drainage, in times of high waters in the Hérault, the Peyne River is unable to release its contribution of flow. This is because the Hérault itself

is forcing its own water upwards through the mouth of the tributary and results in a flash flood caused by heightened Peyne river levels due to stagnant flow and even backflow within the Peyne river itself. This may not only result in floods near the mouth of the river, but also further upstream to the mature stage of the river (where slope is decreasing) and including the locations where tributaries merge with the Peyne, such as at Pézenas (Giraud et al., 2007).

2.2. Flash flood Formation and Characteristics

Flash floods are a rapid response to intense and short lived precipitation events, during which water levels in stream networks reach peak discharge within minutes to hours. Such storm events can cause between 50mm of precipitation in 1 hour (in areas of 10-100km^2) to over 200mm in less than 6 hrs (in areas 25km^2 to 2500km^2) (Creutin and Borga 2003; Collier 2007 in Younis et al., 2008).
The European project, Hydrate (Hydro-meteorological data resources and technologies, for effective flash flood forecasting) has collated information on flash floods across the continent. The project aim is to enable in-depth research into past flood trends in order to improve efficiency in future prediction methodologies. For this study reduced peak discharges (60% of maximum peak) were focused upon, and first observations indicated that flash flooding in Mediterranean regions is greater in magnitude than any other region on the continent (HYDRATE, 2010). According to Gaume et al., (2009) there are few locations globally on such similar spatial scales (less than 500km^2) that produce discharges to contend with those of the Mediterranean maximums. Of the 7 countries with the highest flash flood rate, France scored highest in the occurrence of reduced peak discharges between 75-100 $(m^3/s/(km^2))^{0.6}$ with only Italy rarely experiencing larger peak discharges of over 100 $(m^3/s/(km^2))^{0.6}$ (table 2.4). Peak discharges are observed as they provide a more stable estimate of the pressure experienced by a catchment than the individual peaks themselves.

***Table 2.4**: Proportion of events in each reduced peak discharge category (%). (HYDRATE, 2010)*

	0–25m^3/s	**25–50m^3/s**	**50–75m^3/s**	**75–100m^3/s**	**>100m^3/s**
Catalonia	45	33	11	11	0
France	17	43	27	13	0
Italy	33	43	7	10	7
Slovakia	87	13	0	0	0
Greece	75	25	0	0	0
Romania	77	23	0	0	0
Austria	100	0	0	0	0

Measurable characteristics of such flash floods such as time to peak and peak flood depend upon specific parameters within the flooding catchments. The primary variables involved in flash flood formation include; parameters which restrict the initial amount of water reaching the soil layer such as direct runoff fraction; soil parameters such as hydraulic conductivity, infiltration and sorptivity; and the topographical parameters which influence the routing of flow such as Manning's N of stream channels and land surfaces, sub surface flow and anthropogenic obstructions including reservoirs, dams, bridges , concrete floodplains.

2.2.1 Direct runoff fraction (DRF)

The direct runoff fraction is dependent upon geology, soil and land cover. Paved urban areas (including buildings), roads and areas where geology is exposed with little or no soil are considered as impervious areas and produce higher levels of direct runoff compared to pervious areas (e.g. soils) (Weng, 2008). The direct runoff fraction is represented in models as the quantity (a fraction) of area per model grid cell that is impervious (i.e. where infiltration is approaching 0).

2.2.2 Hydraulic conductivity (k)

Hydraulic conductivity is a measure of the rate of water flow through a porous medium. Direct runoff can develop on porous media via two different processes, Dunnian overland flow and Hortonian overland flow. Both processes are dependent upon hydraulic conductivity of the medium in question. Dunnian overland flow is essentially soil saturation excess water occurring when the saturated hydraulic transmissivity is not fast enough to drain the soil in time to accept all the available precipitation. Hortonian overland flow is soil infiltration excess occurring when the precipitation rate exceeds the soil infiltration rate and thus creates a layer of direct runoff on the soil surface (Horton, 1933). Hydraulic conductivity can continuously vary at one location depending on the antecedent soil conditions (esp. initial soil moisture), seasonality of weather, and land management. A typical example are vineyards within the Peyne catchment. The vineyards are comprised of mostly bare soil with rows of vines approximately 1.5 m apart. This bare soil, usually of low moisture content during the dry season, is vulnerable to crusting in the wetting season. Crusting will occur after precipitation events due to sediment filling of pores at the surface and thus causing a decrease of hydraulic conductivity of the top soil. From field observation in 2009 no significant crusting could be seen on soils during September. Simultaneously, local inhabitants highlighted the fact that the summer of 2009 was a very dry summer, supporting the idea that crusting is related to wetting and subsequent drying of soils, and was confirmed after the first rain event late September 2009 when soils began to once again dry with a crust layer (Duijsings, 2008).

2.2.3 Manning's Roughness (n)

Manning's n is a coefficient for the roughness of a surface over which water will flow. The higher the value the more friction the water will experience and resulting in a lower specific discharge. A smooth surface such as the paved floodplain of the river at Pézenas will have a low Manning's n value and therefore specific discharge will be high. This affects the time to peak of the flood and the intensity of the peak flood.

2.2.4 Sorptivity (s)

Sorptivity is the measure of the ability of a soil to absorb or desorb by capillary motion and is relied upon by soils for lateral flow and ultimately for the saturation of a soil in the vadose zone. When sorptivity of a soil reaches a value of 0, saturated hydraulic conductivity commences. Antecedent soil moisture conditions therefore are dependent upon sorptivity to retain the moisture from previous rain events and thus affect the soils reaction to future precipitation. (Hillel, 2004)

Sorptivity can highly influence the time to pond (tp) of a soil. In this sense sorptivity becomes an important variable to be considered when analysing the cause(s) and source areas of flooding.

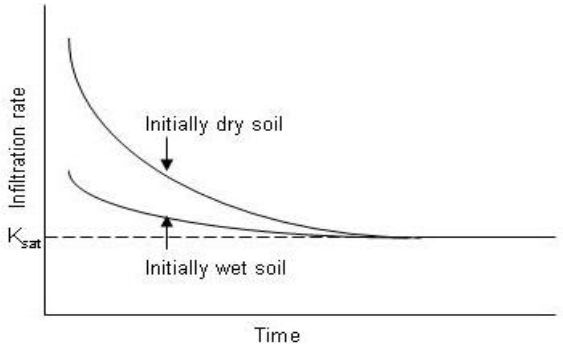

Graph 2.3: *Influence of antecedent conditions on the Sorptivity and Infiltration rate as a function of time (Hillel, 2004)*

2.2.5 Reservoirs

The initial conditions of a reservoir at the onset of a precipitation event are paramount to the hydrological response of the catchment. That such as Lac des Olivettes, when unfilled can store a proportion of the total precipitation entering the catchment and thus reduces the peak flood. For modelling purposes, when full the reservoir can be considered as not in service, leaving the catchment to cope alone with all subsequent input of water and therefore the intensified peak flow will induce a higher risk of flood.

2.2.6 Subsurface flow

Sub surface flow develops from water that has infiltrated the soil and develops a flow path underground. It can reappear at the surface later enroute at a lower altitude such as at the bottom of a hill or in a spring.

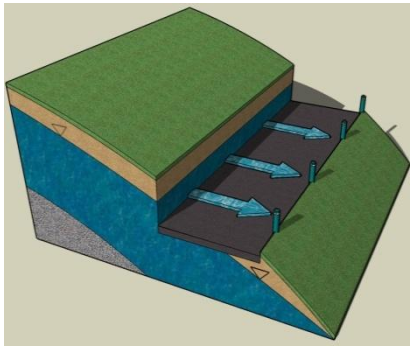

Figure 2.6: *Schematic display of subsurface flow and resurfacing of the shallow groundwater*

3. Data and Method description

3.1 Introduction to the LISFLOOD Model

There are a wide range of models which are able to simulate the effects of landuse change, changing climate, to assess the effect of river regulation measures or for flood forecasting. However there are merely a few models which are able to model all these together. The main objective for the LISFLOOD model was to develop a model which is capable of modelling and assessing all of these processes and influences for the larger European catchments (van der Knijf et al., 2008a & van der Knijf et al., 2008b, Thielen et al., 2008).

The LISFLOOD model is a hybrid between a conceptual and a physically based spatially distributed, grid-based rainfall runoff model. Within LISFLOOD this rainfall runoff part is combined with a routing module in the river channel part (van der Knijf et al., 2008a, Younis et al., 2008; Thielen et al., 2008).

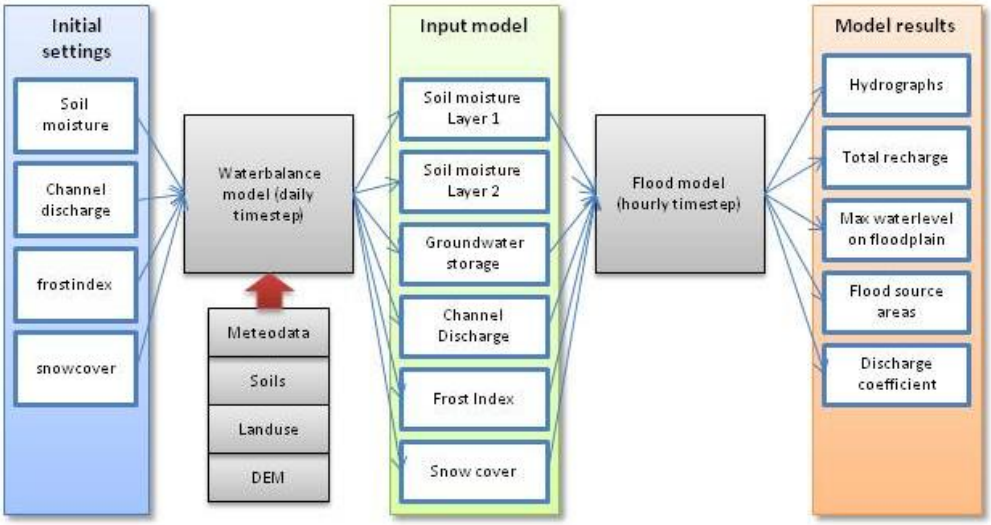

Figure 3.1: *Schematic representation of the LISFLOOD model (based on Everhardus* et al., *2002)*

The LISFLOOD model is especially designed for the larger (pan) European river catchments (catchments of magnitude 10^2-10^4 km^2) as being the model core of the European Flood Alert System (EFAS) (JRC, 2010). This implies that some of the small-scale processes are simplified. Thus working with a high resolution does not necessarily result in better and reliable model output. The recommended grid resolution lies between 100m and 10km (van der Knijf et al., 2008a), nevertheless the model is also applied to smaller catchments with varying results (Everhardus et al., 2002).

3.1.1 Model processes and theoretical background

The key processes within the model will be described in the following paragraphs. A more detailed description can be found in the LISFLOOD manual (van der Knijf et al., 2008a) and van der Knijf et al., (2008b).
The processes described in the LISFLOOD model are represented can roughly be divided into the three following groups (Thielen et al., 2008):

- Soil and groundwater system
- River channel
- Canopy and surface

The processes described in this part highly influence the model output. Four important processes are: interception, infiltration capacity, evapotranspiration and runoff generation.

Soil and groundwater system:

Infiltration capacity

Infiltration capacity is determined by using the VIC/ARNO (or Xinanjiang) method. In contrast to other methods it incorporates heterogeneity of infiltration capacity within the grid cell (Thielen et al., 2008). This method determines the amount of runoff contributing cell fraction, based on the amount of soil moisture (saturation). It works under the assumption that this relationship can be reproduced by a nonlinear distribution function (van der Knijf et al., 2008b).

Runoff generation

The runoff part in the model is build up out of two main sources: direct runoff and dune overland flow. The amount of direct runoff depends on the impervious area fraction within a grid cell. The total amount of precipitation which will fall on the impervious area is assumed to become direct runoff. The amount of dune overland flow is influenced by the interception, infiltration capacity and the preferential flow to the deep groundwater. The calculated runoff will be routed to the nearest river channel pixel by using a four-point implicit finite-difference solution of the kinematic wave equations (van de Knijf et al., 2008a)

One remark to be made in relation to the subsurface runoff: all water outflow from the upper and lower groundwater zones is routed to the closest downstream river pixel within the same time step. This implies the treatment of upstream pixels as spatially lumped units (van der Knijf et al., 2008a). It is not expected that this lumping influences stream flow in the channel in an extreme way, provided that the flow paths are not too long (van der Knijf et al., 2008a).

As runoff is the parameter vital to flash flood research, only the topsoil will be truly represented in the model; the subsoil and ground water will remain underrepresented in this case. This is made possible by the fact that in the case of flash flooding often precipitation and runoff is received by a soil surface at a rate faster than the infiltration capacity of the topsoil, thus the short term cause of excess runoff is not that the storage capacity of the entire soil matrix has been exceeded. A More detailed description of runoff generation within LISFLOOD is outlined below.

Within LISFLOOD, runoff generation is parameterised by the following equation for surface runoff:

$$\mathbf{R_s = R_d + (1-f_{dr}) * (W_{av} - D_{pref,\,gw} - INF_{act})} \quad [1]$$

Rd = direct runoff which is generated using a direct runoff fraction (F_{dr}) in each pixel (mm)

Fdr = direct runoff fraction related to impervious areas such as concrete landscapes and frozen land) in which infiltration is considered 0 (-)

W_{av} = the actual water available for infiltration (mm)

D_{pref} = the water flow that follows preferential pathways leading it directly to the ground water without infiltrating the soil matrix (mm)

INFact = the actual infiltration that occurs in each pixel (mm)

Groundwater:

The model describes the groundwater system by using two parallel interconnected linear reservoirs. There is a significant difference between the two reservoirs. The first represents the fast subsurface- and shallow ground water flow whereas the second behaves far slower and represents the base flow generation (Thielen et al., 2007)

It is important to note that the moisture fluxes in the unsaturated soil and between the two groundwater reservoirs, due to simplification, are completely gravity driven. Therefore no capillary rise occurs. This downward flux equals the hydraulic conductivity of the soil. Under unsaturated conditions the conductivity is calculated by using the van Genuchten equation (van der Knijf et al., 2008 a, van der Knijf et al., 2008b).

Also preferential flow (water which bypasses the soil matrix and directly drains into the deeper groundwater) is incorporated. However until now there is not yet a common equation to describe this process. Nevertheless the process cannot be disregarded as this will, especially during extreme rainfall conditions, lead to unrealistic model behaviour. To counteract this, a fraction of the available water for infiltration is directly added to the deep groundwater. The power function used in the model assumes a direct relation with the saturation of the topsoil, and consequently the preferential flow component becomes increasingly important under wetter soil conditions (Thielen et al., 2007, van der Knijf et al., 2008b).

River channel:
The LISFLOOD model offers two methods for river routing: the dynamic or kinematic wave descriptions. Under default settings the kinematic wave approximation is used (van der Knijf et al., 2008b). By using the kinematic wave the mass balance is still included, it assumes pseudo uniform flow conditions and is driven by the slope entirely (Hager et al., 1985). The use of the kimematic wave approximation exludes the possibility of for example backflow floodingmodelling. To apply the dynamic wave approximation more detailed information about the river cross section is needed.

The LISFLOOD model offers the possibility to extend the water system with special features as polders, reservoirs and lakes (van der Knijf 2008b). As example: the side flow (in m^3/s^{-1}) into the river (which represents the runoff entering the channel per unit channel length), is under default settings, calculated by using the following equation:

$$q_{ch} = (Q_{sr} + Q_{uz} + Q_{lz} + Q_{in} + Q_{res}) / L_{ch} \quad [2]$$

The first three parameters are related to surface runoff (m^3) whereas L_{ch} is the channel length (m). The two other parameters have the value zero under default settings and represent an external 'inflow hydrograph' (Q_{in}) which can be used only when part of the catchment is modelled and the inflow from a controlled reservoir (Q_{res}) flows into the channel (van der Knijf et al., 2008b).

Interception:
The LISFLOOD model calculates interception by using the simplified approach of Aston. This approach assumes an exponential relation to fill the canopy storage, as defined by the equation below (de Jong et al., 2009).

$$Int = S_{max} * (1-exp^{(-k * R\Delta t/Smax)}) \quad [3]$$

$$K = 0{,}046 * LAI \quad [4]$$

Int = Interception per time step (mm)
S_{max} = Maximum storage capacity (mm)
K = factor accounting for vegetation density (-)
LAI = Leaf area index (m^2/m^2)
R = Rainfallintensity (mm/day)

This approach includes a maximum storage which is based on an empirical relation given by von Hoyningen/Huene (Bulcock, 2010; van der Knijf et al., 2008b & de Jong et al., 2009).

$$S_{max} = 0{,}935 + 0{,}498LAI - 0{,}00575LAI^2 \quad [5]$$

The intercepted precipitation (which can never exceed S_{max}) will reduce to zero over time due to leaf drainage and evaporation (van der Knijf et al., 2008a).

***Evapotranspiration**:*

The LISFLOOD model approaches evaporation from the soil and transpiration from the vegetation as separate processes. The used equations are mainly based on the Penman Monteith method (van der Knijf et al., 2008b).

3.1.2 Model Input

As can been seen in the schematisation of the model (figure 3.1) an extensive dataset is required. This data can be divided into five main topics:

- Data related to topography
- Data related to vegetation
- Data related to the stream network
- Meteorological data
- Soil related data.

The related data is displayed in table 3.1. As stated above LISFLOOD originally was designed for the larger pan European catchment. This is something to be aware of as it affects the accuracy of parameterisation. An extensive set of parameters is inputted as detailed spatially heterogeneous data (e.g. maps) another part of the data is inputted as single homogeneous values, constant throughout a complete land cover or soil texture class (e.g. look up tables).

***Table 3.1:** List of the required input maps and tables (van der Knijf et al. 2008)*

	Maps	**Tables**
Topography	Area, DEM Forest fraction per cell, Elevation range per cell Outlets location, Direct runoff fraction	
Drainage network	Channel locations, dimensions, Manning's roughness	
Soil properties	Soil class	kSat
	Xinjiang b value per cell	Van Genuchten parameters
	Initial soil moisture	Thetas, thetar, Poresize, Van Genuchten Parameter,
Meteorological data	Precipitation, average temperature	
	Evapotranspiration of bare soil, water, example crop (et, ew & es)	
Vegetation	Leaf Area Index (LAI)	Crop coefficient, cropgroupnr, rooting depth, Manning's N

3.1.3 Model restrictions

LISFLOOD offers the possibility to incorporate lakes or reservoirs into the model, however the limited capabilities of the LISFLOOD reservoir function are not sufficient to illustrate the mechanisms in use at Barrage Des Olivettes. This is why the model simulations in this study omit the presence of any reservoir. This is counteracted after model simulation with interpretation that includes manual calculations relating the capacity of the lake to the amount of discharge created north of the barrage and finally to total discharge, time to peak and peak flow intensity of the river Peyne (appendix X).

The lake is an important factor affecting all modelling phases, the calibration, validation and scenario simulation. It was not possible to find a method to simulate the behaviour of the reservoir and dam release thresholds within LISFLOOD. Consequently the lake was omitted from the modelling process. To compensate for this, a mass balance was calculated manually to analyse the error that would consequently arise from this omission.

The evolution of a soil crust over time is not incorporated within LISFLOOD. There is not yet an option within the model to change the infiltration capacity due to crusting after a precipitation event during a single model run. Nevertheless, it is known, that reduced infiltration of rain water occurs on vineyard soils due to inhibiting crust layers and also due to tractor compaction of soil pores. (Van Asch et al. 2001). In order to simulate crusted vineyards, the direct runoff fraction of vineyards was increased to higher fractions representing increasing area of crusting. The fractions ranged between 0.05 (uncrusted vineyards) to 0.8 (urban area equivalent).

For more information about the integral details of LISFLOOD please refer to the manual (Van der Knijff, de Roo, 2008)

3.1.4 Modelling Scenarios

The model was used to gain insight in the response of the catchment. To confirm or reject the formulated hypotheses an extensive set of scenarios was run with LISFLOOD. The following scenarios where ran during this research:

- Changing all the land cover classes in a uniform class
  Aim of this scenario was to determine the most hazardous land cover class.

- Changing all the soil texture classes in a single uniform class
  Aim of this scenario was to determine the most hazardous soiltexture class.

- Changing the direct runoff fraction (to increasing simulate crusting) of the vineyards
  Aim of this scenario was to research the effect of crusting on total discharge in Pézenas and the shape of the hydrograph.

- Running the model under extreme precipitation conditions (February 1996)
  Aim of this scenario was to study the catchment response (peak flow propagation, time to peak) during an extreme event.

- Running the model under extreme conditions with observation points at the outlet of each tributary
  Aim of this scenario was to determine the contribution of each single tributary to the hydrograph in Pézenas and to determine the most important source areas.

3.2. Input Data Acquisition

As mentioned in paragraph 3.1, an extensive spatial database on soil properties, topographical characteristics and meteorological data was required to fulfil LISFLOOD input requirements. This input data for the Peyne catchment was generated from three main sources:

- Databases of Utrecht University and external organisations
- Digital databases accessible over the internet
- A fieldwork campaign conducted in September and October 2009

Table 3.2 outlines the composition of the database and related sources. Overall, the database gives a detailed description of the catchment from geology to land cover, excluding in-depth information on deep groundwater and the saturated zone as there was no project requirement for this, considering the short time scale of individual flash flood existence.

Table 3.2: *Peyne catchment database features*

Topography		
Land cover	Corine land cover	Maps (grid)
DEM	Utrecht University	Map (grid)
Appearance of crusting	Infield observations	Map (points)
Appearance of Rills and Gullies	Infield observations	Map (points)
Appearance of Tractor trampling	Infield observations	Map (points)
LAI values	Literature	Map (grid)
Meteorological Data		
Precipitation	Infield/digital database/JRC	
Evapotransipiration of reference crop, Water bodies & soil (E_t, E_w, E_s)	JRC	Maps (grid)
Average temperature (T_{avg})	JRC	Maps (grid)
Soil properties		
Manning's N	Infield observations	Map (grid)
Sorptivity	Infield observations	Map (points)
pF curves	Laboratory/literature	Table
Porosity	Laboratory/literature	Table
Bulk density	Laboratory/literature	Table
Soil Moisture	Laboratory/literature	Maps (grid)
Van Genuchten Parameters	Literature	Table
kSat	Infield observations/literature	Table
Stream network		
Stream dimensions	Infield observations/literature	Map (grid)
Manning's N	Infield observations/literature	Map (grid)
Stream ordering	Sandre.fr	Map (.shp)

3.2.1 The fieldwork campaign

In September and October 2009 a field campaign was carried out in the Peyne catchment to collect data and gain insight into the (hydrological) characteristics of the catchment. Data on soil properties and stream dimensions were compiled from infield observation. Measurements were taken at approximately 120 predefined locations (appendix I). The 120 points were selected using the ArcGIS tool 'Create Random Points'. Random sampling allowed for a weighted representation of soil and land cover classes, as the majority classes had more sample locations assigned to them than the minority soil classes. In practice, measurements were confined to these locations or as close to these locations as possible in the case of difficult accessibility.

The following tests were performed in the field:

- Surface roughness (Chain measurements)
- Infiltration (Mariotte bottle tests)
- Sorptivity (Falling head single ring infiltration)
- Soil moisture (TDR)
- Tipping buckets

Infiltration observations:

The infiltration measurement described by Duijsings (2008), requiring a Mariotte bottle to release a continuous fixed discharge on an area of bare soil, was used. Time is given until equilibrium is reached (soil reaches saturation and horizontal flow has become minimum) before the test would end. It was assumed that after 20 minutes an equilibrium was reached (this time window of 20 minutes was tested several times to confirm this assumption).

Figure 3.2: *a) Locations of the infield observations b) Measuring the wetted perimeter c) Infiltration location after 20min of water supplying*

After 20 minutes the wetted area and discharge from the Mariotte bottle were measured. With these two values the kSat was determined by using the following formula:

$$Q/A = I \qquad [6]$$

Q = Discharge (cm^3/s^{-1})
A = Wetted area (cm^2)
I = Infiltration under steady state conditions (cm/s^{-1})

Infiltration measurements were performed according to the methodology of Duijsings (2008). This technique is only reported to have been tested on crusted largely bare soil, nevertheless it was decided to use this technique on the entire catchment regardless of soil class. This decision was made due to the benefits of the minimal apparatus and simplicity associated with the technique,

which allowed increased mobility, enabling the sampler to reach the predefined sample locations with higher accuracy. Saturated hydraulic conductivities (kSat) recorded using this method followed a normal distribution, however values experience overestimation with a consistent magnitude of error.

Sorptivity test.

During the fieldwork campaign, infiltration experiments highlighted the importance of sorptivity. Taking advantage of this finding, single ring falling head experiments were performed (Touma et al. 2007). A single ring with a diameter of 9 cm is placed 0.5cm to 4cm deep into the soil surface. A 100ml volume of water is applied to the soil within the ring and the time taken for full infiltration is measured. This is repeated with consecutive 100ml installments of water applied until the soil becomes saturated and equilibrium is reached. Equilibrium can be identified when the time measurements for infiltration of the 100ml applications of water stabilize (Farrel, 2010)
The raw field measurement values were imported into an Excel sheet containing the Brutsaert formula for 3D infiltration (van Beek, 2009, pers comm.).

$$q=Ks*0,5S\sqrt{t}*(1+\frac{Ks*\sqrt{t}}{S})-2 \quad [7]$$

q = Infiltration in (cm^3/h)
ks = Saturated conductivity (cm/h^{-1})
t = Timestep (min)
S = Sorptivity ($cm/h^{-0,5}$)

This formula was fitted to the observed data to determine the sorptivity value. The best result was found by using the Solver option within Excel with the RMSE and the 'LinEst' as objective functions.

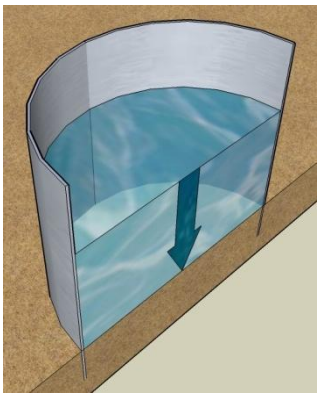

Figure 3.3: *Schematic representation of the single ring falling head method applied in the field to determine the sorptivity values of the different soil texture classes*

Uncertainty exists in the results of the experiment, especially in the crusted soil where the metal ring will damage the crust.

Saleh roughness factor

To determine the surface roughness a fine chain of 1m length is placed on the ground with consideration given to ensuring the surface roughness is incorporated (the chain takes the shape of the surface.
The subsequent length of the chain is measured and imported into the following sequence of equations to determine the Saleh roughness factor and convert this into Manning's N values. 5 to 10 measurements are taken per location and averages are taken to ensure heterogeneity is accounted for (Gomez et al. 2005 & Gilley et al. 1995, Stone et al. 1992)

$$Crr = 100 * (1-(L2/L1)) \quad [8]$$

$$RR = (1-exp[-4,82*10-3(R + 19]) * Crr \quad [9]$$

$$F = 1.0 + 13 * (1.0 – e^(-0,0773 *RR)) + 18,52 * ((SC/100)^1,267) \quad [10]$$

$$C = (8g/F)0,5 \quad [11]$$

$$C = k * [R1/6 /n] \quad [12]$$

Crr = Saleh roughness (-)
L 1 = Length total chain (cm)
L2 = Length draped chain (cm)
RR = Random roughness (cm)
F = Darcy-Weisbach friction (-)
C = Chézy roughness (-)
K = Conversion factor (1.49 from feet to m)
N = Manning's N surface roughness (-)

Soil Moisture

Soil moisture content was measured at more than 50 locations before and after the infiltration tests using a Frequency Domain Reflector measurements. FDR methodology measures signal reflections travelling within a medium. The energy signal leaves one of two metal pins inserted into the soil. The received frequency at the second pin will be the same frequency as the incident (sweep) signal but in a different phase (JDSU, 2010). Pulse frequency is dependent upon moisture available in the soil (Eijkelkamp, 2010). The used FDR device offered two options separating mineral soils form organic rich soils. Based on the infield situation it was decided which to use.

Tipping buckets

To acquire high resolution precipitation data two typing buckets where installed in the field during the fieldwork campaign. These tipping buckets registered every tip on a digital hobo device. The first tipping bucket was placed at Neffiès and the second one along the reservoir (UTM X 0522674; Y 4820217 and X 0526859; Y 4823804).

Figure 3.4: *The infield installed typing bucket at the reservoir location (Gortmaker, 2010)*

3.2.2 External sources

A significant proportion of the data was retrieved from existing datasets which were accessed using the internet, and by contacting specific organisations and institutes. The following paragraph outlines the more important datasets and sources.

Meteorological Data

Meteorological data was gathered from 3 sources. Twenty years (1990-2009) of low resolution meteorological data gathered from the MARS repository (maintained by the European Centre for Medium-Range Weather Forecasts (ECMWF, 2010)) was provided by the Joint Research Council. The resolution of precipitation data was increased by comparison with data acquired from two tipping buckets during the field campaign and two additional datasets. Firstly, precipitation data gathered at the St. Majan meteorological station near Roujan (Lambertian X 678820, Y 1836010) and in the vicinity of Lac des Olivettes (Lambertian X 677718; Y 1840090) was acquired from OMERE via Montpellier University for the period 30/06/2009 – present. Secondly, data was downloaded manually from the RDBRMC website (Rhone-Mediterranean-Corsica Basin Water Data Network) (Lambertian X 678820,Y 1836010 and X 677718; Y 1840090) (RDMBC, 2010)

LAI and Forest fraction

Forest fraction values were derived from the OLSON land cover characteristics (Hagemann et al, 1995). For land cover types that were not incorporated in the OLSON table, mean values were used. The OLSON table also provided the input for the following equation (R. van Beek, pers comm., 2009.) which was used to determine the monthly Leaf Area Index (LAI) values.

$$LAI_d + LAI_{Re} \text{ (per month) } * (LAI_G - LAI_D) = \text{LAI per month} \quad [13]$$

LAI_{re} = Leaf area index compensation factor per month
LAI_g = Leaf area index during the growing season (m^2/m^2)
LAI_d = Leaf area index during dormancy (m^2/m^2)

Discharge data

Discharge and water height data of the St. Majan measuring station (Lambertian X 678820, Y 1836010) was downloaded manually from a French governmental ecological website (vigicrues, 2010). The dataset covers the period of 30/6/2009 – 30/03/2010.

Land cover

Spatial mapping of land cover was retrieved from the Corine online database which uses Spot HRVXS and Landsat TM and MSS imagery. The map has a resolution of 1:100000, is based on the Lambertian coordinate system and was validated by observation during the infield phase. (Corine, 2006)

3.3 Input data preparation

PCRASTER and *ArcGIS* applications were used to convert the acquired data into maps with proper extent and dimensions. A more detailed description of the data conversion and the steps taken in PCRaster is included as Appendix XVIII).

All prepared data is summarized in the LISFLOOD settings file (.xml type), which contains all file paths and initial values required to run the LISFLOOD model. This settings file also gives access to the activation switches of preferred features to simulate (e.g. simulate water levels, reservoirs, dynamic wave) and preferred reported output data.

3.4 Model Calibration & Validation

3.4.1 Sensitivity analysis

Sensitivity analyses were performed on 19 different input parameters to gain insight into the sensitivities of the LISFLOOD model. Six out of the nineteen tested parameters are shown in the spider diagrams of graph 3.1. All three parameters were tested by increasing and decreasing their value by a factor 2 and 0.5 respectively. By using these factors the non linear response of the model to certain parameters is partly ignored. The resultants were then compared to the original output discharge.

.

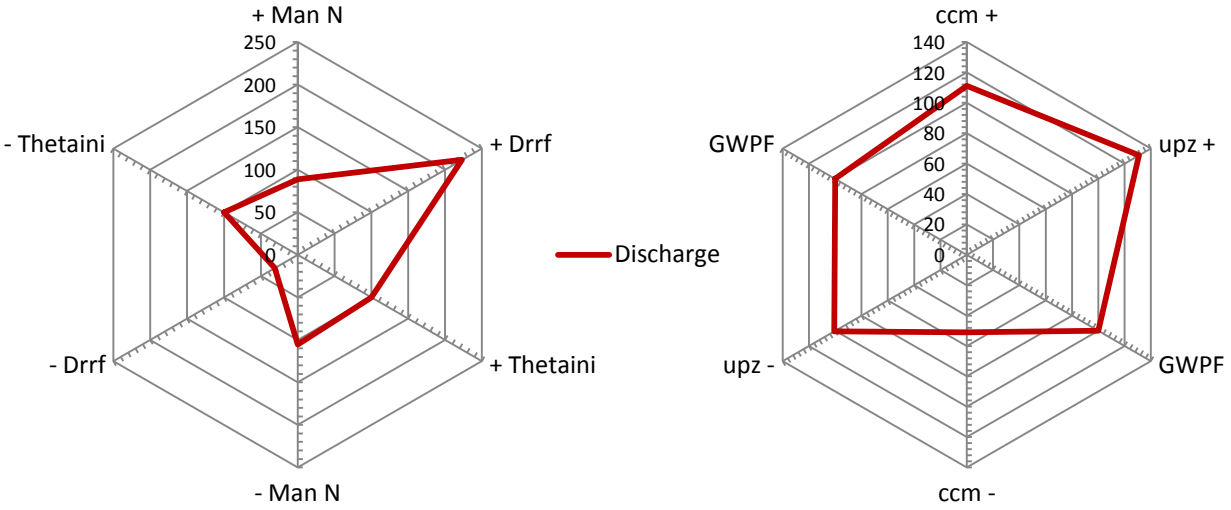

Graph 3.1: *Spiderdiagrams displaying the sensitivity of the LISFLOOD model to six important parameters. The diagram displays the change in the total discharge relative to the discharge modelled under normal parameterisation (a discharge equal to 100%)*

Remarkable is the insensitive behaviour of the model to initial soil moisture conditions which affect the total discharge by no more than 1%. In contrast, the model discharges appear to be very dependent upon the direct runoff fraction. A doubling of the direct runoff fraction results in a discharge increase of 122% compared to discharge under normal conditions. By halving the initial direct runoff fraction the actual discharge will be reduced by 70%. The model shows less sensitivity to changes in surface roughness where halving the values result in an increase of 5% and doubling the values result in a change of approximately 12%. In comparison to the Manning's N, related to land cover classes, the model shows a large sensitivity to the CCM which is affecting the surface roughness of the riverbed. By changing this value the total discharge can be reduced by 50% (by doubling the value) or increased by 10% when the value is halved. When looking at the hydrograph of the total catchment discharge at the outlet (graph 3.2), it can be seen that sensitivity of this hydrograph to changes in CCM of the streams is high. However when looking at individual discharges of each stream, the relative influence of CCM changes is much less. The explanation for this is that the discharge at the outlet, is comprised of the combined individual discharges, each containing its own element of error. The combined error of the individual tributaries plus the error of the Peyne river itself results in a significantly altered final hydrograph. As figure 3.2 below illustrates, CCM values of 4.617 (blue hydrograph) and 7.5 (red hydrograph) result in very different hydrograph responses. The higher CCM value resulted in lower peak formation and extended peak durations .

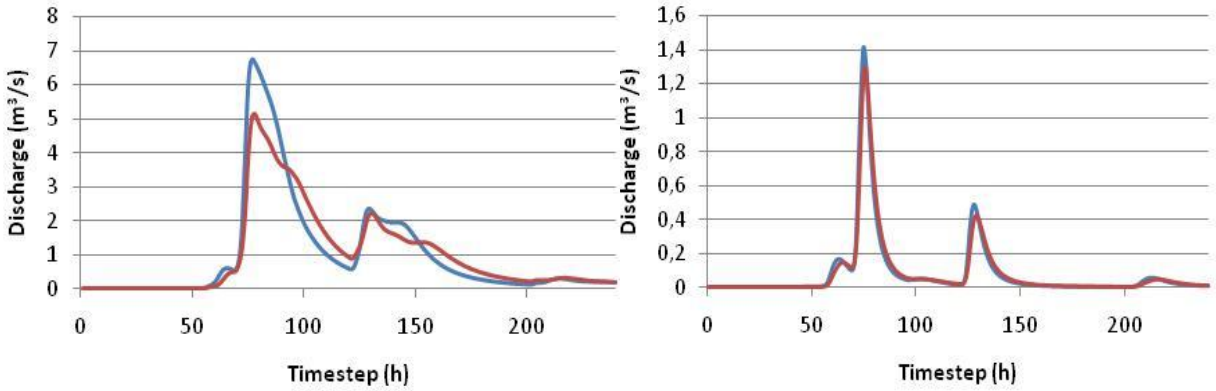

Graph 3.2: *The above graphs show the sensitivity to a changing CCM.*

3.4.2 Nimbus & the SCEUA algorithm

Calibration was performed using NIMBUS, a calibration application developed specifically for the LISFLOOD model. The Nimbus software contains several calibration algorithms (e.g. SCEM, SCEUA, Amalgam, PEST). However restrictions exist regarding the possibilities of these algorithms such as specific operating system requirements (Windows versus Unix). Under current conditions the JRC advise for relatively smooth operational use to apply the SCEAU algorithm (Pannemans, 2008).

The SCEUA algorithm uses a (global search) shuffled complex evolution method (SCE) which is developed at the University of Arizona (UA). For LISFLOOD purposes the SCEUA algorithm was translated from Fortran to Python environment. (Pannemans, 2008 & Duan et al., 1993). SCUA offers several objective functions (Nash Sutcliff, Pearson, RMSE, rRMSE) which can be used to measure the goodness of fit between the observed and calculated data. For this research it was found optimum to use Nash Sutcliffe as the primary objective function while observing Relative Root Mean Squared Error (rRMSE) as the secondary objective function (as SCUEPY uses a single objective function only) (please refer to appendix XIX for a more extensive description).

The Nimbus application offers by default 8 calibration parameters. After an initial sensitivity analyses it was decided to use three parameters to calibrate upon as outlined in table 3.3 below.
The three calibration parameters are applied to the whole catchment being spatially uniform.

Table 3.3: *the calibration parameters*

	Minimum value	Maximum value
[1]Bxinj	0.01	1
[2]PWPF	0.5	8
[3]CCM	0.1	15

[1]Infiltration in LISFLOOD uses the VIC/ARNO model (also known as the Xinanjiang model) which is a non linear distribution function to illustrate the relation between the runoff contributing fraction of each grid cell and the total soil moisture content. A shape parameter (b) within the infiltration equation defines the level of heterogeneity within each grid cell. In the case of no heterogeneity, b is zero and the model becomes a simplistic overflowing bucket model (Van der Knijff, de Roo, 2008).
[2] An empirical shape parameter that defines the proportional increase of preferential flow with respect to increase soil moisture storage (van der Knijf et al.,2008).
[3] CalChanMan is a multiplier that is applied only to manning's n of the stream channels and affects the timing of peakflows in the channel routing (van der Knijf et al.,2008).

3.4.3 Calibration and validation data

Data for the calibration involved use of meteorological and discharge data from February 2010 as it was of a higher reliability due to a large absence of incorrect or missing values relative to other time periods. The precipitation and discharge data was acquired from the Olivettes (precipitation) and St. Majan (precipitation and discharge) observation points. (tavg, Es, Ew and Et) was complemented by using average values based on a 10 year period extracted from the MARS repository (1990 to 2000).

The calibration was performed on a hourly basis rather than the default daily time step used in NIMBUS. This was done in order to improve the temporal resolution of the output, as flash flooding occurs on an hourly scale rather than a daily scale. Taking daily discharge values would imply a large underestimation of peak flows (Appendix XIX).

Two time periods were taken for the calibration and validation:

- *Calibration: 14 – 23 February 2010*
- *Validation: 1 – 8 February 2010*

As mentioned above the choice of these time periods was highly influenced by the available datasets. As a consequence of this decision it was expected and incorporated in the further process that the model would not be able to reliable reproduce summer events.

3.4.4 Calibration and validation runs

The first calibration run resulted in a Nash Sutcliff of 0,86 which can be classified as a 'good' model performance. The range of tested values was large as can be observed in table 3.4.

Table3.4: *The range of the calibration parameters within the most successive calibration run*

	bXinj	PWPF	CCM
Min	0,012	0,52	0,16
Max	0,999	7,97	14,89
Mean	0,490	4,11	5,07
Best	0,316	0,55	4,62

The calibrated parameter values are displayed in table 3.5.

Table 3.5: *The original and optimized CCM parameter values*

	bXinj	PWPF	Ccm	Nash Sutcliffe	Period
Calib 1	0.316	0.551	4.617	0.86	14-23feb
Calib 2	0.186	0.5523	10.94	0.83	1-8feb
Calib 3	0.316	0.551	7.5	0.72	14-23feb
Valid 1	0.316	0.551	4.617	0.5	1-8feb
Valid 2	0.316	0.551	7.5	0.74	1-8feb

In contrast to the calibration run the validation run resulted in a Nash Sutcliff of 0,52 which can be classified as poor performance.
A second calibration run was performed to reduce the error. In this second calibration run the validation period was used as calibration period. The resulting Nash Sutcliff was 0,83. The calibrated parameters of run 1 and run 2 showed a high correlation with exception of the CCM which resulted in a optimum value of 10,94.

By manually changing the CCM value into an intermediate value (based on the probability density function (appendix XIX)), a more robust calibrated model was achieved. The NS for the original calibration period decreased to 0,72 but the validation period resulted in a NS of 0,74.

The following scatterplots (graph 3.3) display and support the influence of the cross calibration/validation. A certain amount of hysteresis can be observed in the scatterplots. This is mainly due to the time to peak. In general the hydrographs calculated by LISFLOOD tend to peak earlier and show a more smooth shape this in contrast to the observed hydrographs of the Peyne which show a more instant peak and a less smooth shape.

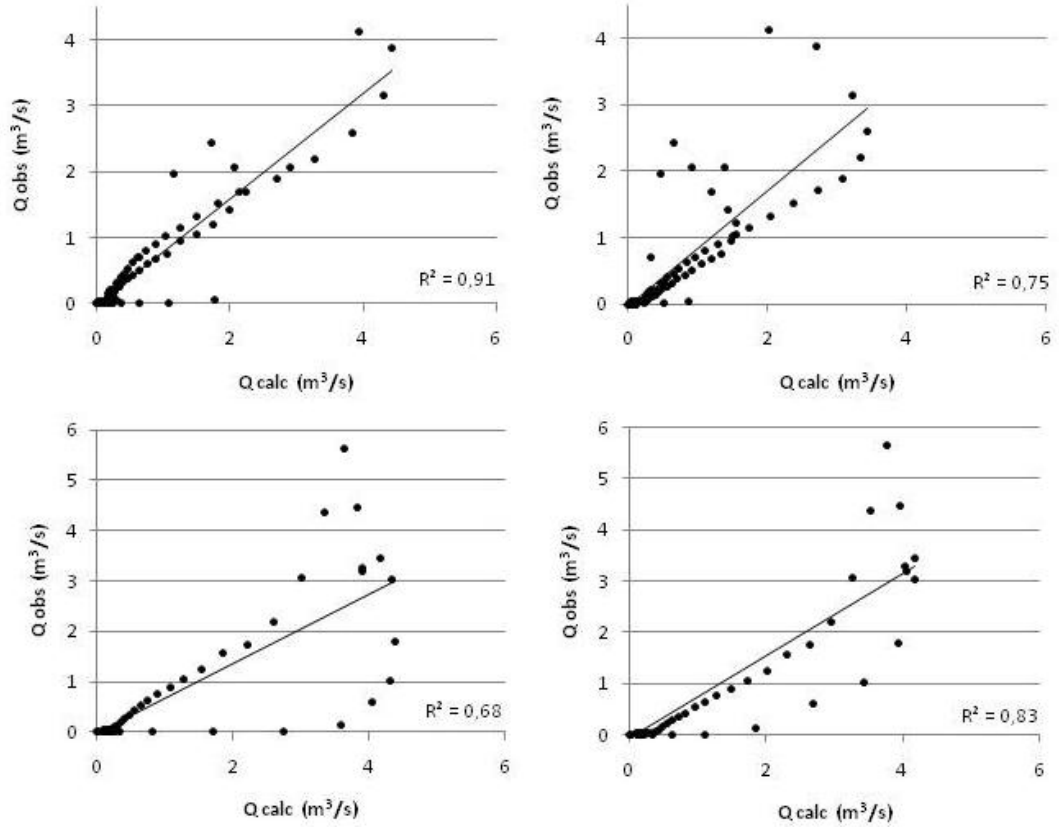

***Graph 3.3**: The observed discharges plotted against the by LISFLOOF calculated discharge. From left to right: a) calibration run b) calibrations run 2 c) validation run 1 d) validation run 2*

4. Results

During this research an extensive set of results where found, modelled and determined. The results can be subdivided into four classes related to:

- Data(base) analysis
- Fieldwork observations
- Scenario modelling
- Model behaviour

4.1 Database analysis

4.1.1 Lake Mass Balance

A mass balance for the lake was calculated using cumulative infiltration occurring between 11/10/09 - 10/02/10 and is outlined in table 4.1 below (Appendix X).

Table 4.1: *Mass balance of Lac des Olivettes for 11/10/09 to 10/02/10*

	mm (relative to area)	**Million m^3**
Input		
Pr	329,5	9,7
Output from the reservoir		
Q	20,2	0,6
E_t	86,6	2,6
E_w	0,9	0,3
Storage		
Soil	101,7	3
Lake	120,1	3,2

This equates to a total of 5.8Mm^3 of storage required in the lake which corresponds to ~166m.a.s.l of water depth. It is known that this calculation is an overestimation of water volume due to the rough estimation of the upper catchment dimensions and properties (soil moisture content, porosity, soil depth) and absence of interception.

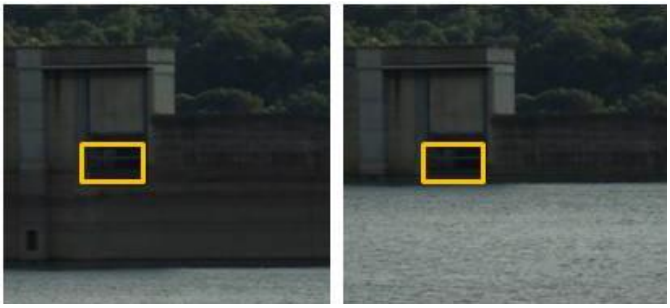

Figure 4.1: *The water level before October 11th 2009 and the expected (manipulated) water level on February 10th 2010 relative to the 22m^3/s spill (yellow cube).*

Photographic evidence (figure 4.1) from October 2009 indicates that the lake had an initial storage of 2.6Mm^3 with base flow of 50l/s as the only outflow from the lake. Also known from discharge data is that the lake outflow did not increase from the base flow level during this time period October-February. Therefore the outflow threshold at 163m with potential discharge of 22m^3/s must not have been breached (please refer to paragraph 3.1 and graph 3.2). The storage of the lake in this case must not have exceeded 4.37Mm^3. Thus, the additional water added to the initial lake storage must have reached a maximum 1.83Mm^3. This results in mass balance over estimation of

approximately 1.4Mm^3. Finally, the part of the catchment above the lake would have contributed 1.83Mm^3 of water to the lower part of the catchment if the lake had not facilitated.

4.1.2 Precipitation and discharge data analysis

An extensive precipitation dataset (ranging from 1992 to 2005) was statistically analyzed to gain more in depth insight in the event properties over the year. Based on the analyzes of these 12 years it was observed that the most intensive events tend to happen in the summer months and early autumn, whereas the longer less intense events tend to happen in late autumn and winter season (graph 4.1).

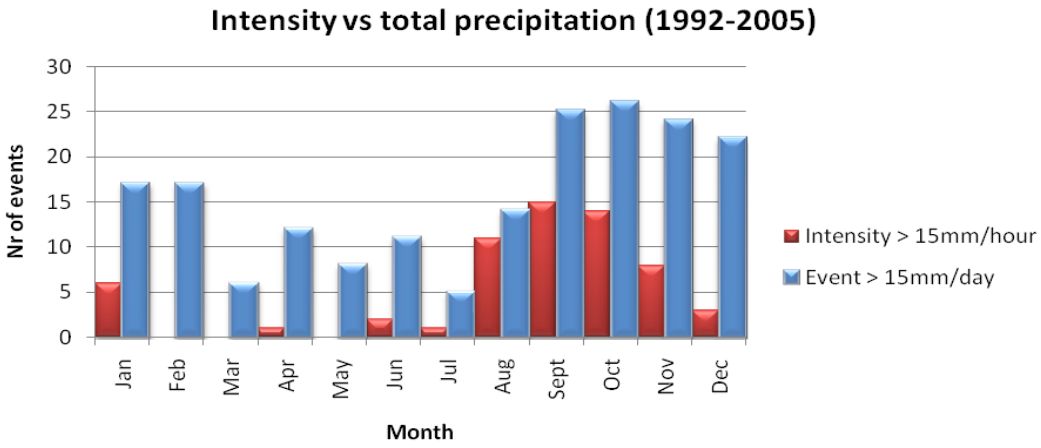

Graph 4.1: *Precipitation intensity versus the total precipitation based on 13 years of data (Omere, 2009).*

Looking at graph 4.2 below it is apparent that the catchment has irregular response behaviour to precipitation events of similar character (A & B). The different discharge response of the catchment is related to three factors. Firstly precipitation event A is a long and mild precipitation event of 26.5mm lasting 24 hours whereas precipitation event B occurs in several hours spread over two days is more intense and has a larger cumulative total over two days of 48mm. Secondly the soil is less saturated at event A than event B which implies more soil storage for incoming water at event A, reducing peak discharge. Thirdly, the lake is not full at precipitation event A, but has reached the 22m^3/s spillway at event B thus a large proportion of the discharge peak at St. Majan is due to the outflow of the dam from the upstream area into the river Peyne.

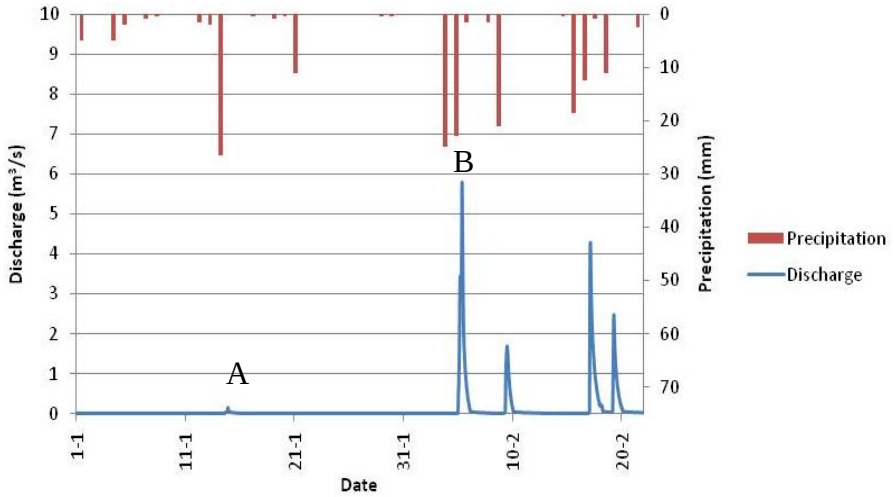

Graph 4.2: *Discharge and precipitation data ranging from 01/01/10 to 22/03/10 showing the irregular behavior of the catchment (Vigicrues 2010).*

4.1.3 Normalized Difference Vegetation Index

The NDVI was determined for June 2002 and February 2003. The two following figures (figure 4.2) show an extract of the complete map (included in appendix XI). The two figures clearly bring to attention the monthly differences between the vineyards in the southern part of the catchment, and the schlerophyllous and forest in the upper part. It also highlights the higher seasonal vegetative variation of vineyards in comparison to the forested area. This will affect the temporal heterogeneity of the topographical characteristics and thus the catchment response to precipitation events. The first image of vegetative cover in vineyards in June shows a more extensive coverage of vegetation than in February. This supports the annual changes of LAI which in turn affects the interception of rainfall. Thus during February more direct rainfall will reach the soil compared to June.

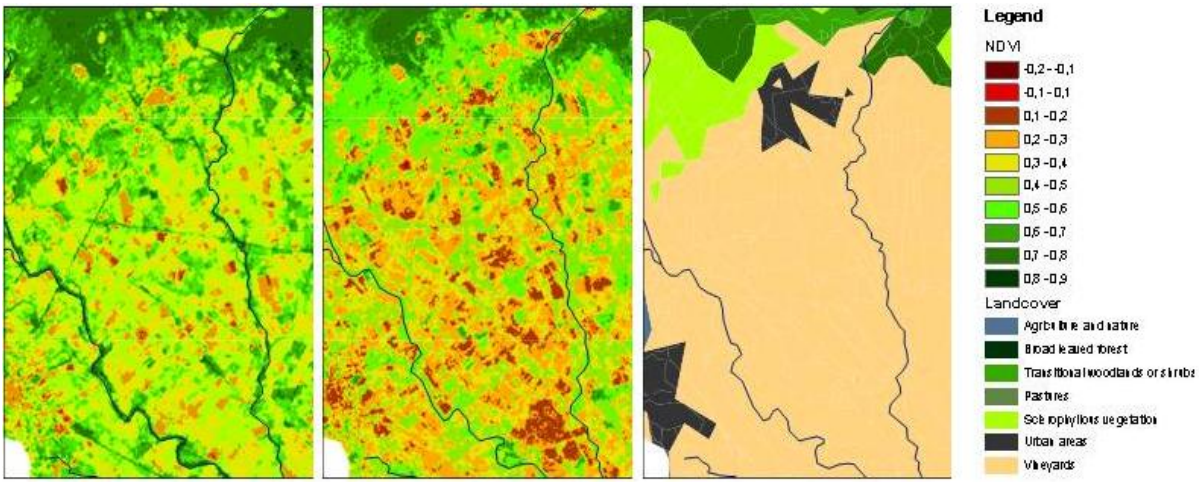

Figure: 4.2 *The NDVI for June 2002 and February 2003 and the related land cover classes*

4.2 Fieldwork data

4.2.1 Infiltration

Model input

The observed kSat values showed a large heterogeneity within the soil texture classes. It was decided to use the median values over the mean values. Due to the large variance within the observations mainly caused by large differences within soil texture classes (for instance a high values due to recent ploughing) the mean values often showed extreme values:

Table 4.2: *The statistics related to the infield observed infiltration values*

Soiltexture	N	Min	Median	Mean	Max	Stdev
Clayey	12	1,20	4,56	50,90	465,19	132,35
clayey sand	33	1,11	6,40	9,70	43,13	8,40
Sandy	12	0,93	4,66	4,73	8,01	2,13
Silty	18	1,15	3,74	4,73	12,76	2,71
silty clayey	6	1,46	9,03	8,82	19,79	6,85
silty clayey sand	139	0,40	7,82	20,21	186,07	31,08
silty sand	38	1,54	6,36	18,67	200,96	35,75
silty sandy	3	5,09	5,33	5,96	7,47	1,31
silty sandy clay	99	0,35	6,77	18,35	194,63	33,72
urban other	21	1,74	5,23	13,23	131,88	27,98

Crusting

Of the 153 locations measured for crusting and Hydraulic conductivity (appendix XIII), 24%, 26% and 50% were crusted, mildly crusted and not crusted respectively. There lies a clear difference between mean kSat values of the three classes, with non-crusted soils experiencing the largest mean ksat value of 10.52cm/hr, mildly crusted soils have a mean of 7.23 cm/hr and crusted soils having the lowest mean kSat value of 4.91 cm/hr.

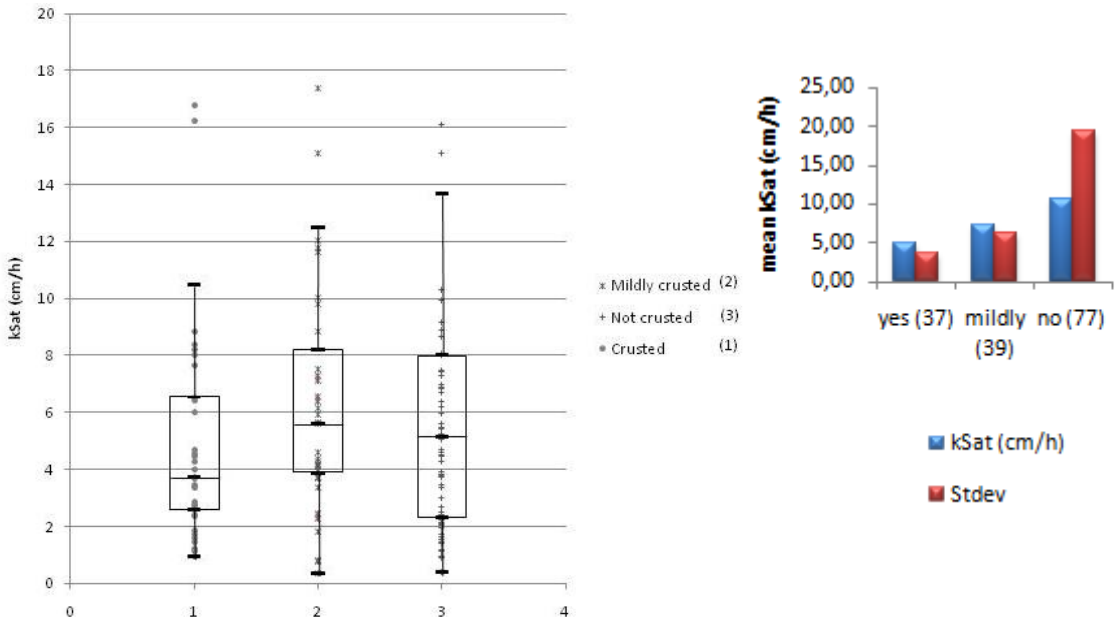

Graph 4.3: *a) Boxplot diagrams of the infield measured hydraulic conductivity classified on crusting appearance*
b) Mean and standard deviation values related to the boxplot diagrams

4.2.2 Surface roughness

Model input

The model only needed one single value for each land cover class. It was decided to use the mean value as model input. The variance was in case of most land cover classes relatively small. Mean and median differed within a minimal range. The calculated maning's N values and the related variances are displayed in table 4.3.

Table 4.3: *Statistical analysis of infield measured Manning's N displaying the mean median and variance values.*

Land cover	min	mean	median	max	stdev	n
Vineyards	0,028	0,033	0,034	0,034	0,002	433
bare soil	0,022	0,027	0,028	0,028	0,002	83
broad leaved forest	0,033	0,057	0,058	0,058	0,004	50
complex cultivation pattern	0,054	0,058	0,059	0,060	0,002	60
agriculture with significant areas of nature	0,027	0,046	0,052	0,053	0,010	10
mineral extraction site	0,008	0,028	0,034	0,034	0,010	10
mixed forest	0,034	0,058	0,060	0,060	0,004	39
natural grasslands	0,049	0,058	0,059	0,060	0,003	60
pastures	0,036	0,055	0,060	0,062	0,010	15
schlerophyllous vegetation	0,051	0,055	0,055	0,057	0,002	30
sport and leisure facilities	0,037	0,041	0,042	0,043	0,002	10
transitional woodland	0,051	0,057	0,057	0,057	0,002	24

4.2.3 Sorptivity

The sorptivity value was determined for 27 observations and shows large heterogeneity on the small scale (appendix XIII). Values within one vineyard can differ with more than a factor 3. Crusted areas not necessarily show lower values in sorptivity which might be due to the occurrence of cracks and the used experiment to determine the sorptivity values. No statistical relation was yet found between effective conductivity and soil moisture.

4.2.4 Direct runoff fraction

During the field campaign a first estimation of impervious area (or direct runoff fraction) was determined. During the classification rock outcrops, roads, buildings and paved areas where considered as impervious. These values where checked at a later stage using topographic maps and satellite imagery as can be seen in figure 4.3 (Geoportail, 2010). The land cover classes were divided into 5 different groups which are displayed in table 4.4.

Table 4.4: *The five direct runoff fraction classes*

Group	Direct runoff fraction (%)
Vines and agricultural area	5
Forested areas	15
Schlerophyllous vegetation	25
Mineral extraction site	50
Urban area	80

Figure 4 3: *Examples of visual data used to validate the infield observed direct runoff fractions for a vineyard area (5%) and the schlerophyllous vegetation (25%)(Geoportail, 2010)*

4.3 Scenario modelling

4.3.1 Tributaries

LISFLOOD simulations of the 1996 precipitation event in which 304 mm rain fell in 240 hours were used to determine the influence of the 18 tributaries of the Peyne. Table 4.5 below ranks the tributaries in order of largest to smallest total discharges, based on this 1996 event.

In order of highest to lowest discharge, the three largest contributors are the Bayelle, the Rieutord, and the Saint Martial (appendices III, VII and XX). The Bayelle delivers the largest discharge (7775.87m /100m and a total discharge of 635173.08 m3) to the river Peyne which is attributed to the large quantity of urban area in the sub catchment. The Rieutord discharges the second largest total discharge and this is likely to be related to the steep plateau topography. The Saint Martial is the 3rd largest contributor mainly due to its length, as it is the longest tributary according to SANDRE (2010). The Vallat produces the smallest discharge and the Roquemaliere is the shortest river providing the 7th smallest total discharge. All tributaries have the same peak travel times (time to peak approximately 2 hours). The accumulated peak arrives 3 hours later at the outlet located at Pézenas and the Peyne peak wave arrives 3 hourly times steps later (time to peak approximately 5 hours)

Table 4.5: *Tributaries ranked from largest to smallest total discharges*

Name	Length (km)	Discharge(m^3)	Peak wave (m^3)	Tp (hour)	Strahler	Sandre Stream order
Peyne	32.9	3673980.59	53.10	151	4	3
Bayelle	8.4	653173.92	15.05	148	3	5
Rieutord	6.7	373133.28	8.98	148	2	5
saint martial	10.5	309534.38	7.24	148	2	4
Boudic	4.2	231959.09	5.52	148	2	6
Levers	4.7	231228.23	5.63	148	1	6
Tartuguier	7.6	204965.02	4.50	148	2	5
Pouzes	4.4	179955.25	4.41	148	2	6
Margaride	4.2	152622.14	3.74	148	2	6
Mourissou	3.7	104843.01	2.55	148	2	6
Ribouyrel	3	104833.3	2.57	148	1	6
font rarens	1.8	95627.75	2.36	148	1	6
Roquemaliere	1.2	66115.13	1.63	148	1	6
de la bayse	1.8	65234.52	1.60	148	1	6
Rounel	2.7	64291.62	1.56	148	1	6
de la Charette	2.1	42060.82	1.02	148	1	6
de Fer	1.3	26862.12	0.66	148	1	6
de maro	1.5	25719.52	0.60	148	1	6
le vallat	2.1	19114.63	0.46	148	2	6

If the values are approached in a relative way (runoff per hectare) rather than observing the absolute values (total discharge per tributary) a different ordering of the tributary orders is revealed.

In this comparison the sub catchments mainly covered with schleropyllous vegetation stand out followed by the (broadleaved) forested catchments and the sub catchments mainly in use by viniculture (table 4.6).

Table 4.6: *Three sub catchments covered by one particular land cover type and the related runoff generation*

Tributary	Main landuse	Area (hectare)	Runoff (mm)
Roquemalier	Sclerophyllous (94,8%)	96.48	68.53
De Pouzes	Broadleaved forest (98,1)	424.89	42.35
De Maro	Vineyards (100%)	183.58	14.01

Each subcatchment was assigned to one of the three classes (vines, forest, schlerophyllous). The summed values of the total discharges, runoff and the complete area the cover are displayed in table 4.7.

Table 4.7: *The summed discharges and generated runoff of the three main land cover classes*

	Forest (7)	Sclerophyllous (3)	Vines/urban (8)
Discharge (m3)	802806,03	266576.20	1881886.52
Area (hectares)	2063,93	465.81	6534.48
Runoff (mm)	38,90	57.23	28.80

4.3.2 The influence of crusted vineyards

To examine the influences of crusting a scenario was ran with increasing crusted area. To simulate a larger percentage of impervious area in the catchment, the direct runoff fraction of the vineyards in the downstream part was increased stepwise. The direct runoff fraction was varied ranging between 5% and 80%. It needs to be stated that increasing the direct runoff fraction to simulate the increasing crusting is not the most accurate way. As observed during the fieldwork, crusted soils still have a (low) hydraulic conductivity. Within the original LISFLOOD calculation a low direct runoff fraction was used (based on infield observation). Under influence of an increasing crusted area the total discharges enhanced (graph 4.4). The total discharge increase from a total of 596353m^3 to a maximum of 2608016m^3 when 80 percent of the vineyards is crusted. The peak flow increases with the same rate froim 4.03m^3/s (at timstep 88) normal to 42.08m^3/s (at timestep 75).

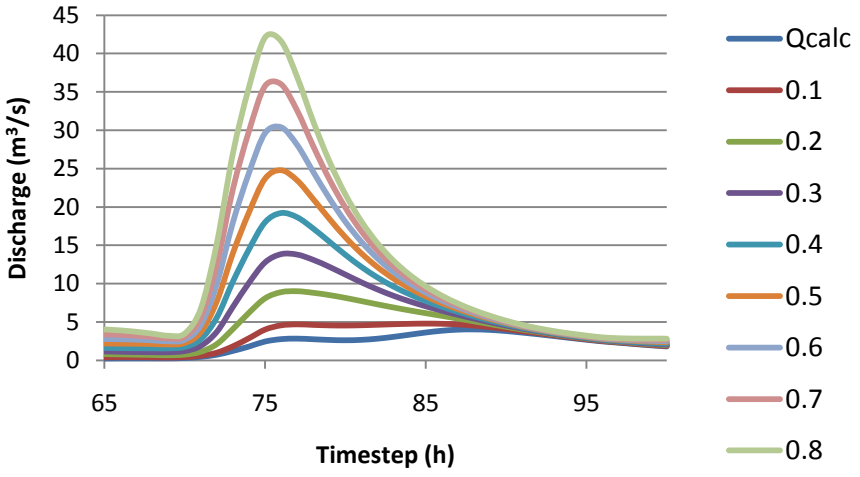

Graph 4.4: *The influence of an increasing direct runoff fraction in the downstream vineyards on the hydrograph in Pezenas*

4.3.3 Soil textures classes

Simulations of the catchment containing only one soil type per model run results in minor differences between total discharge response (appendix XX). The total differences in (percentages) of the tributaries and the Peyne are displayed in table 4.8.

The Morissou experiences highest increase in runoff generation of all subcatchments when exposed to complete coverage of soil 2 (clayey sand) and soil 8 (silty sandy). The Levers had overall highest sensitivity to all soil types. This sensitivity is caused by shallow soils in the area which becomes saturated quicker due to lesser soil storage capacity than a deeper soil, thus a quicker response to changes in soil type.

Table 4.8: *The influence of a changing soil type on the tributary and total discharge(s)*

	Orig	S 1	S 2	S 3	S 4	S 5	S 6	S 7	S 8	S 9	S 10
Mourissou	0,000	-0,015	1,424	0,005	-0,005	-0,002	0,018	0,003	1,317	0,004	-0,015
Levers	0,000	-0,186	0,599	-0,153	-0,164	-0,177	-0,158	-0,146	0,550	-0,161	-0,186
Pouzes	0,000	-0,006	-0,006	0,014	0,006	0,009	-0,009	0,013	0,008	-0,006	-0,006
Margaride	0,000	-0,003	-0,004	0,017	0,009	0,011	-0,008	0,015	0,010	-0,004	-0,004
Bayse	0,000	-0,002	-0,003	0,017	0,009	0,012	-0,006	0,016	0,011	-0,002	-0,003
Fer	0,000	-0,005	-0,005	0,016	0,008	0,010	-0,009	0,015	0,010	-0,005	-0,005
Charette	0,000	-0,003	-0,004	0,018	0,009	0,012	-0,007	0,016	0,011	-0,004	-0,004
Rarens	0,000	-0,001	-0,001	0,014	0,008	0,010	-0,004	0,013	0,009	-0,001	-0,002
Ribouyrel	0,000	-0,003	-0,004	0,011	0,005	0,007	-0,006	0,010	0,007	-0,004	-0,004
Roquemaliere	0,000	-0,003	-0,004	0,008	0,003	0,004	-0,005	0,007	0,004	-0,003	-0,004
Rounel	0,000	-0,010	-0,001	0,045	0,024	0,024	-0,014	0,042	0,034	-0,005	-0,011
Bayelle	0,000	-0,026	0,009	0,032	0,013	-0,005	-0,014	0,035	0,040	-0,008	-0,026
Boudic	0,000	-0,051	0,042	0,057	0,025	-0,026	-0,012	0,069	0,092	-0,004	-0,049
Vallat	0,000	-0,018	-0,005	0,047	0,023	0,020	-0,021	0,045	0,036	-0,011	-0,020
Maro	0,000	-0,059	-0,036	0,058	0,015	0,010	-0,064	0,054	0,037	-0,046	-0,062
Saint Martial	0,000	-0,030	0,034	0,055	0,028	-0,005	-0,005	0,063	0,076	0,002	-0,030
Rieutord	0,000	-0,029	0,056	0,054	0,030	-0,017	0,009	0,066	0,092	0,014	-0,027
Tartuguier	0,000	-0,046	-0,032	0,033	0,003	0,001	-0,051	0,030	0,018	-0,039	-0,049
Peyne	0,000	-0,036	0,097	0,024	0,005	-0,018	-0,017	0,029	0,120	-0,012	-0,036

SCALE
1,5
1
0,5
0
-0,05
-0,1
-0,15
-0,18

Abbreviation	**Soil type**
S1	clayey
S2	clayey sand
S3	Sandy
S4	Silty
S5	silty clayey sand
S6	silty clayey
S7	silty sand
S8	silty sandy
S9	silty sandy clay
S10	urban other

4.3.4 Land cover classes

Simulations of the catchment containing only one land cover class, besides the urban area, per model run results in large variation between total discharge responses. Total discharges (after 51,25mm of rain) of the river Peyne, per land cover class are outlined in table 4.9.

Table 4.9: *Land cover classes ranked from largest to smallest total discharges (table continued on following page) .*

Land cover	Runoff (mm)	Runoff ratio (-)	Peak flood (m^3/s)	Tp (timestep)
Urban area	34,50	67,32	63.84	75
Vineyards (high level of soil crusting)	33,75	65,85	59.63	76
Sport and leisure facilities	32,00	62,44	52.99	76
Mineral extraction site	21,83	42,60	33.52	76
Transitional woodland or shrubs	10,75	20,98	11.14	80
Moors and Heathland	7,00	13,66	6.07	77
Coniferous forest	6,83	13,33	5.73	77
Broad leaved forest	6,75	13,17	5.47	78
Original	5,00	9,76	4.03	88
Vineyards	3,08	6,02	2.36	77
Pastures	3,08	6,02	2.07	77
Sclerophyllous vegetation	3,00	5,85	2.03	77
Natural grasslands	3,00	5,85	1.72	85
Complex cultivationpatterns	3,00	5,85	2.00	77
Mixed forest	2,92	5,69	1.93	77
Agriculture and Nature	2,92	5,69	2.04	77

Urban area produces the largest discharge, followed by vineyards, and agriculture and nature provide the least discharge. Urban area delivers the fastest peak discharge at timestep 75, while vineyards deliver at timestep 76. The original catchment layout delivers the slowest peak flood occurring at timestep 88.

L2 (urban areas) and L11 (sport and leisure facilities) caused the largest percentage difference in discharges produced by all subcatchments. The Maro subcatchment produced the highest discharge under the influence of urban areas and sport and leisure facilities with an increase of more than 1500%. Table 4.10 on the following page gives an overview of the percentages of change per subcatchment relative to the discharge under normal parameterisation. As can be observed some sub catchments show larger fluctuations than others. This is mainly due to the 'land cover homogeneity' of each subcatchment under the current conditions (appendix VI).

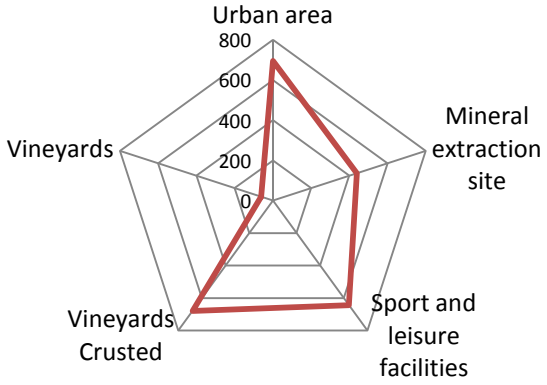

Graph 4.5*: An illustration of the most extreme response is shown in spider diagram format relative to the modelled discharge under normal parameterization(equal to 100%).*

Looking at graph 4.5 it is apparent that urban area and crusted vineyards contribute the largest portion of water to the stream networks total discharge. It needs to be stated that within this scenario several stages of crusting are simulated by increasing the direct runoff fraction which is known to be a simplification of reality.

Table 4.10 *The influence of a changing land cover type on the tributary and total discharge(s)*

	Orig	L2	L7	L11	L15	L18	L20	L21	L23	L24	L25	L26	L27	L28	L29
Mourissou	0	588	328	570	-59	-59	-59	-60	23	25	-60	-59	25	107	108
Levers	0	417	222	404	-69	-69	-69	-70	-7	-6	-70	-69	-6	56	57
Pouzes	0	460	249	446	-66	-67	-67	-67	1	2	-67	-67	2	69	70
Margaride	0	479	261	464	-65	-65	-66	-66	4	5	-66	-66	6	75	76
Bayse	0	444	240	430	-67	-68	-68	-68	-2	-1	-68	-68	-1	64	65
Fer	0	452	245	438	-67	-67	-67	-67	-1	0	-68	-67	1	67	68
Charette	0	454	246	440	-67	-67	-67	-68	-1	0	-68	-67	1	67	68
Font rarens	0	344	177	333	-73	-73	-74	-74	-20	-19	-74	-74	-19	34	35
Ribouyrel	0	342	176	330	-74	-74	-74	-74	-21	-20	-74	-74	-20	33	33
Roquemaliere	0	245	115	236	-79	-79	-80	-80	-38	-38	-80	-80	-37	4	4
Rounel	0	842	488	816	-44	-44	-45	-45	68	70	-45	-44	71	183	185
Bayelle	0	594	338	572	-40	-41	-41	-41	39	40	-41	-41	40	153	121
Boudic	0	658	394	637	0	-1	-1	-1	82	84	-2	-1	84	257	168
Vallat	0	854	497	829	-43	-43	-44	-44	71	73	-44	-44	73	187	189
Maro	0	1584	949	1537	0	-1	-2	-2	200	202	-3	-2	204	405	407
Saint martial	0	741	439	717	-12	-13	-13	-13	82	83	-14	-13	84	242	180
Rieutord	0	436	256	422	-13	-14	-14	-14	43	44	-14	-14	45	196	102
Tartuguier	0	1134	666	1097	-29	-30	-30	-30	116	118	-31	-30	119	265	267
Peyne	0	585	331	565	-37	-38	-38	-38	40	41	-38	-38	41	239	119

Scale

-80

-50

0

300

600

900

1200

1500

Abbreviation	**Landcover**
L2	Urban area
L7	Mineral extraction site
L11	Sport and leisure facilities
L15	Vineyards
L18	Pastures
L20	Complex cultivation patterns
L21	Agiculture and Nature
L23	Broad leaved forest
L24	Coniferous forest
L25	Mixed forest
L26	Natural grasslands
L27	Moors and heatland
L28	Sclerophyllous vegetation
L29	Transitional woodland or shrubs

4.3.5 The flash flood of 1996

During the convective storm of 28th of January 1996 304mm of rain was released within 240 hours over the 120km^2 catchment. LISFLOOD simulates that peak discharges begin travelling downstream from upstream sub catchments at the onset of the intense precipitation event (timestep 148).

Graph 4.6a, 4.6b and 4.6c show respectively the preferential flow, infiltration and soil moisture at outlets of the Levers (upstream), Bayelle (midstream) and Peyne (downstream). Graph 4.6d gives locations of these streams.

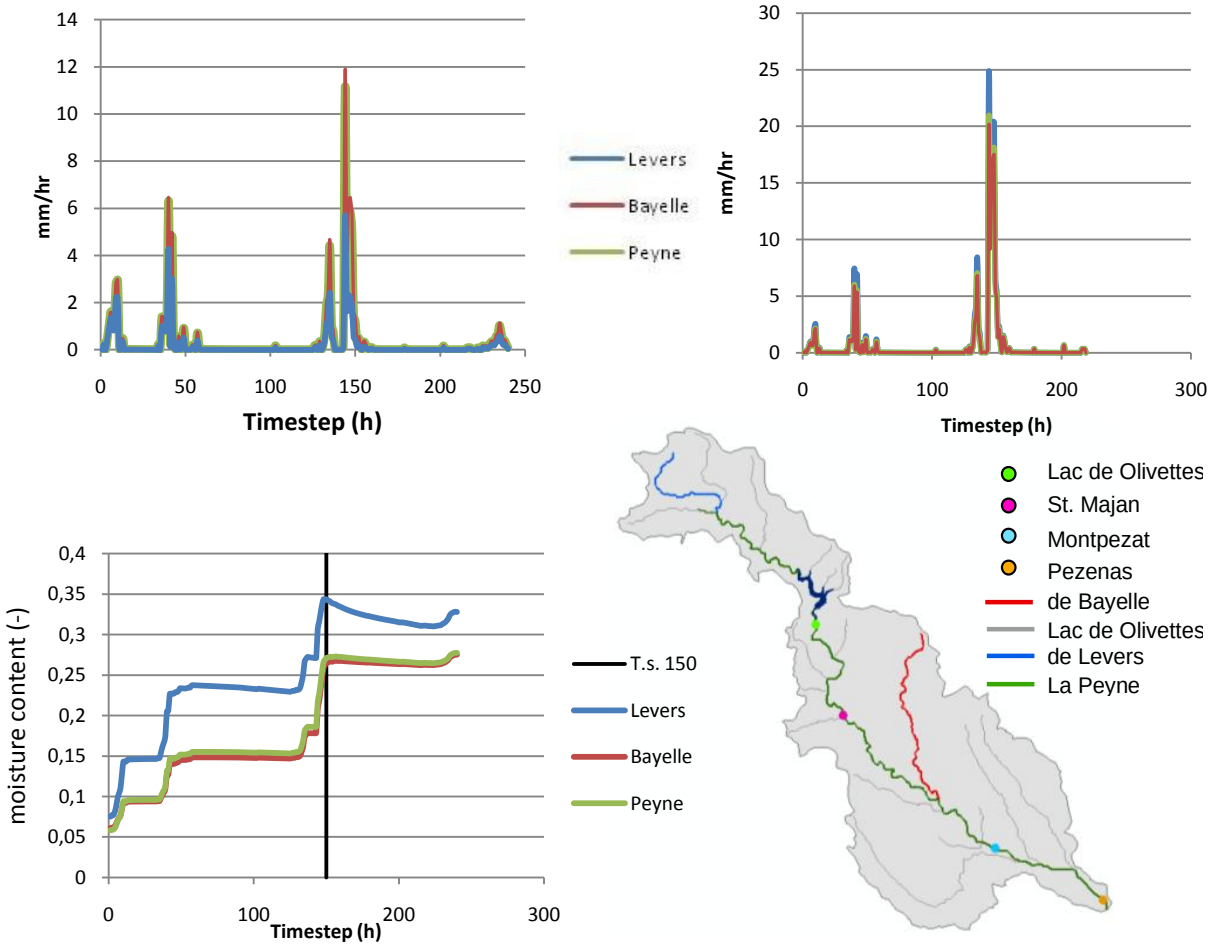

***Graph 4.6**: a) preferential as a function of time during the 1996 event; b) infiltration as a function of time during the 1996 event; c) moisture conditions as function of time during the 1996 event; d) the location of the points of interests*

The soil infiltration and preferential flow reach a maximum at all 3 stream outlets at timestep 148, when intense precipitation occurs, however soil moisture reaches a maximum at timestep 150. This time difference is attributed to the time it takes for the water to infiltrate into the soil profile. The Bayelle and Peyne experience similar moisture contents of 0.26 and 0.27 respectively at timestep 150. However the Levers has acquired a higher soil moisture content of 0.34 due the lower soil storage capacity associated with the areas shallow soil depth and a different texture class as can be seen in appendix II.

The greatest discharge arrives downstream in the vicinity of Pézenas. Accumulation of the peak flows occurs between timestep 148-153 as subcatchment discharges accumulate along the river Peyne as

shown in the propagation diagrams in figure 4.4. These diagrams display the discharges (m^3/s) at the critical timesteps (148 to 153).

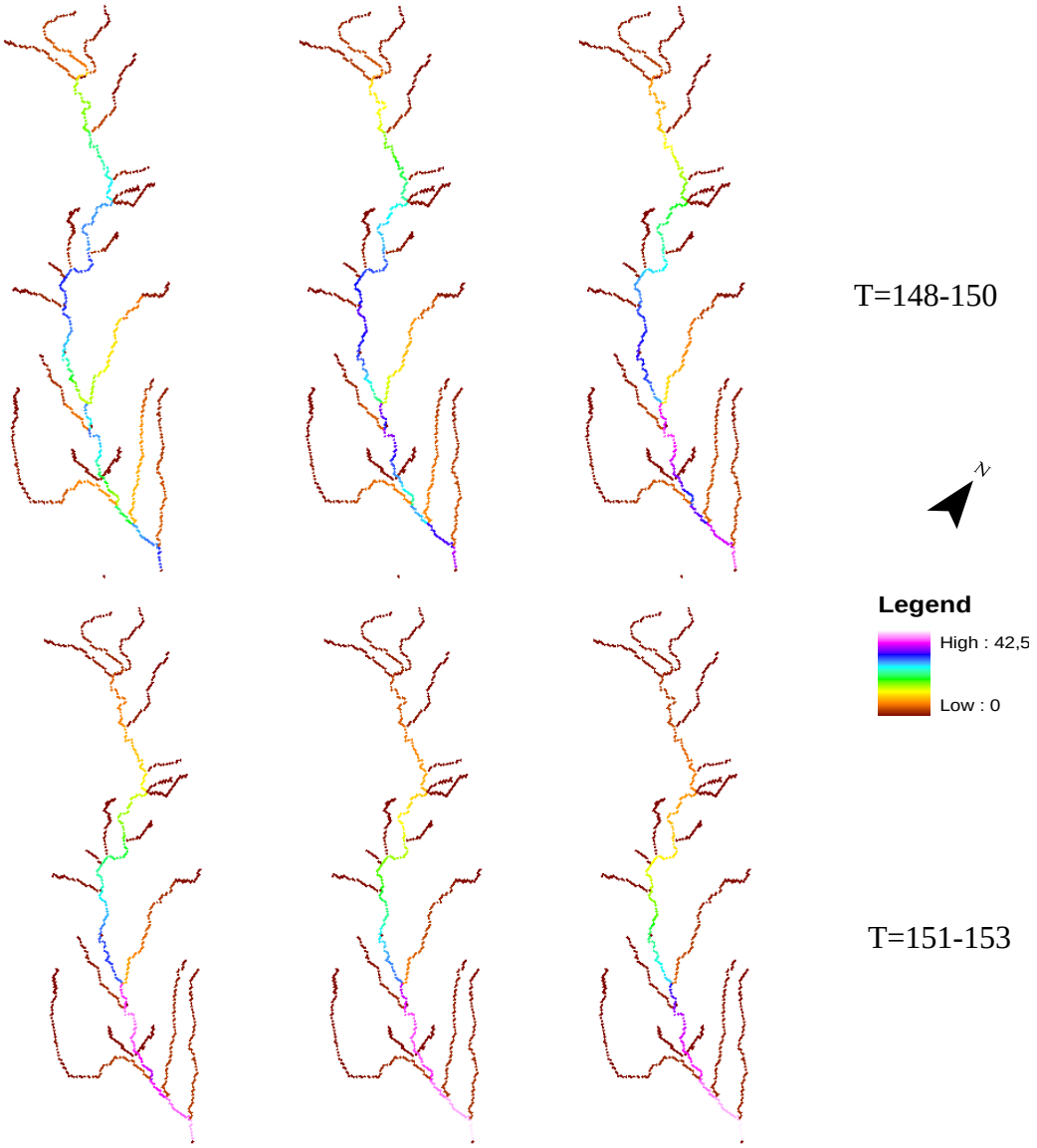

Figure 4.4: *The simulated propagation of discharges through the stream network during the 1996 event*

This peak flow raises water level to 4m which is above the maximum water level facilitated by the river banks of 3.75m (graph 4.7). River banks are consequently breached and Pézenas is experiencing a flood

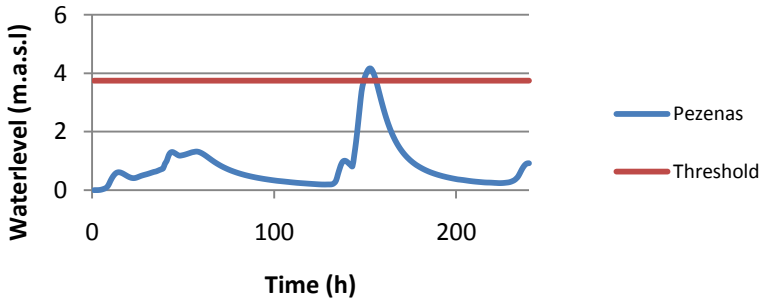

Graph 4.7: *The waterlevel in the Pézenas floodplain during the 1996 event*

4.4 Model behaviour

4.4.1 Preferential flow versus Infiltration

Graph 4.8 shows an inverse relation between infiltration and preferential flow under varying soil moist conditions. The total water entering the soil system stays the same (263.96mm) under dry, field capacity, and wet initial soil moisture contents. The variation lies in the decreasing contribution of infiltration as soil moisture increases and thus soil storage is filling. The simultaneous increase in the contribution of preferential flow has an equalising effect, restricting fluctuation of the total amount of water entering the soil system.

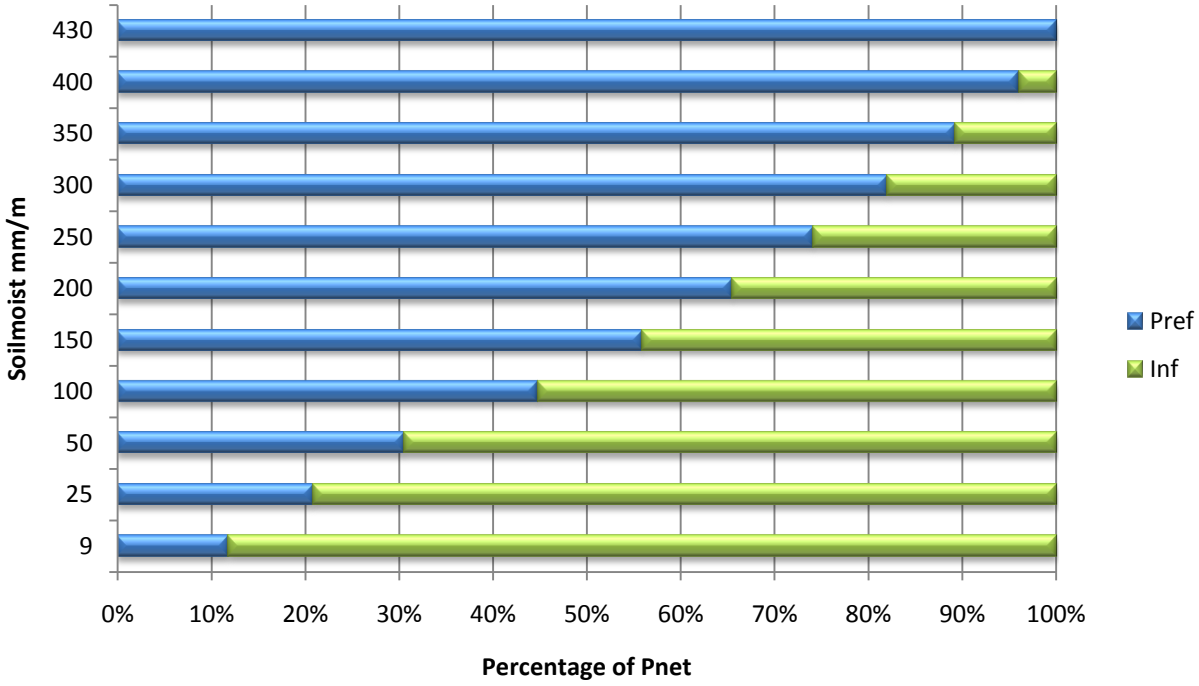

Graph 4.8: *The interaction between preferential flow and infiltration rate under different initial moisture conditions which highly influences and balances the total discharge*

Table 4.10 below briefly compares the model representation of the relation between infiltration and preferential flow with the realistic behaviour observed infield. A negative correlation lies between the two mechanisms within the model representations whereas the reality invokes a fairly positive correlation between the two mechanisms.

Table 4.10: *Infiltration rate and preferential flow behaviour of the LISFLOOD model and the infield observed situation*

	Infiltration	**Preferential flow**	**Total discharge**
Model behaviour			
Dry	High	Low	Same
Wet	Low	High	Same
Infield observed behaviour			
Dry	High	High	Moderate
Wet	Low	Moderate	High

Based on intensive modeling sessions it was thus noted that the 100% net precipitation (minus the direct runoff (fallen on impervious area)) is divided over the preferential flow and infiltration. Only

by using some extreme calibration values, additional surface runoff was generated. The exact proportions of preferential flow versus infiltration depend on the soil moisture content as can be seen in table 4.11:

Table 4.11: *The interaction between preferential flow and infiltration rate under different initial moisture conditions which highly influences and balances the total discharge*

Watercontent (mm)	As (-)	Infpot (mm)	Dpref (mm)	Infact (mm)	Runoff (mm)	PWPF (-)	Beta VIC/ARNO (-)
9	0,00	364,93	9,50	70,50	4,00	0,55	0,15
25	0,01	349,02	16,68	63,32	4,00	0,55	0,15
50	0,02	324,36	24,44	55,56	4,00	0,55	0,15
100	0,04	275,79	35,81	44,19	4,00	0,55	0,15
150	0,06	228,30	44,78	35,22	4,00	0,55	0,15
200	0,09	182,08	52,47	27,53	4,00	0,55	0,15
250	0,12	137,36	59,34	20,66	4,00	0,55	0,15
300	0,16	94,47	65,61	14,39	4,00	0,55	0,15
350	0,22	54,05	71,42	8,58	4,00	0,55	0,15
400	0,33	17,50	76,87	3,13	4,00	0,55	0,15
430	1,00	0,00	80,00	0,00	4,00	0,55	0,15

This implies that no extra water is converted into surface runoff and hence runoff is insensitive to soil moisture conditions. This results in runoff values, completely dependent upon the chosen direct runoff fraction (equation 1 and 2) and is highly arbitrary.

The actual runoff within LISFLOOD is calculated as follows:

$$R_s = R_d\,(1\text{-}fdr)*(W_{av}\text{-}\,D_{pref,gw} - Inf_{act}) \qquad [14]$$

R_s = Surface runoff (mm)
R_d = Direct runoff (mm)
fdr = Fraction impervious area (-)
W_{av} = Available water (mm)
$D_{pref,gw}$ = Preferential flow to groundwater (mm)
Inf_{act} = Actual infiltration (mm)

The potential infiltration is extremely high under dry conditions and decreases under wetter conditions. These extreme values are calculated using the following equations based on the VIC/ARNO scheme:

$$Inf_{pot} = \frac{W_{s1}}{b+1} - \frac{W_{s1}}{b+1}\left[\,1 - (1 - A_s)^{\frac{b+1}{b}}\,\right] \qquad [15]$$

Within this formula the saturated fraction of the cell is calculated as follows:

$$As = 1\text{-}\,(1\text{-}\frac{W_1}{W_{s1}})b \qquad [16]$$

Inf_{pot} = Potential infiltration (mm)
W_{s1} = Saturated watercontent (mm)

W_1 = Actual watercontent (mm)
b =empirical shape parameter (-)
A_s = Saturated fraction of the cell

The actual infiltration is then calculated by subtracting the preferential flow of the available water. The fraction of the available water converted to preferential flow depends on the soil moisture of the soil. The following equations show that preferential flow increases when the soil becomes more moist. Remarkable is the suggestion that under saturated conditions the complete available water is converted into preferential flow (W1/Ws1 becomes 1):

$$D_{pref,\,gw} = W_{av} \left(\frac{W_1}{W_{s1}}\right) C_{pref} \qquad [17]$$

W_{av} = Available water (mm)
W_1 = Actual soil moist
W_{s1} = Saturated soil moist
C_{pref} = Calibration parameters

The soil interaction is in this sense underestimated in the model on these small time scales. It was expected that this would partly be counteracted by the subsurface flow from the upper zone, Quz. The formula for flow from the upper zone would imply a reasonable outflow (even on an hourly basis) depending on the moisture status of the soil, nevertheless no nameworhty outflows where observed in the model output neither under dry or wet conditions.
The following formula is used by LISFLOOD to calculate the upper zone outflow to the stream network:

$$Q_{uz} = 1/T_{uz} * UZ_{\Delta t} \qquad [18]$$

Q_{uz} = Outflow upperzone to streamnetwork (mm)
T_{uz} = Timezone constant (days)
$UZ_{\Delta t}$ =Watercontent in upperzone (mm)

4.4.2 Equifinality

Looking at table 4.12 it is apparent that a wide range of calibration parameter values result in a satisfying Nash Sutcliff value of >0.8 (83%). For example: a Nash Sutcliff of 0.8 can be reached with a CCM value of 4.16 or 9 within the same calibration run, implying the presence of equifinality when the model is ran on an hourly timescale.

Table 4.12: *The frequency of Nash Sutcliffe values generated by NIMBUS*

Nash Sutcliff	Frequency	Fraction (%)	Cumulative (%)
0,1	18	3,43	3,44
0,2	1	0,19	3,63
0,3	3	0,57	4,20
0,4	7	1,34	5,53
0,5	11	2,10	7,63
0,6	17	3,24	10,88
0,7	20	3,82	14,69
0,8	63	12,02	26,72
0,9	384	73,28	100
More	0	0	0
Total	524	100	100

5. Discussion

5.1 The catchment response to Mediterranean precipitation

The objective of this project was to understand the mechanisms of runoff generation within the Peyne catchment. Data was collated from infield measurements within the study area and a calibrated model was established based upon LISFLOOD. Using these resources, scenarios of changing landcover, soil type and rainfall intensities were simulated. Overall this modelling exercise was successful in identifying the source areas and the primary mechanisms involved in creating the flash floods in the Peyne catchment. The Curve Number method, which is a coarse estimate method to calculate the peak flow and source areas, had a similar result for time to peak of flood yet produced overestimated total discharge values. (Backwell & Bijkerk, 2009 b). The benefit of using LISFLOOD over using the less labour intensive Curve Number method, is that it gives not only the discharge and the status of the peak flows but also provides insight into the dynamics of runoff generation mechanisms and an appreciation of the most important parameter interactions. (please refer to appendix XXI)

Hortonian overland flow is the most important runoff generating mechanism within this catchment. The inability of a surfaces infiltration capacity to absorb the net precipitation falling, results in water ponding or mobilising along flow paths towards the stream network. Paved areas, vineyards and soils with a low hydraulic conductivity such as that in figure 5.1 b (no subsurface flow indicating high hortonian runoff) are all locations in which this mechanism is highly active.

One known buffer to such runoff generating processes is the reservoir at Lac des Olivettes. The aim of the lake was to minimise the intensities of peak flows.

Figure 5.1: *a) A flooded vineyard observed on the 21st of October during the fieldwork (X: 525048; Y: 4820707)*
b) Runoff flowing into the Peyne where no water was discharged through the drainpipe

It was originally hypothesised that hazardous runoff generation would occur due to a combination of crust development on bare vineyard soils after the first post summer intense rain events. This would result in high volumes of Hortonian excess runoff from the vineyards, which would run into local streams but also into other agricultural land causing Dunnian saturation excess flow and eventually drain into the local stream network. (Weng, 2008) Model outcomes show that dominant source areas for runoff generation lie within land use classes containing a high impervious fraction. This is in accordance with the preset model values of impervious fractions per landuse class, in which urban area and crusted vineyards have the highest direct runoff fraction.

Large differences were found between the tributary discharges and this is due to the topographical characteristics of their subcatchments. For instance, The Bayelle, Rieutord and St. Martial tributaries deliver the highest discharges to the river Peyne. The Bayelle catchment has a high

spatial coverage by urban area and vineyards which have the highest direct runoff fraction of all land cover classes. The Rieutord has a steep topography in its subcatchment which is represented in the LISFLOOD input map of elevation ranges and the directions of the local drainage direction map. The St. Martial is the longest tributary and therefore receives a larger quantity of runoff from the local land which has high vineyard coverage.

A non linear relation found between tributary length and discharge highlights the important role of land cover, soil properties and topographical characteristics in the formation of flash floods. Simulations ran for a single land coverage for the entire catchment gave no clear trend related solely to land cover class, and therefore the existence of other influential factors is evident (I.e. soil properties, and local elevation ranges). A minor trend is apparent in simulated discharges and does hold a relation with land cover. The trend found between tributary length and total discharges is largely related to direct runoff fractions which range from 0.05 to 0.8 within this catchment.
The rain events at the beginning of the rain season in September and October are usually shorter in duration and more intense than the longer lasting rain events of the latter part of the rain season in January/February. It is as the rain events become longer that the soil reaches true saturation and finally the reservoir reaches maximum capacity. Therefore it is apparent that it is not the intensity of the rain event that is highly influential to discharge of this reservoir, but rather the longevity of the rain event, the antecedent soil conditions of subcatchments and the capacity of the reservoir at the time of rainfall.

The post modelling mass balance calculations carried out to compensate for this absence of reservoir activity indicated that the capacity of the reservoir is in fact sufficient in terms of its location and capacity, but that behaviour of the dam does not efficiently maintain a relatively consistent water level within the reservoir. Calculations and infield observations, show that at the onset of the rain season the reservoir is not at full capacity. Over time the water level rises as the reservoir fills with input from the upper part of the catchment and overlying rain events. It is when the water level in the reservoir reaches the threshold of the $22m^3/s$ spillway that the behaviour of the reservoir changes and becomes a hazard to the downstream area. Activations of this spill implies that the reservoir has reached its buffering capacity as it can no longer store the upstream discharge. The water is then released into the Peyne at $22m^3/s$ which is equivalent to recorded flooding discharges (Devez, 2004). Thus if the reservoir inflow is faster than $22m^3/s$, the water level will rise past the activated spillway and reach the next threshold at 166.5m which discharges maximum $290m^3/s$, inevitably causing a destructive flash flood.

5.2 Factors influencing model outcomes

The modelling process was successful in terms of gaining insight into catchment behaviour and runoff mechanisms, However it is not sufficient to investigate accurate flash flood predictions. Reasons are as follows:

Meteorological data used for this modelling exercise was relatively coarse and short in time length due to the resolution of the data acquired and downtime of meteorological measuring stations. This provided a lower resolution of seasonal data and the behaviour of the rainfall in the area, which increased overall model error, reduced the length of sound data strings upon which the model can run and reduced the overall resolution of the model. Another important point to mention is that discharge data is not available at the outlet (Pézenas) and to have access to such data would certainly increase the accuracy of the model as actual discharge at Pézenas could be used to calibrate and validate the model.

Nevertheless, the calibration was carried out using NIMBUS on two rainfall events within the month of February. These rain events were chosen as they were both recorded without any absence of

data and they both lie within the same season (thus no uncertainty due to seasonal changes). Numerous calibration runs were performed to define an optimum set of calibrated parameters. The calibrated parameters that were settled upon were created by running a NIMBUS calibration which gave considerably optimum values, followed by manually altering the CCM values before validation. The alteration was made with guidance from observing the results of previous calibrations. The final validation gave stable results as the objective function remained very similar to those of the original calibration run. (Pannemans, 2008)

To gain insight into the reliability of the model outcome, it is a priority to investigate the variance of the input parameters on the model outcomes. A sensitivity analysis was carried out to define the most sensitive parameters and ultimately the potential pathways for error propagation. From the sensitivity analysis it is apparent that CCM (calibrated multiplier assigned to stream bed roughness), and DRF (direct runoff fraction) are the parameters most sensitive within the model. Spatial heterogeneity within each land cover class is known to be high. The larger the heterogeneity of the stream bed, the larger potential error associated with the time to peak of flow. It has been noted that a slight change in DRF results in a significant increase in discharge. However, the heterogeneity of direct runoff fraction values within one class shows less variance over the entire catchment than that of the CCM. IT is therefore expected that the main error propagated throughout the model is a result of CCM rather than DRF.

Due to the fact that one value is assigned to a single soil texture class, the associated variance of this value will be high. However because of the issue of the perfect inverse relation between infiltration and preferential flow, kSat does not influence the total discharge on used model timescales and hence in this case, the effect of kSat variance is negligible.
Manning's N is a parameter that the model is slightly sensitive to (relative to the sensitivity of other parameters). However the observed variance within the field observations of mannings N is within such a range that the differences of model outcomes based on various mannings N values, are less than 1%, relative to the original model outcome.

Of all LISFLOOD calibrations, 83% finished with Nash Sutcliffe values of 0.8 or higher indicating the presence of equifinality within the model when it runs on an hourly timescale. This is a phenomenon in which many different model representations can be consistent with the realistic measurements of one specific scenario. Allowing an uncertainty level with which the model can predict will result in many acceptable models to describe a single reality. (Beven, 2006) The main reason for this to occur is over-parameterisation due to the complexity of the scenario being simulated, but also due to errors that propagate throughout the model simulations which consequently produce different parameter values during the calibration. LISFLOOD has many parameters and upon commencing the modelling phase, little prior knowledge was acquired regarding inherent model error and error associated with using an exceptionally small catchment. (Beven et al, 2006 & Van der Knijf , Roo (2008b))

The Dynamic wave of the St. Venant equations is incorporated within LISFLOOD, but in this case we restricted the type of flow to steady state uniform flow (kinematic wave approximation). The use of the kinematic wave causes an underestimation of the calculated discharges (and hence water height).

The bridges in Pézenas, which cross the concrete floodplain of the Peyne, were not included in the model due to model resolution limitations. Due to the omission of the bridges the simulated water levels are expected to be underestimated because of damming up by debris. From first hand observations of a flash flood event (21st of October 2009) it can be concluded that the water level, in the concrete floodplain crossing Pézenas, changes from the 25cm ditch into a 30m wide river within

the time span of a few hours (figure 5.2a &5.2b). The water flow at Pézenas happens with moderate to high velocities (please refer to video 21_10.mp4 included on the data DVD).
This flow transports much debris from forested upstream areas such as the sub catchments of the Rieutord and Tartiguier. These two tributaries are known for their debris contribution as they pass through mixed and broad leaved forested areas (appendix 3 & 4). During flood events the pillars supporting the bridge and the bridge itself act as debris blockages (figure 5.2c).

Figure 5.2: *a) The concrete floodplain with the Peyne centered in a 25cm wide ditch under normal conditions (18 September 2009); b) The concrete floodplain during a minor flash flood (21st October 2009); c) One of the bridges in the Pézenas floodplain acting as an obstacle for flooding debris during a minor flash flood (21s October 2009)*

One of these bridges the 'Pont du Peyne' at Pézenas (were the D39 crosses the Peyne) is of specific interest in this issue (figure 5.3). Due to its low height it restricts river flow causing build up of water and eventually a breach of the river banks. No exact dimensions were measured during the field campaign, however it is estimated using Google Earth (Google Maps, 2010) that the vertical area through which water can flow, is approximately 62m^2. Further analysis of this bridge may help explain the local factors involved in the flooding that occurs specifically in the centre of Pézenas.

Figure 5.3: *Pont du Peyne crossing the concrete floodplain in Pézenas (Janberg, 2010)*

Caution was taken in interpreting the modelled discharges as it is considered that LISFLOOD has misplaced a portion of the water that is discharged from the Rieutord. Rather than being created in the subcatchment of the Rieutord (as in the model), it is thought that the discharge should be created in the neighbouring Tartiguier subcatchment. This belief stems from field observation of both rivers, their relative channel dimensions and also from local inhabitants stating that the discharge coming from the upstream Tartiguier heightens flood risk of Pézenas. No changes were

made to the model to rectify this as it was not found to affect the overall water balance and formation of floods in the model simulations.

Other points of caution reported during this modelling phase are:
All tributaries deliver peak discharge to the Peyne at the same timestep which is not realistic. One remark to be made about this is in relation to LISFLOODs technique of routing subsurface runoff. All water outflow from the upper and lower groundwater zones is routed within the same timestep to the closest pixel identified as a river pixel. This implies the treatment of near stream pixels as spatially lumped units (van der Knijf et al., 2008a) and increases the speed of subsurface flow for all cells that are not direct neighbours of a river cell. This can potentially create a scenario in which tributaries appear more similar to one another in terms of length and travel times, than exists in reality. (van der Knijf et al., 2008a). However in this scenario the groundwater outflow amounts are so small that they hardly have a significant effect on the water amounts reaching the river per time step.

Within LISFLOOD, vineyards with soil crusts are different to non crusted vineyards due to changes in the direct runoff fraction parameter only. In reality the lack of infiltration due to crusting can be counteracted by the existence of macropores and cracks in the soil which have not closed over during precipitation events (refer to Appendix XV). It is at these locations that vertical and horizontal Infiltration will occur and could potentially supply the dry soil below the crusts with an amount of moisture.

Also raised was the question of the effect of heterogeneity within the model. Manning's n related to surface roughness, is one such topographical characteristic that holds strong relation with the timing of peak discharge. The magnitude and timing of peak flow is dependent upon manning's n which varies per land cover class i.e. a larger manning's n value lengthens time to peak, reduces peak intensity and lengthens the time of the peaks duration. However it is apparent that although surface roughness itself has a strong effect on timing of peak flow, increased spatial variation of surface roughness has a stronger effect in increasing time to peak. This can be concluded from the land cover scenario which was run with the model. The model run with the original land cover resulted in the longest (less extreme) peak flow relative to the runs with a single land cover class. This might imply that the current calculated values are still an overestimation. As stated above a more heterogenic cover influences the peak flow. Under the current model settings there is no heterogeneity within the land cover classes. This is not in line with reality where especially in vineyards large heterogeneity was observed.

5.3 The model

LISFLOOD is suitable for small catchments such as the 120km^2 catchment of the Peyne used in this research, however its suitability depends upon the purpose simulations are intended for. Once calibrated the model can give reliable results, however the detail of the catchments mechanisms, such as Hortonian and Dunnian overland flow, used in forming such floods at high resolution is not well defined. This model in combination with a higher resolution model which shows processes at field scale, would provide a more robust analysis of the scenario in hand.

The temporal resolution of the model is an important consideration for such a hydrological model. LISFLOOD is originally intended to model at a daily time scale which is acceptable for such large European catchments where the detail of high resolution is less important to understand the catchment dynamics. However for a catchment as small as 120km^2 the travel times of peak waves are in hours rather than days and response of the model to interactions of parameters will become apparent in a shorter period of time (Ruin et al., 2008). Therefore the time step for such small catchments should be on an hourly basis which requires all input data to have an hourly resolution.

If one is modelling hourly time steps using LISFLOOD as done in this research, the modeller should be especially conscious of the units of parameters used in calculations when using the NIMBUS application. The RMSE and hence the rRMSE are based on the mass balance which is by default calculated on a daily basis. Adaptations in the mass balance python file are necessary to compensate for this in order to avoid overestimation of the RMSE. (Pannemans, 2008)

A restriction within the LISFLOOD model is its insensitivity to soil processes due to the inverse relation between infiltration and preferential flow. It is known that LISFLOOD's preferential flow mechanism is a simplification in which preferential flow increases as infiltration decreases, maintaining a constant rate of soil water flow. Thus no water from precipitation becomes surface runoff under normal calibration values. This model behaviour is apparent during soil type scenario runs in which there was little to no variation observed in the calculated surface runoff between soil types. This is supported by the models insensitivity to change in soil moisture content represented by parameter 'Theta initial'. Theta Initial does affect the infiltration and preferential flow mechanisms, however as these two parameter always account for 100% of net precipitation, theta Initial therefore does not influence the total discharge. It is possible that this insensitivity is related to running the model on an hourly timescale, and it is expected that this characteristic run on a daily timescale holds a less prominent influence. Therefore caution should be taken when running the model on an hourly timescale.
A preferable scenario for this catchment is a relatively positive correlation in which preferential flow decreases as infiltration decreases and surface runoff increases. This would provide a more realistic representation of the reality and is supported by the inverse relation between infiltration and runoff production.
The dependency on such accurate direct runoff fractions highly reduces the flexibility and applicability of this calibrated model on other catchments. It also gives opportunity for considerable model error to arise, as an overestimation in direct runoff fraction will result in an overestimation in runoff generated in an area. In the case of the modelling efforts within this research, realistic direct runoff values were obtained through infield observations.

A second restriction within this study is the lack of reservoir activity due to the insufficient representation of the dam behaviour. This can be perceived as either the absence of the reservoir entirely or that the reservoir is at full capacity and thus has no more buffering capability. Based on a mass balance, it was estimated that the lake level at the time of calibration was at the $22m^3/s$ spillway threshold (i.e. the lake was not completely full). This implies all water coming from the upstream area, until the threshold of $22m^3/s$ will not become retained within the reservoir (as the water does not enter the lake faster than the rate of $22m^3/s$).

The results of this study reject the initial hypothesis that the reservoir is insufficient to satisfactorily minimise flood risk, as there have been 5 destructive floods in the last 25 years. In fact under the current management regime, the reservoir is accepting of all discharge from north of the reservoir in summer, releasing only a baseflow of less than or equal to 50l/s in the summer months and up to 50l/s in the early part of rain season when the rain events are most intense. This means that all water that occurs south of the dam during this time is essentially created by that area itself and not received by that area from above. However, further into the rain season the reservoir reaches full capacity at the threshold of the baseflow rate, thus any new input of water into the reservoir will be released directly through the dam into the river Peyne at the higher flow rate of $22m^3/s$. Based on this passive method of dam management, the timing of this $22m^3/s$ input has a considerable affect on the flood risk of the catchment during the winter season, when rain events are less intense but rather longer lasting. It is therefore not reservoir characteristics that are insufficient but rather the management of the reservoir is not optimum.

6. Conclusion

This study has explored the sources of flash floods in the Peyne catchment, a catchment vulnerable to intense Mediterranean precipitation and anthropogenic alterations to the natural landscape. LISFLOOD modelling of the catchment scenario gave insight into the catchment mechanisms of surface runoff production and solutions to why Pézenas is a hotspot of flooding.

From precipitation data it can be said that the rain season begins with short intense rain events and ends with less intense longer duration rain events. During rain events the time to peak of flows in this catchment is approximately 5 hours for all tributaries, according to LISFLOOD. Variations from this are largely related to heterogeneity of land cover within subcatchments. The largest contributing tribuatries are the Bayele, Rieutord and the St. Martial, due to land cover, topography and spatial length respectively. Land with high impervious fractions are dominant source areas of surface runoff. In this catchment, urban area and crusted vineyards generate the largest surface runoff of all land cover classes. Vineyards cover 53% of the catchment, however only a portion of that is crusted. Soil properties such as soil storage, infiltration, and local elevation ranges are found to influence the variation within areas of the same land cover. In the case of vineyards without crusting and other land covers with lower impervious fractions (e.g. agriculture), their significant contributions to surface runoff will occur only when soil reaches saturation and hence Dunnian excess overland flow occurs. This explains flash flood occurance throughout the catchment and within Pézenas in winter. This rejects the original hypothesis that the timing of flash floods occurred upon soil crust formation after the intense first events of the rain season in autumn. The model also confirms that due to canopy interception and higher infiltration capacities (including macropores), true forested areas will contribute a much lower amount of runoff than urban or vineyard areas. However in reality, the northern forested catchment area has a significant proportion of area that consists of impervious bare rock outcrops, which would counteract the modest surface runoff of the forest. Information kindly supplied by Conseil Général d'Hérault, such as details of the event on 28th January 1996 during which 106m^3/s of water entered the lake and only 42m^3/s left, accompanied by the calculated reservoir behaviour of Lac des Olivettes, results in the conclusion, that the reservoir is in fact large enough to efficiently receive all incoming water peak flow volumes from the north of the catchment. This provides a facility to buffer the peak flows, however outflow of 42m^3/s is still capable of causing significant flooding downstream. Ultimately however, it is the timing of release of the stored water that is not efficient, as it does not allow the lake to empty fast enough once it has reached maximum capacity, in order to create new storage before the next event. This can only be ensured by use of specific management techniques.

The LISFLOOD model is suitable for use on a small scale catchment such as 120km^2, which is 10 times smaller than the smallest documented catchment tested within LISFLOOD. (Everhardus 2002). However, caution should be taken when interpreting output. The most prominent challenge faced relates to changes of the temporal resolution within the calibration software, NIMBUS.

Meteorological data used for this modelling exercise was relatively coarse and short in time length providing a lower resolution of seasonal data and the behaviour of the rainfall in the area, which increased overall model error, reduced the length of sound data strings

The insensitive behaviour of the model to infiltration and preferential flow implies that the model underestimates the influence of subsurface flow on the short timescales. As observed during the field campaign this process plays an important role during the extreme precipitation events.

Management recommendations

A preferable management alternative could be performed through observation of local meteorological centre weather predictions and during times of dry spells, water could be released via

manual control of the dam in order to lower the water level in the dam. To allow release of the reservoir water at the higher flow rate of 22m^3/s during drier times would create more reservoir storage for the rainfall during the latter part of rain season. This would preserve a low outflow from the reservoir in times when the banks of the river Peyne are under most pressure due to direct rainfall input, local saturation excess runoff and high tributary discharges in the lower part of the catchment. An additional benefit of such management would be that channel roughness would be maintained at a minimum as a constant flow of water through the channel would reduce the vegetation growth observed in the channels during the field work campaign. The water released during these drier spells could also be considered as irrigation water to the agriculture of the lower part of the catchment.

7. Further Research

In addition to the data acquired during this research project, many new potential sources of data and information were discovered which could greatly benefit higher accuracy modelling and further research in the following areas:

- To acquire a full clarification of the behaviour of the Barrage des Olivettes. Although it is assumed that the dam is passive for this project, it is known that there is a manual control option only used in times of scheduled maintenance of the lake. The possibility of using this manual control to empty the lake during drier spells could be investigated.
- To clarify the true configuration of water volumes discharged by the Tartiguier and the Rieutord subcatchments.
- To investigate the difference in catchment response to the same inputs using the dynamic wave rather than the kinematic wave.
- To perform a detailed field scale analysis of the interaction between soil crusting and water entering the upper soil layer (i.e. vertical and horizontal infiltration, preferential flow and macropores)
- To analyse the influence of heterogeneity of topographical properties on the timing and intensity of flood peaks within the catchment. And to analyse the transferability of optimal parameters across the spatial and temporal scales.
- To calibrate upon a longer time period. A possible calibration technique could be a cross correlation based on two data sets of summer and winter seasons. This would ensure representation of the variation in catchment response through the seasons.
- To describe a more efficient method of calibrating LISFLOOD upon more than one objective function within NIMBUS.
- To perform an analysis on the prominent sources of model uncertainty and investigating the effects of an increase/decrease of parameterisation on the model error.

8. References

Antoinne, J. M., Desailly, B., Gazelle, F. (2001). Les Crues Meurtrières, du Rousillon aux Cévennes. Annales de Géographie, vol. 110, (622), pp. 597-623 (2001).

Backwell & Bijkerk. (2009 a). A Literature Review. Flash Floods- Why at Pézenas.Universiteit Utrecht.

Backwell & Bijkerk. (2009 b).Defining sources areas in the Peyne Catchment- A curve number Quick scan. Universiteit Utrecht.

Beven, K. (2006). A Manifest for the Equifinality Thesis. Journal of Hydrology. Vol 320 pp. 18-36 (2006).

Bonfils, P. (1993). Carte Pédologique de la France 1:100 000; Feuille Lodève. INRA, Olivet

Borga M, Gaume E, Creutin JD, Marchi L. (2008). Surveying flash flood response: gauging the ungauged extremes. Hydrological Processes vol. 22 (18), pp.3883-3885 (2008).

Bulcock , H. H., Jewitt, G. P. W. (2010). Spatial mapping of leaf area index using hyperspectral remote sensing for hydrological applications with a particular focus on canopy interception. Hydrol. Earth Syst. Sci., 14, 383–392 (2010).

Collier, C. (2007). Flash Flood Forecasting: What are the limits of predictability? Q.J.RM.S., 133, 622A, 3–23 (2007).

Conseil Géneral d'Hérault. (2010 a). Barrage des Olivettes. Commune de Vailhan (34.230). Présentation Géneral de l' ouvrage. Pôle environnement, eau
cadre de vie et aménagement rural (Received March 2010).

Conseil Géneral d'Hérault. (2010 b). Caracteristiques de l'ouvrage et de son dispositif d'auscultation. Pôle environnement, eau cadre de vie et aménagement rural (Received March 2010).

Conseil Géneral d'Hérault. (2010 c). Les Olivettes en chiffres. Pôle environnement, eau cadre de vie et aménagement rural (Received March 2010).

Conseil Géneral d'Hérault. (2010 d). Présentation du barrage. Pôle environnement, eau
cadre de vie et aménagement rural (Received March 2010).

Corine. (2006). http://www.eea.europa.eu. (Last accessed November 2009).

Creutin, J. D. and Borga, M. (2003). Radar Hydrology modifies the monitoring of flash flood hazard, Hydrological processes, 17(7), 1453–1456 (2003).

De Jong, S., Addink, E., van Beek, R., Duisings D. (2009). Mapping of soil surface crusts using airborne hyperspectral HyMap imagery in a Mediterranean environment. Anais XIV Simpósio Brasileiro de Sensoriamento Remoto, Natal, Brasil, 25-30 April 2009, INPE, pp. 7725-7732.

De Roo, A., Schmuck, G., Perdigao, V., Thielan, J. (2002).The influence of historic land use changes and future planned land use scenarios on floods in the Oder catchment. Physics and Chemistry of the Earth, Parts A/B/C, Vol. 28, Issues 33-36, Pages 1291-1300 (2003).

Devez, A. (2004). These- Caractrisation des Risques Induits par les Activites Agricoles sur les Ecosystemes Aquatiques. Ecole Nationale du genie Rual, des Eaux et des Forets. Unite Mixte de Recherche no. 5569 (2004).

Diren Languedoc Roussillon. (2007). Atlas des Zone Inondables sur le Basin Versant de l'Hérault. http://www.languedoc-roussillon.ecologie.gouv.fr/zi/hydrogeomorphologie/Hérault/CDROM/fichiers/Rapport_AZI_Hérault.pdf (Last accessed, April 2010).

Drobinsky P., Ducrocq V. (2008). Towards a major field experiment in 2010-2020; HyMeX: Hydrological cycle in Mediterranean Experiment (draft version 1.3.2) http://www.hymex.org/global/documents/WB_1.3.2.pdf (Last accessed May 2010).

Duan, Q.Y., Guptal, V.K., Sorooshian, S. (1993). Shuffled complex evolution approach for effective and efficient global minimization. Journal of Optimization Theory and Applications, Vol. 76 (3), pp. 501-521 (1993).

Duijsings, D. (2008). Physical Characterization and Spectral Response of soil surface crusts in the Peyne Area, fr. Department Physical Geography, Faculty Geosciences, Universiteit Utrecht. Chapter 4.5, pp. 25 (2008).

ECMWF (European Centre for Medium Range Weather Forecasts). (2010). http://www.ecmwf.int/services/archive/ (Last accessed February 2010).

Eijkelkamp. (2010). http://www.eijkelkamp.com/Products/Catalogueseсtion/tabid/76/CategoryID/17/List/1/Level/a/ProductID/72/Default.aspx (Last accessed April 2010).

Everhardus, C., de Roo, A., de Jong, S. (2002). Validation of the LISFLOOD runoff model for a mountainous catchment. Report of the European Commission, Joint Research Centre, EUR 20514 EN (2002).

Farrel. (2010). http://www.usyd.edu.au/agric/web04/Single%20ring% 20final.htm# (Last accessed March 2010).

Feyen L., Vrugt J.A., O´ Nualláin B., van der Knijf J., de Roo A. (2007). Parameter optimisation and uncertainty assessment for large-scale streamflow simulation with the LISFLOOD model; Journal of Hydrology vol. 332, pp 276– 289 (2007).

Gaume, E., Livet, M., Desbordes, M. & Villeneuve, J. P. (2004). Hydrological analysis of the river Aude, France, flash flood on 12 and 13 November 1999. J. Hydrol. 286, 135-154 (2004).

Gaume, E. (2006). Post Flash-flood Investigations Methodological Note; Report Number T23-06-02, Floodsite (2006).

Gaume, E., Bain, V., Bernardara, P., Newinger, O., Barbuc, M., Bateman A., Blaškovicˇová, L., Blöschl, G., Borga, M., Dumitrescu, A., Daliakopoulos, I., Garcia, J., Irimescu, A., Kohnova, S., Koutroulis, A,. Marchi, L., Matreata, S., Medina, V., Precis, E., Sempere-Torres, D., Stancalie, g., Szolgay, J., Tsanis, I., Velasco, D., Viglione, A. (2009). A compilation of data on European Flash Floods. Journal of Hydrology 367, pp. 70–78 (2009).

Gilley, J. E., Kottwitz, E.R. (1995). Randomn Roughness Assessment by the Pin and chain method. American Society of Agricultural Engineers, Vol. 12 (1) pp. 39-43 (1995).
Giraud E. P., Negrel P. (2007). Geochemical flood deconvolution in a Mediterranean catchment (Hérault, France) by Sr isotopes, major and trace elements; Journal of Hydrology vol. 337, pp. 224–241 (2007).

Gomez, J. A., Van der Linden, K., Nearing, M. A. (2005). Spatial variability of surface roughness and hydraulic conductivity after disk tillage: implications for runoff variability. Journal of Hydrology. Vol. 311, pp.143-156 (2005).

Google Maps. (2010). http://maps.google.nl/maps?hl=nl&tab=wl (Last accessed March 2010).

Gruntfest E. Handmer J. (2001). Coping with flash floods NATO Science Series; 2. Environmental Security, Vol. 77 (2001).

Hager W., Hager K., (1985) Application Limits forthe Kinematic Wave Approximation; Nordic Hydrology, vol 16, pp 203-212

Hillel, D. (2004). Introduction to environmental soil physics. Elsevier/Acad. Press, San Diego, CA. pp. 494 (2004).

Horton, R.E. (1933). The role of infiltration in the hydrologic cycle. EOS, Transaction, American Geophysical union (1933).

Huet, P., Martin, X., Prime, J.-L., Foin, P., Laurain, C., and Cannard, P. (2003). Retour d'experience des crues de septembre 2002 dans les d´epartements du Gard, de l'Hérault, du Vaucluse, des Bouches-du-Rhone, de l'Ard`eche et de la Drome. Technical report, Minist`ere de l'Ecologie et du D´eveloppement Durable, R´epublique Française, 133 pp (2003).

HYDRATE. (2010). http://www.hydrate.tesaf.unipd.it/ (Last accessed April 2010).

International association for hydrological sciences, (1974). Flash-floods, proceedings of the Paris symposium, September 1974, IAHS-UNESCO-WMO, Publication 112.

Janberg, N, (2010). ICS. http://fr.structurae.de/structures/data/index.cfm?ID=s0040486) (Last accessed April 2010).

JDSU. (2010). http://www.jdsu.com/product-literature/FDRdefine.pdf. (Last accessed June 2010).

Leerwiki (2010) www.leerwiki.nl (last accessed June 2010)

Meteopassion (2010) www.meteopassion (last accessed June 2010)

Midi-France. (2010). http://www.languedoc-france.info/1114_mediterranean.htm (Last accessed April 2010).

OMERE (Observatoire Méditerranéen de l'Environnement Rural et de l'Eau). (2009). http://www.umr-lisah.fr/omere/ (Last accessed December 2009).

Pannemans, B. (2008). NIMBUS Calibration Tool. Manual version 3.0.

PRIM (Porteil de la Prévention des Risques Majeurs). (2010). http://www.prim.net/ (Last accessed April 2010).

RDBRMC (Rhone-Mediterranean-Corsica Basin Water Data Network). (2010). http://www.rdbrmc.com/hydroreel2/carto.php?vphp=x_-525,y_-1700,z_566 (Last accessed April 2010).

République Française. (2009). Région Laungedoc Rousillon- L'atlas des paysages du Languedoc Roussillon. http://www.languedoc-roussillon.ecologie.gouv.fr/Hérault/ (Last accessed November 2009).

Risson, M. (1995). These-'Incidence de la complexitédu milieu physique et des lois de comportement sur la réponse hydrologique d'un bassin versant. Modèle de représentation et de dynamique. Application au bassin de la Peyne (Hérault, France). L'Université de Montpellier.

Ruin I., Creutin J.D., Anquetin, S., Lutoff C (2008). Human exposure to flash floods – Relation between flood parameters and human vulnerability during a storm of September 2002 in Southern France. Journal of Hydrology 361, 199– 213, 2008

SAGE (Schéma d'Amenagement et de Gestion des Eaux) Hérault (2005). DIAGNOSTIC. Last accessed March 2010)

SANDRE (2010). http://sandre.eaufrance.fr/app/chainage/courdo/htm/Y2340500.php?cg=Y2340500 (Last accessed March 2010).

S´en´esi, S., Bougeault, P., Ch`eze, J. L., and Cosentino, P. (1996). The Vaison le Romaine Flash flood: Meso-Scale Analysis and Predictability Issues. Wea. Forecasting, vol. 11, pp. 417–442 (1996).

Stone, J.J., Jane, L.J., Shirley, E.G. (1992). Infiltration and Runoff Simulation on a Plane. Soil and Water Division of Americcan Society of Agricultural Engineers . Vol.35 (1) (1992).

Thielen J., Bartholmes J., Ramos M.H., de Roo A. (2008). The European Flood Alert System – Part 1: Concept and development; Hydrol. Earth Syst. Sci., vol.13, pp.125–140, (2009)

Touma, J., Voltz, M., Albergel, J. (2007). Determining soil saturated hydraulic conductivity and sorptivity from single ring infiltration tests. European Journal of Soil Science Vol. 58, pp. 229–238 (2007).

Valarie P., Coeur D. (2004) Vulnérabilité de la région Languedoc-Roussillon aux crues méditerranéennes : perspectives historiques et enjeux actuels; LA Houille Blanche/N° 6 (2004).

Van Asch, T., Van Dijck, S.J.E., Hendriks, M.R. (2001). The role of overland flowand subsurface flow on the spatial distribution of soil water in the topsoil. Hydrol processes. Vol. 15, pp. 2325-2340 (2001).

Van Der Knijff, J. M., Younis, J. and De Roo, A. P. J. (2008a). LISFLOOD: a GIS-based distributed model for river basin scale water balance and flood simulation, International Journal of Geographical Information Science, vol. 99999 (1) (2008).

Van der Knijf J.M., de Roo A. (2008b). LISFLOOD Distributed Water Balance and Flood Simulation Model Revised User Manual JRC Scientific and Technical Reports EUR 22166 EN/2 ISSN 1018-5593. http://natural-hazards.jrc.ec.europa.eu/activities_LISFLOOD.html (Last accessed April 2010)

Vigicrues. (2010). http://www.vigicrues.ecologie.gouv.fr/niveau3.php?idspc=21&idstation=78#271 (Last accessed March 2010).

Weng, Q. (2008). Remote sensing of impervious surfaces. CRC Press. Taylor and Francis Group.

Younis, J., Anquetin, S., Thielen, J. (2008). The Benefit of High Resolution Operational Weather Forecasts for Flash Flood Warning. J. Hydrology and Earth Sciences Vol. 12, pp. 1039-1051.

Table of contents

Appendix I. Sample location map 69
Appendix II. Texture map 70
Appendix III. Tributary map 71
Appendix IV. Land use 72
Appendix V. The Peyne catchment in numbers 73
Appendix VI. Tributary Subcatchment Land Cover Characteristics (%) 74
Appendix VII. Precipitation and runoff in the Peyne catchment 75
Appendix VIII. Meteorological data 76
Appendix IX. Observed Discharge of the river Peyne 77
Appendix X. Lac des Olivettes. 78
Appendix XI. NDVI Maps 80
Appendix XII. Field form 81
Appendix XIII. Fieldwork statistics 83
Appendix XIV. Heterogeneity vineyards 89
Appendix XV. Crusting and Macropores 90
Appendix XVI. Precipitation Events 91
Appendix XVII. pF curves 93
Appendix XVIII. Data preparation ArcGIS and PCraster 94
Appendix XIX. Validation Calibration 97
Appendix XX. Scenarios 103
Appendix XXI. Curve Number vs. LISFLOOD 108
Appendix XXII. A non technical glossary of the annual scenario 109

Appendix I. Sample location map

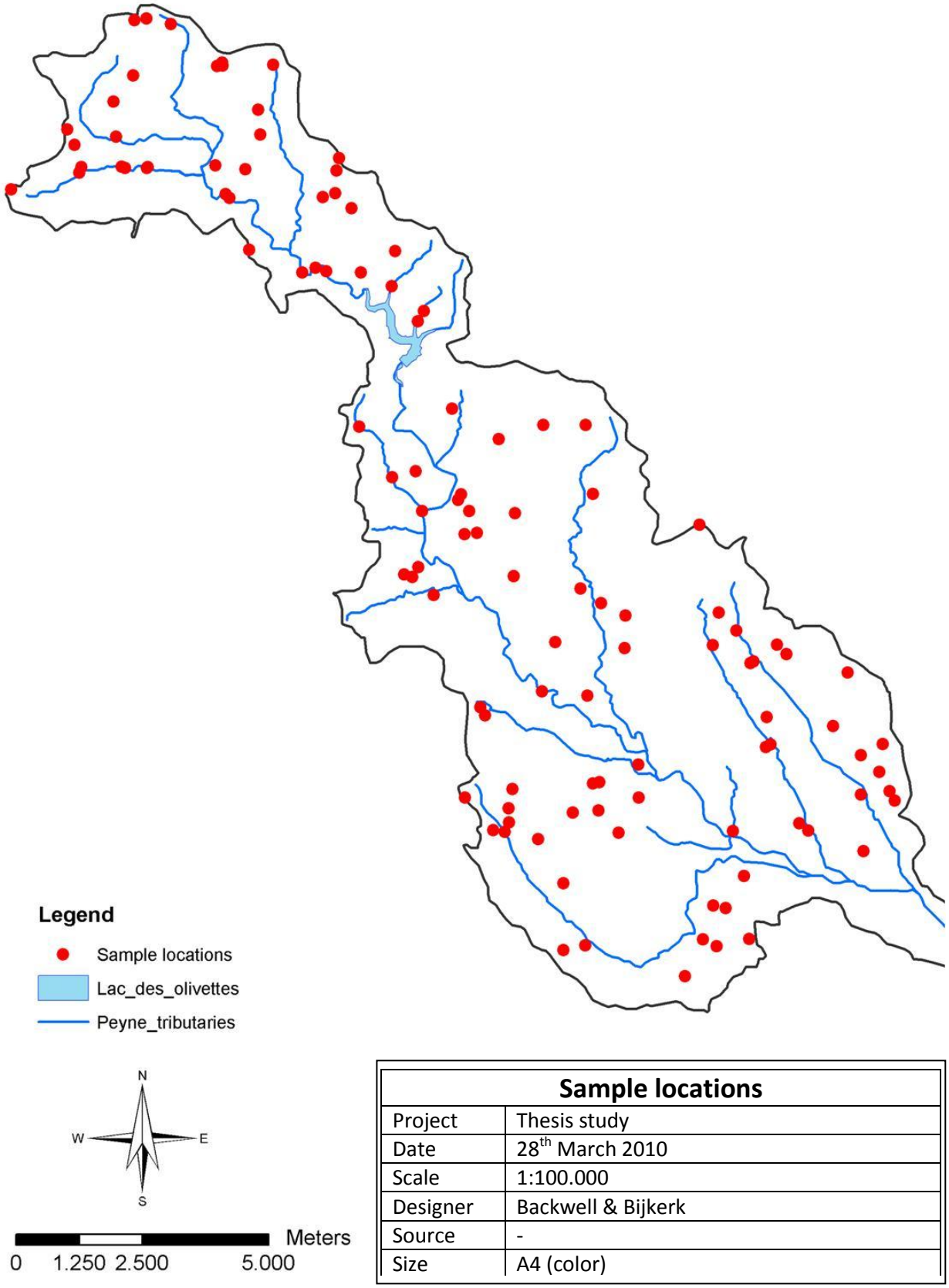

Sample locations	
Project	Thesis study
Date	28th March 2010
Scale	1:100.000
Designer	Backwell & Bijkerk
Source	-
Size	A4 (color)

Appendix II. Texture map

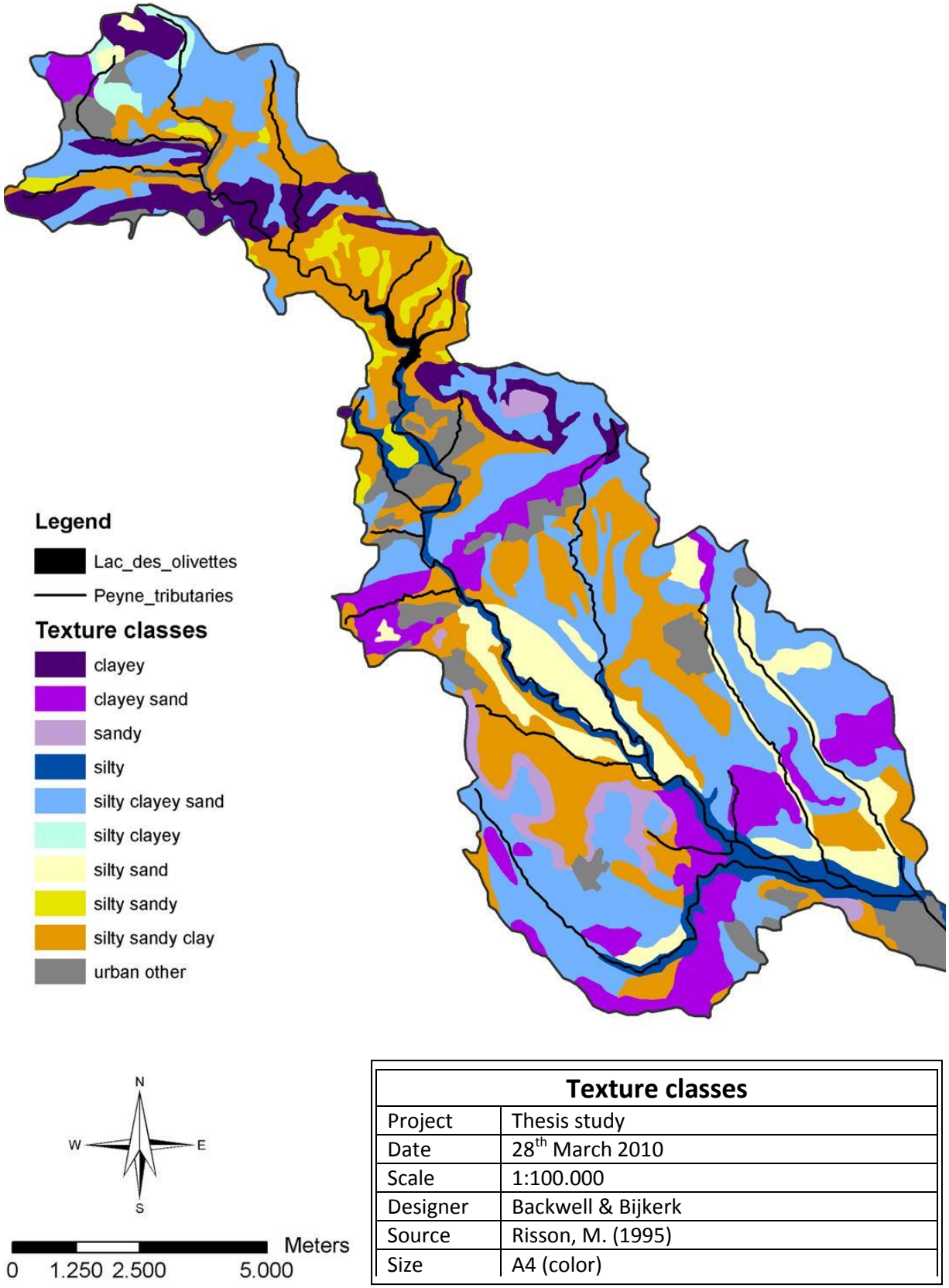

Texture classes	
Project	Thesis study
Date	28th March 2010
Scale	1:100.000
Designer	Backwell & Bijkerk
Source	Risson, M. (1995)
Size	A4 (color)

Appendix III. Tributary map

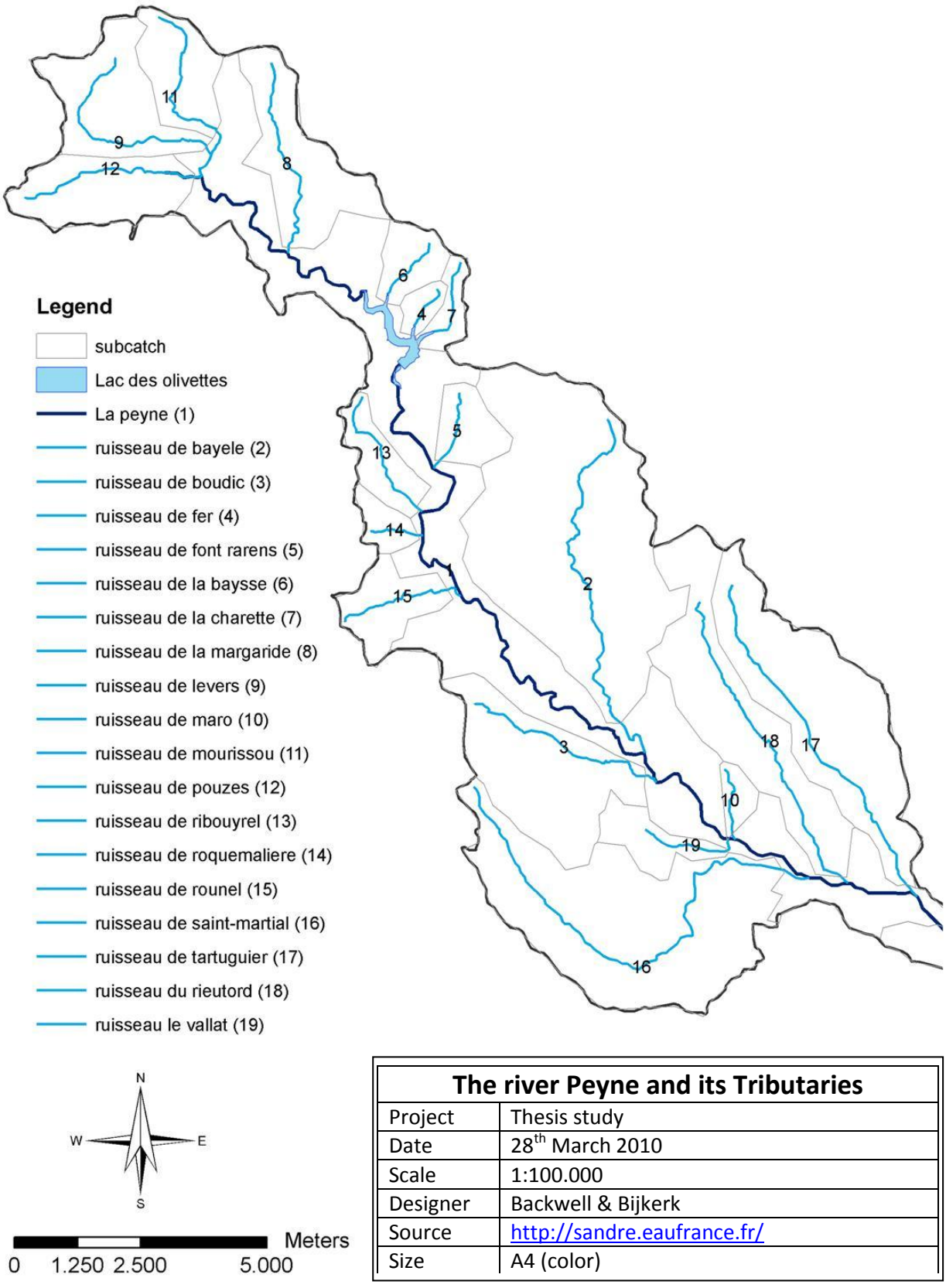

The river Peyne and its Tributaries	
Project	Thesis study
Date	28th March 2010
Scale	1:100.000
Designer	Backwell & Bijkerk
Source	http://sandre.eaufrance.fr/
Size	A4 (color)

Appendix IV. Land use

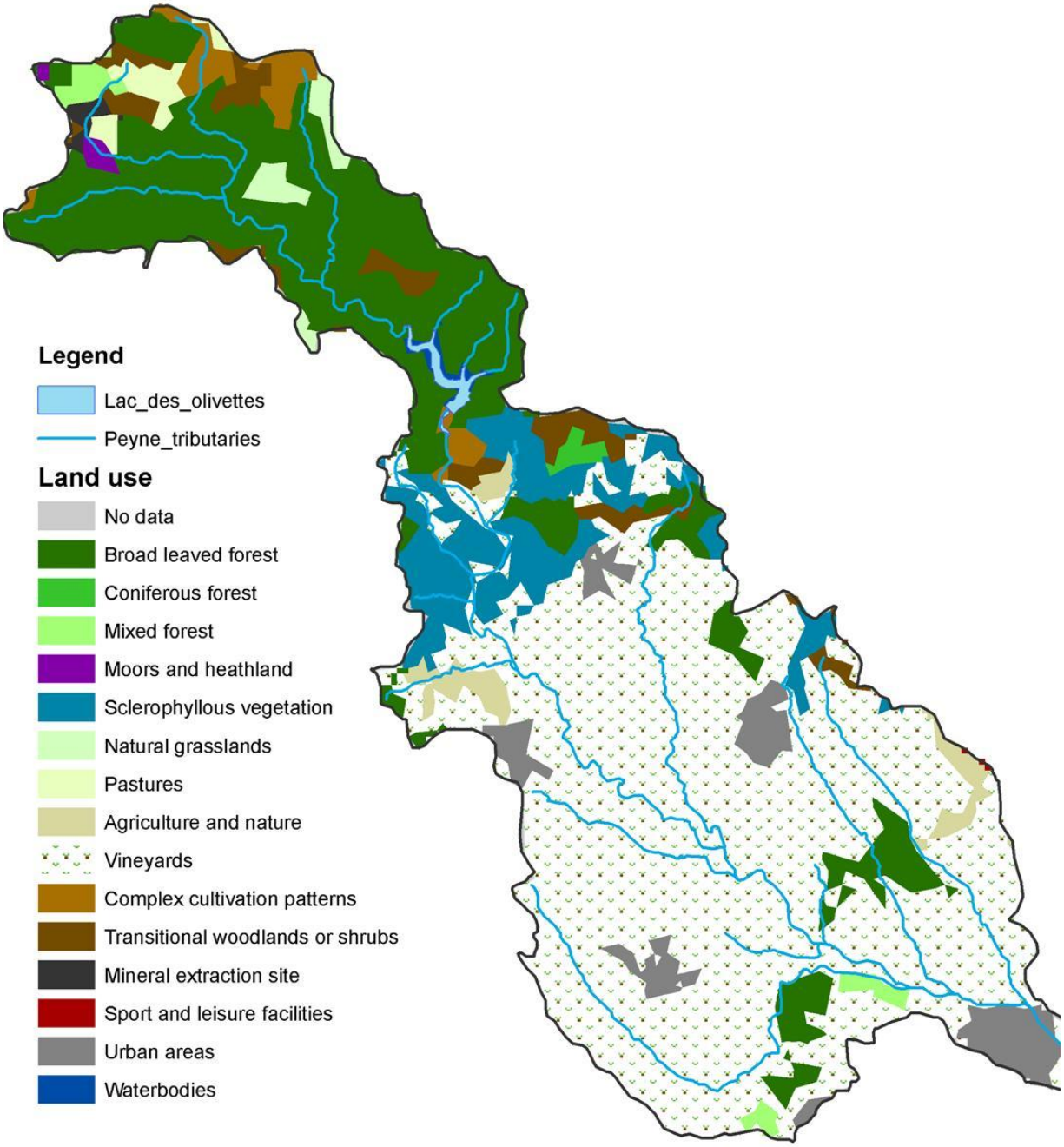

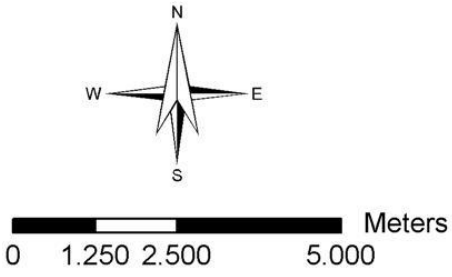

Land cover	
Project	Thesis study
Date	28th March 2010
Scale	1:100.000
Designer	Backwell & Bijkerk
Source	http://www.eea.europa.eu
Size	A4 (color)

Appendix V. The Peyne catchment in numbers

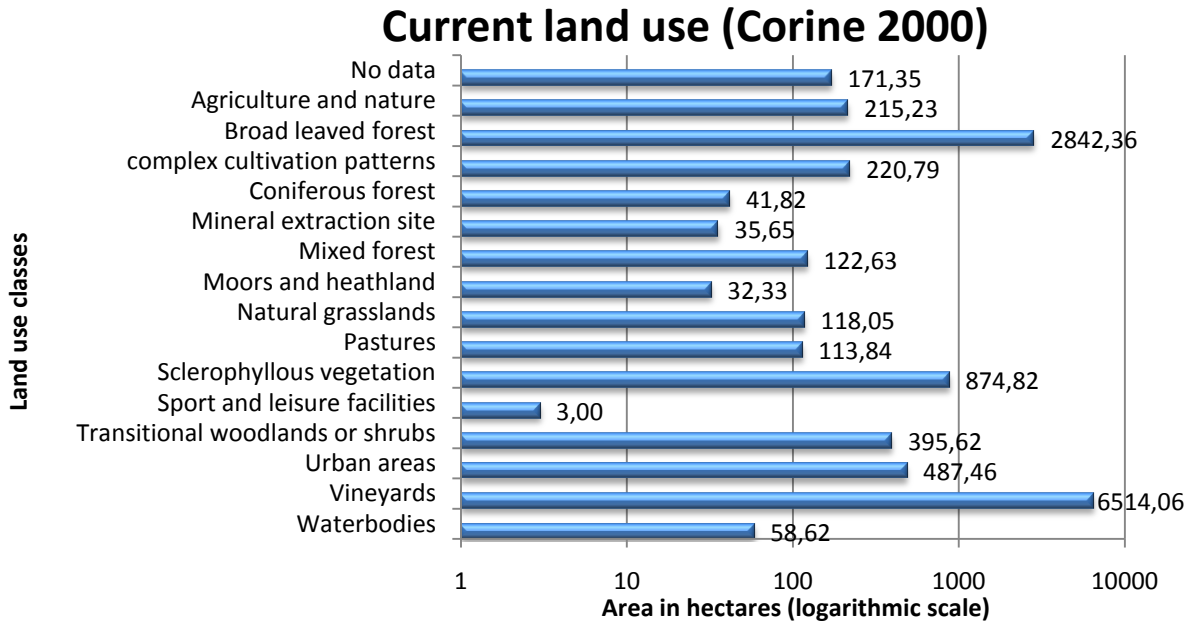

Graph V.1: *Land cover classes according to CORINE 2000 database and their corresponding area of coverage within the catchment*

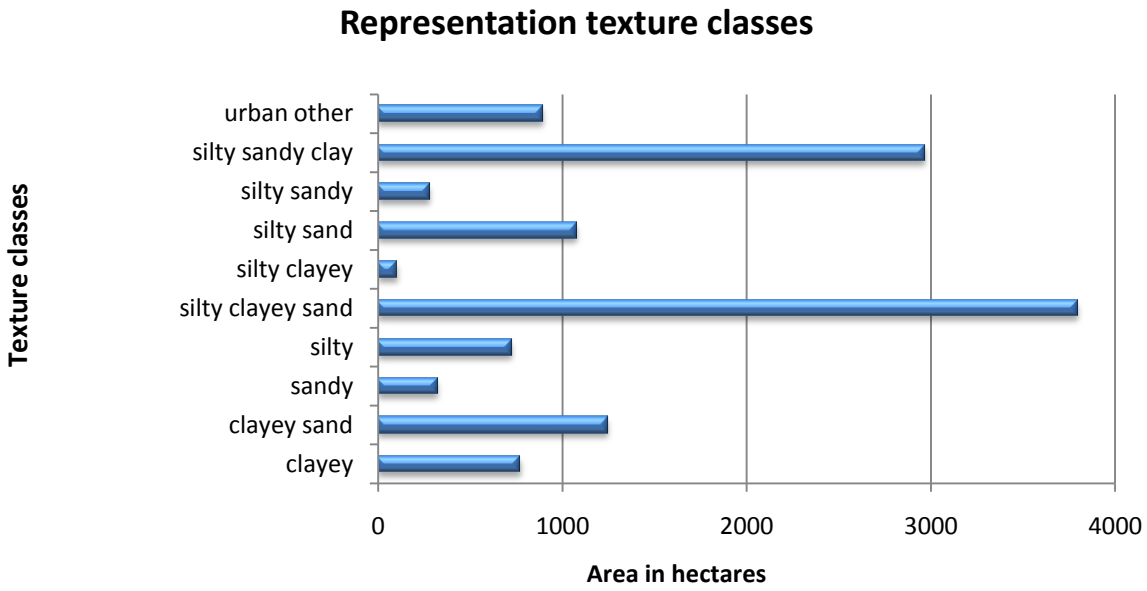

Graph V.2: *Soil texture classes and their corresponding area of coverage within the catchment.*

Appendix VI. Tributary Subcatchment Land Cover Characteristics (%)

	mourissou	de levers	de pouzes	la margaride	de la bayse	de fer	de la charette	de font rarens	de ribouyrel	de roquemaliere	rounel	bayelle	boudic	le vallat	de maro	saint martial	rieutord	de tartuguier	Peyne	Pézenas area
No data	0,4	0,9	0,5	0,4	0,5	0,0	0,7	0,0	0,9	3,0	1,8	0,5	0,7	0,0	0,0	0,4	0,1	0,4	0,3	42,1
complex cultivation patterns	26,9	0,0	1,4	11,1	0,0	0,0	0,0	0,0	0,0	0,0	0,0	0,0	0,0	0,0	0,0	0,0	0,0	0,0	2,6	0,8
Broad leaved forest	51,4	44,7	98,1	75,4	95,6	94,8	93,8	22,0	10,9	1,5	10,3	9,0	0,0	34,4	0,0	8,6	11,4	5,4	26,3	7,3
Vineyards	0,0	0,0	0,0	0,0	0,0	0,0	0,0	6,7	25,0	0,8	44,5	66,6	91,4	65,6	100,0	84,3	73,2	80,6	48,3	16,0
Mineral extraction site	0,0	7,0	0,0	0,0	0,0	0,0	0,0	0,0	0,0	0,0	0,0	0,0	0,0	0,0	0,0	0,0	0,0	0,0	0,0	0,3
Pastures	10,8	16,0	0,0	0,0	0,0	0,0	0,0	0,0	0,0	0,0	0,0	0,0	0,0	0,0	0,0	0,0	0,0	0,0	0,0	0,6
Transitional woodlands or shrubs	10,4	13,1	0,0	0,9	2,4	0,0	0,0	2,5	0,0	0,0	0,0	6,9	0,0	0,0	0,0	0,0	0,3	2,6	4,1	1,6
Moors and heathland	0,0	6,5	0,0	0,0	0,0	0,0	0,0	0,0	0,0	0,0	0,0	0,0	0,0	0,0	0,0	0,0	0,0	0,0	0,0	0,1
Natural grasslands	0,0	0,0	0,0	12,2	0,0	0,0	0,0	0,0	0,0	0,0	0,0	0,0	0,0	0,0	0,0	0,0	0,0	0,0	1,9	0,5
Sclerophyllous vegetation	0,0	0,0	0,0	0,0	0,0	0,0	0,0	55,3	63,2	94,8	14,6	11,7	0,0	0,0	0,0	0,0	3,9	3,3	8,0	2,1
Agriculture and nature	0,0	0,0	0,0	0,0	0,0	0,0	0,0	12,2	0,0	0,0	28,8	0,0	0,0	0,0	0,0	0,0	0,0	7,6	1,4	0,6
Sport and leisure facilities	0,0	0,0	0,0	0,0	0,0	0,0	0,0	0,0	0,0	0,0	0,0	0,0	0,0	0,0	0,0	0,0	0,0	0,2	0,0	0,3
Urban areas	0,0	0,0	0,0	0,0	0,0	0,0	0,0	0,0	0,0	0,0	0,0	3,2	8,0	0,0	0,0	3,7	10,9	0,0	5,0	27,4
Mixed forest	0,0	11,7	0,0	0,0	0,0	0,0	0,0	0,0	0,0	0,0	0,0	0,0	0,0	0,0	0,0	3,1	0,0	0,0	0,6	0,1
Waterbodies	0,0	0,0	0,0	0,0	1,5	5,2	5,5	0,0	0,0	0,0	0,0	0,0	0,0	0,0	0,0	0,0	0,0	0,0	1,6	0,0
Coniferous forest	0,0	0,0	0,0	0,0	0,0	0,0	0,0	1,4	0,0	0,0	0,0	2,1	0,0	0,0	0,0	0,0	0,0	0,0	0,0	0,0
	100	100	100	100	100	100	100	100	100	100	100	100	100	100	100	100	100	100	100	100

Appendix VII. Precipitation and runoff in the Peyne catchment

An extensive database containing meteorological and discharge data for a small region near Roujan is provided by OMERE, 2009. From this a relation was found between extreme precipitation intensities, cumulative rainfall and the extreme runoff generation. Between 1992 and 2002, November experiences the highest frequency of precipitation events, October receives the highest number of events over 15mm/day and September sees the highest occurrence of rainfall intensities of over 15mm/hr.

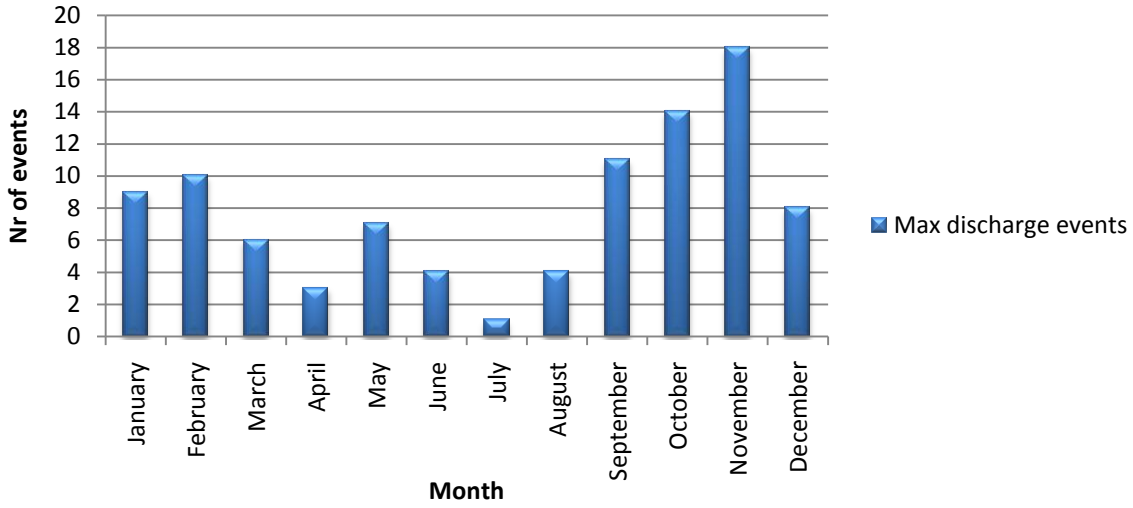

Graph VII.1: *Extreme runoff events in Roujan between 1992 and 2002 (Omere, 2009)*

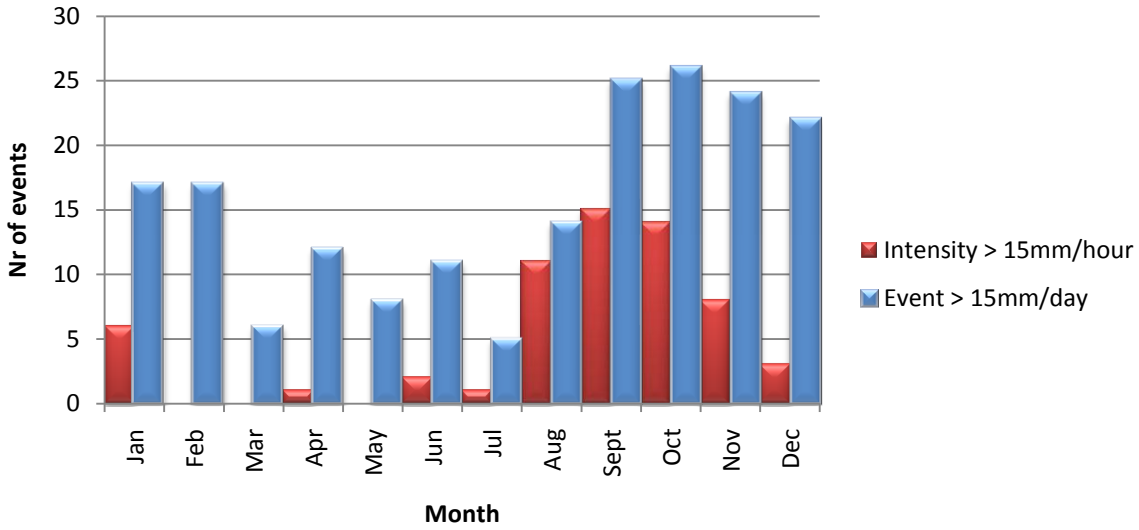

Graph VII.2: *Precipitation intensity in relation to the total precipitation for the period 1992 to 2005(Omere, 2009).*

Appendix VIII. Meteorological data

Calibration and validation required E_t, E_s, E_w and T_{avg} values of 2010. This time period is not part of the available database, hence average values based on Mars satellite data of the JRC between 1990-2000 were used. Daily average values were determined by the LISFLOOD model at 4 outlets in the catchment. The time series were converted to a spatial extent using a PCraster script

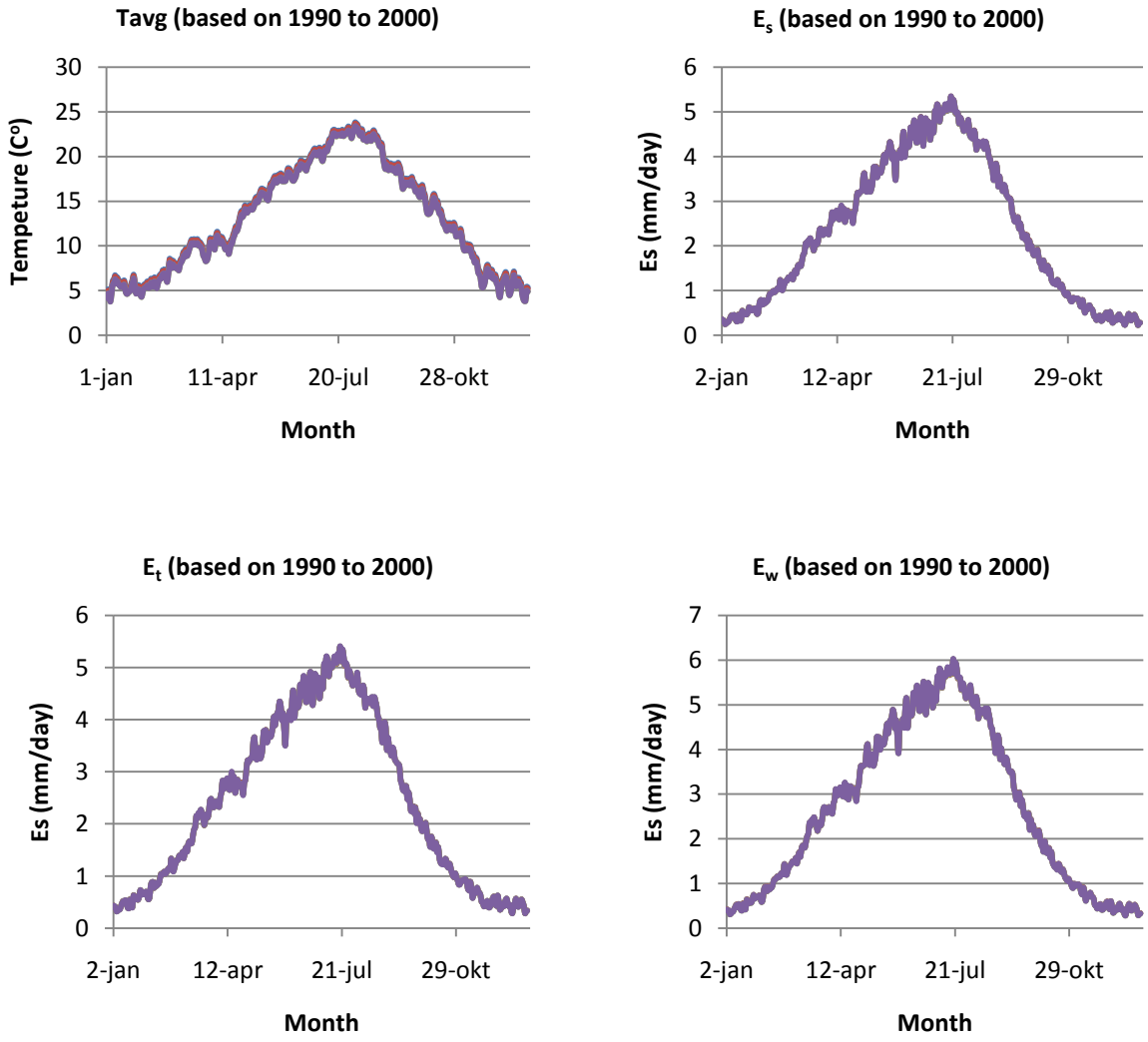

Graph VIII.1a/d: *Averaged meteorological data derived from the mars repository a) Average temperature b) Evapotranspiration from the soil c) Evapotranspiration from a reference crop d) Evaporation from surface water*

Appendix IX. Observed Discharge of the river Peyne

The catchment reacts irregularly to precipitation events within this time period, as can be observed in the hydrograph of graph IX.1. Graph IX. 1 shows the hydrograph with observations taken every 15min and the precipitation data which is measured on a hourly basis. At the beginning of 2010 the Peyne reacts more intense to precipitation than autumn and winter period of 2009.

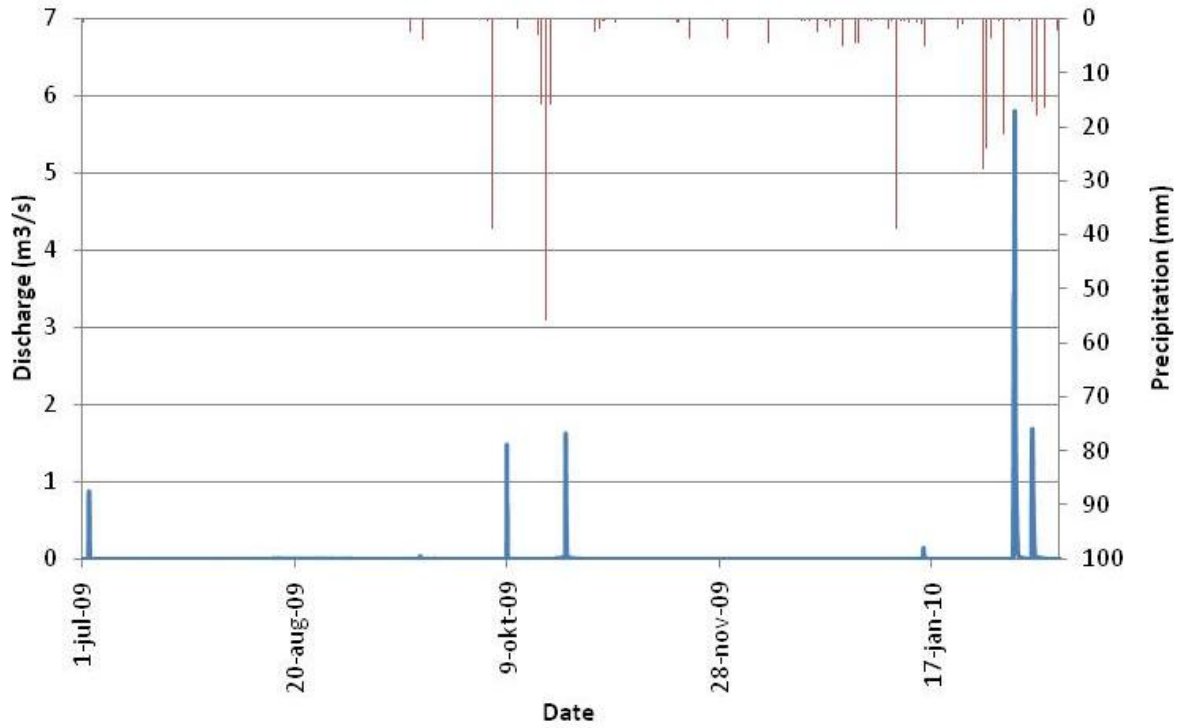

Graph IX.1: *>6 Months (30/06/09 – 22/02/10) discharge(15min) and precipitation (hourly) data for the Peyne river at St Majan*

Table IX.1: *An overview of events between the 1st of July (2009) and the 22nd of February (2010) showing the irregular response of the catchment*

Event	Date	Peak Discharge (m^3/s)	Precipitation (mm)
1	2-jul	0,7	0,75
2	8-okt	1,4	40
3	21-okt	No data	100
4	22-okt	1,5	18
5	14-jan	0,2	30
6	5-feb	5,7	23,5
7	9-feb	1,5	21
8	17-feb	4,2	30
9	19-feb	2,25	15

This irregular response can be explained by two subjects:

- Soil saturation
- Lac des Olivettes (Appendix X)

Appendix X. Lac des Olivettes.

The largest prevention technique to mitigate flash flooding that was carried out in the region during the past decennia, was the creation of Lac des Olivettes by the Département d'Hérault. This artificial lake and its accompanying barrage near Vailhan were first put into action in 1988 to satisfy two goals. Firstly to buffer peak discharges from the 29,5 km^2 upstream forested area and secondly to create a new source of water for irrigation (provides 200hectares with approximately 0,1Mm^3/y). The reservoir protects 2,500 hectares of arable land in the downstream area from inundation during peak discharges. (Groupe chantiers de France, 1987). The reservoir is 'passive'. The discharge will increase during events by reaching the threshold of several spills. Under normal conditions the reservoir provides a small base flow ranging between 0,024 and 0,1 m^3/s. If the water level in the reservoir reaches 163 m.a.s.l. the threshold of the first spill is reached (1,5m * 3m) with a maximum discharge of 22m^3/s. If this is not sufficient and the water level keeps increasing it will reach the next spill located at 166,5 m.a.s.l. The spill with a width of 40m wide has a maximum discharge of 290m^3/s. This spill will only be in use during the most extreme events (Conseil General d'Herault).

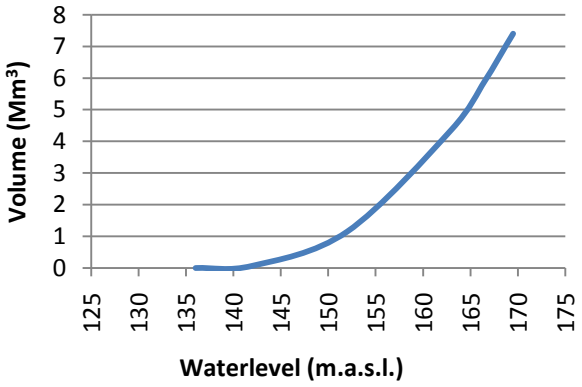

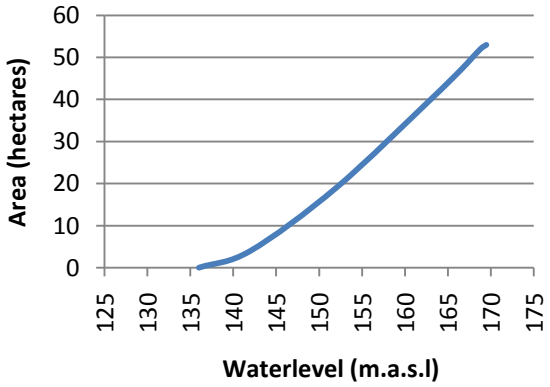

WL (m.a.s.l)	Mm3	Q (m^3/s)
169,5	7,4	323
168,8	7,05	323
166,5	5,9	22
163,0	4,37	0,024/0,05
152,0	1,15	0,024/0,05
142,0	0,07	0,024/0,05
136,0	0	0,024/0,05

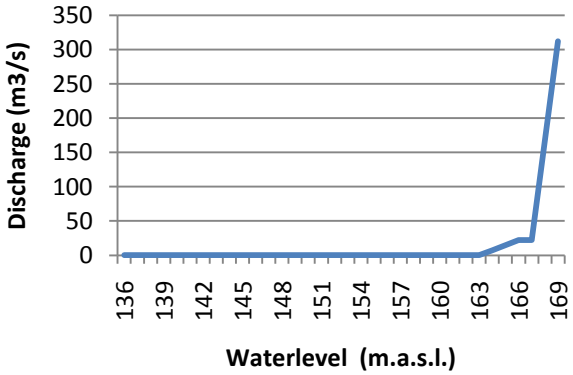

Graph X.1 a-c & Table X.1: *a) the relation between the volume of the lack and the related water level relative to sealevel b) the relation between the water level of the lake and the related surface area c) the relation between the water level and the discharge at the barrage displayed in graphical and tabled form*

An event occurred at the 28th of January 1996. During this event the reservoir showed its value. At the peak of this event 106m^3/s entered the reservoir and only 43m^3/s left the reservoir. The 106m3/s can be described as being between a 1/10 to 1/100 year event (80m^3/s and 190m^3/s respectively).

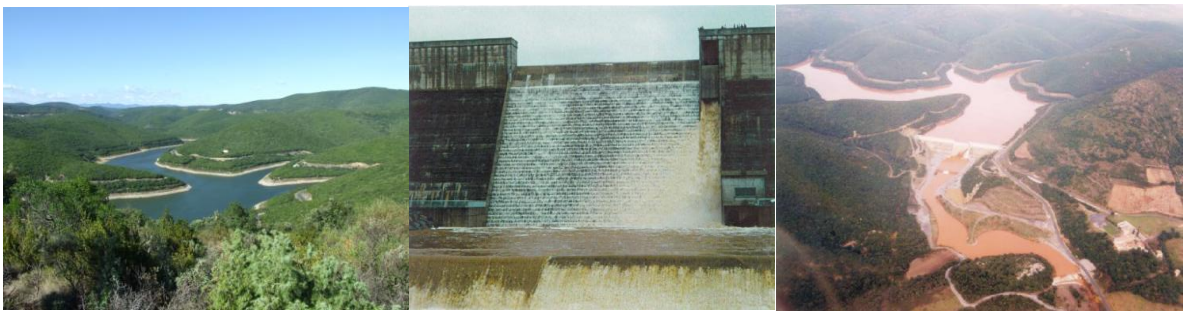

Figure X a-c: *a) The reservoir in birds eye perspective b) the barrage during the 1996 event c) the reservoir filled with sediment after the event*

It appears that the 'passive behavior' of the reservoir plays an important role. To gain insight in the behavior of the reservoir a mass balance is calculated for 9/10/09-10/02/10 for the 29,5km^2 sub catchment north of the reservoir.

The following assumptions were made regarding the following mass balance

- The base flow of the reservoir is 50l/s (based on literature and observations)
- The total E_w is based on average values (averages over the 1990-1999 period)
- The total E_t is based on average values (averages over the 1990-1999 period)
- The total soil storage is 5,2mm^3 (a coarse value based on the available data related to SWC and soil depths). It is assumed that the catchment was not completely dry at the 10th of October (2 days since last precipitation event) and not completely saturated at the 10th of February.
- The precipitation events measured at the Olivettes observation point cover the whole area

Table X.2: *The in and output parameters used to determine the reservoirs mass balance for the period 9/10/09-10/02/10*

	mm (relative to area)	**Mm^3**
Input		
Pr	329,5	9,7
Output		
Q	20,2	0,6
$E_{t\ (evaporation\ soil)}$	86,6	2,6
$E_{w\ (evaporation\ water)}$	0,9	0,3
Storage		
Soil	101,7	3
Lake	120,1	3,2

The initial reservoir storage is approximately 2,6 mm^3 which corresponds to a water level of +/-157 m.a.s.l. (numbers provided by the Conseil Géneral de Hérault) The increase of 3,6mm^3 is assumed to be an overestimation due to unknown losses and the assumptions made in the process.
It is known from the discharge observations that in the mentioned period no additional discharge was observed from the reservoir. This means that the available storage of 1,8Mm^3 was not exceeded. However based on the observed discharges after the mentioned period it was assumed that the water level of the reservoir approached/reached the threshold of the 22m^3 spill which is located at 163m.a.s.l. The result of this is that only small amounts of an event mid February will be stored in the reservoir and the upstream part of the catchment start to contribute (with a maximum of 22m^3/s) to the downstream discharges.

Appendix XI. NDVI Maps

NDVI (Normalized Difference Vegetation Index) indicating the vegetation over the region based on the reflection and absorption (light-absorbing chlorophyll) of Red and Near Infrared light. Based upon the spectrum of vegetation which shows low reflection of red light and high reflection of near infrared, the following equation gives values per pixel ranging between -1 and 1. (Lillesand et. al, 2004).

$$NDVI = \frac{NIR-R}{NIR+R}$$ where Rock/Bare soil < 0.1 < Greenness/quantity of vegetation

Values of 0,22 and higher indicate a vegetation rich cover. NDVI maps based on two Aster images with a resolution of 15m, using band 2 (red) and 3 (NIR). The first image is taken on June 13th 2002 and the second image is taken on February 8th 2003.

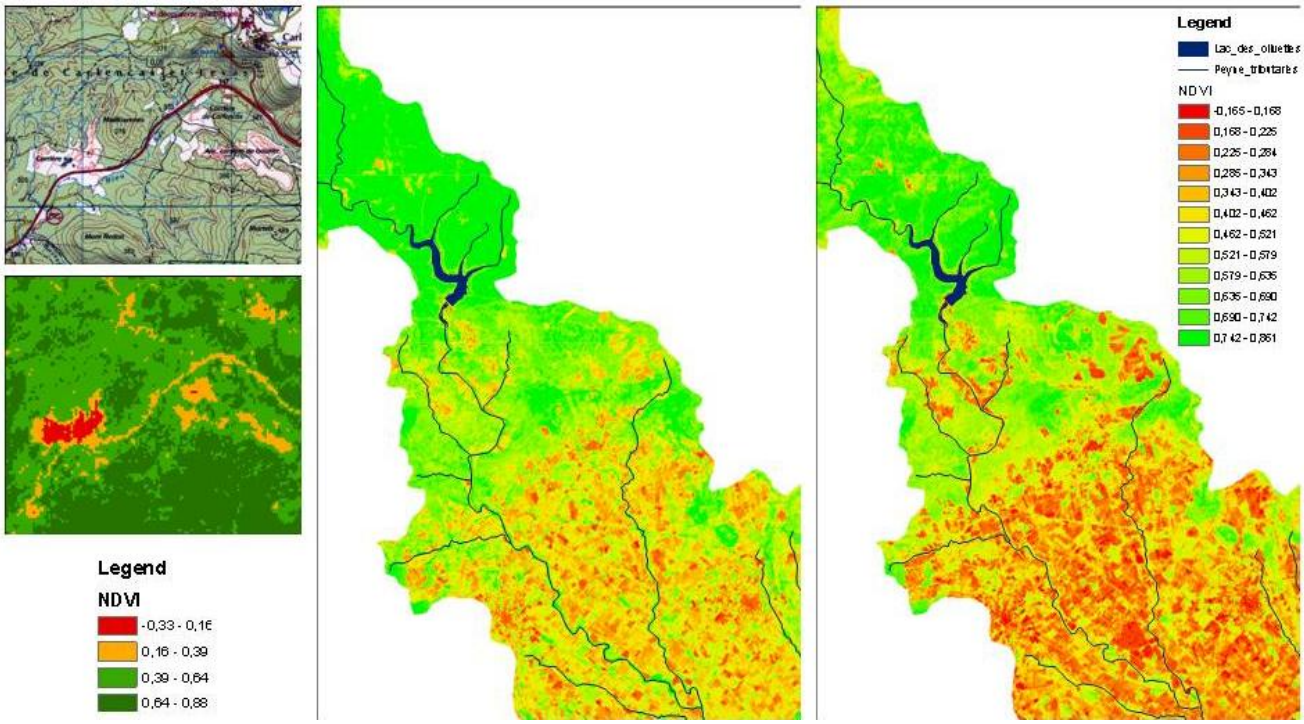

Figure XI.1: *The NDVI for part of the catchment based on ASTER satellite imagery from June 2002 and February 2003. On the left an example is enclosed to show the difference in values for a mineral extraction site and the surrounding forested areas.*

Appendix XII. Field form

General:

Observer	*Backwell/Bijkerk*		Temperature	
Coordinates /EPE		m	Weather conditions	
Time			Wind	
Date			Numbers Pictures	
Sample location nr.			Numbers Soil samples	

Land use:

	Broad leaved forest		Complex cultivation patterns
	Coniferous forest		Moors and heath land
	Mixed forest		Natural grasslands
	Sclerophyllous vegetation		Pastures
	Transnational woodland-shrub		Discontinuous urban fabric
	Vineyards		Sport and leisure facilities
	Land principally occupied by agriculture with significant areas of nature		Mineral extraction sites
Fraction impervious area			0% / 25% / 50% / 75%
Management			

Infiltration capacity

Used experiment	Rainfall/inversed auger	Run off tracers	
Crusting		Rills and Gullies	
Resistance crust		Calcium test (Hydro Chloride acid)	
Infiltration capacity		Tractor Trampling	

Surface Roughness

Slope		Wetted perimeter	
Discharge		Cross sectional area	
Flow velocity			

Waterbody

Waterdepth		Slope Banks	
Width		Discharge	
Vegetation cover river banks			

Precipitation data:

Used device:	Tipping Bucket/Rain Gauges	Precipitation in mm	
Observation period:			

Miscellaneous

Sketch cross section channel:

Appendix XIII. Fieldwork statistics

A complete database can be found on the DVD accompanying this report. The following is a brief statistical overview of the observations.

Saturated hydraulic conductivity.

Infiltration (ksat) measurements were repeated 393 times at more than 120 locations. Values showed a large range illustrated in the following graph:

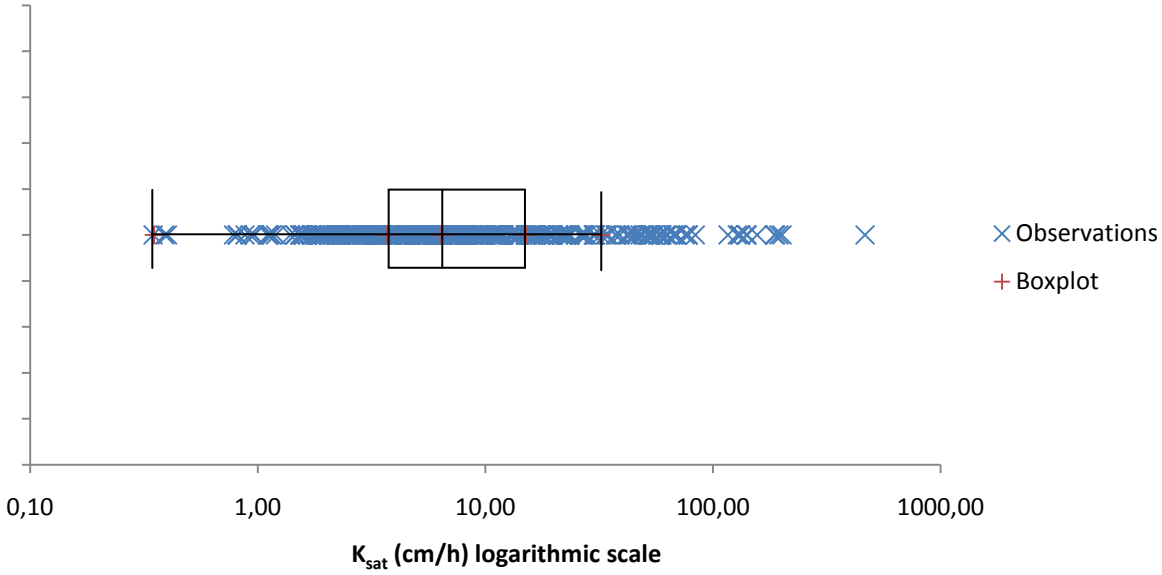

Graph XIII. 1: *Variance of the infield measured k_{sat} values*

k_{sat} values show a skewed Gaussian distribution (Skewness = 1,271) as can be observed in the following graph. The median of the observed values is 6,4cm/h versus a mean of 17,73 cm/h. The measured values range between 0,35cm/h up to the extreme value of 435cm/h (recently ploughed field). Probability density functions show that the majority of observations range between 0 and 75 cm/h. These values are considered high in comparison with literature, and the infiltration values used by the JRC highlight that the measured values are consistently offset by a of factor 10. Despite the fact that measured ksat values seem to be (very) high are in the same order of magnitude as the k_{sat} values determined by the single ring falling head method (mean 17,68cm/h versus a median of 12,10 cm/h on 54 samples).

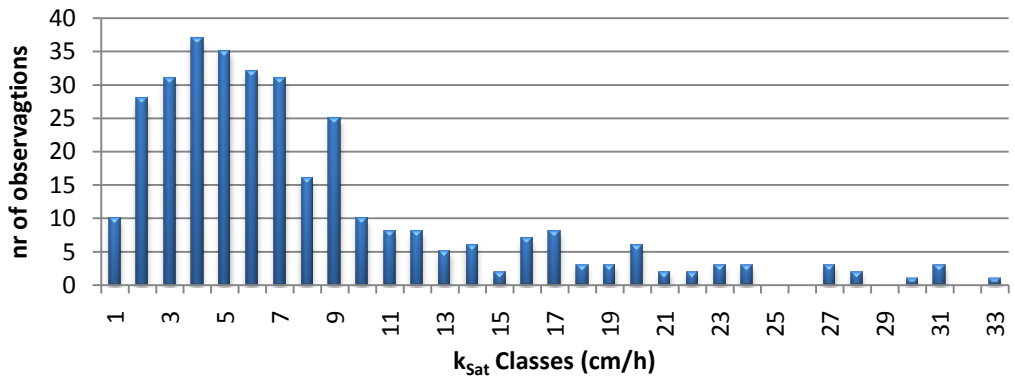

Graph XIII. 2: *The (skewed Gaussian) distribution of the measured k_{sat} values, the median is located at 6,4 the mean at 17,74cm/h*

The following table shows the observed land cover types and the number of k_{sat} observations taken at the cover types.

Table XIII. 1: *The amount of measurements taken per land cover type*

Land cover observed	N	Land cover observed	N
Bare soil	25	Natural grasslands	12
Broad leaved forest	63	Pastures	6
Broad leaved forest (cleared)	3	Sclerophyllous vegetation	25
complex cultivation patterns	19	Sport and leisure facilities	6
Agriculture and nature	6	Transitional woodland	12
Mineral extraction site	3	Urban area	12
Mixed forest	24	Vineyards	140
Moors and heathland	4	Vineyards (abandoned)	18
Natural grasland/Sclerophyllous	9	Vineyard (nursery)	6

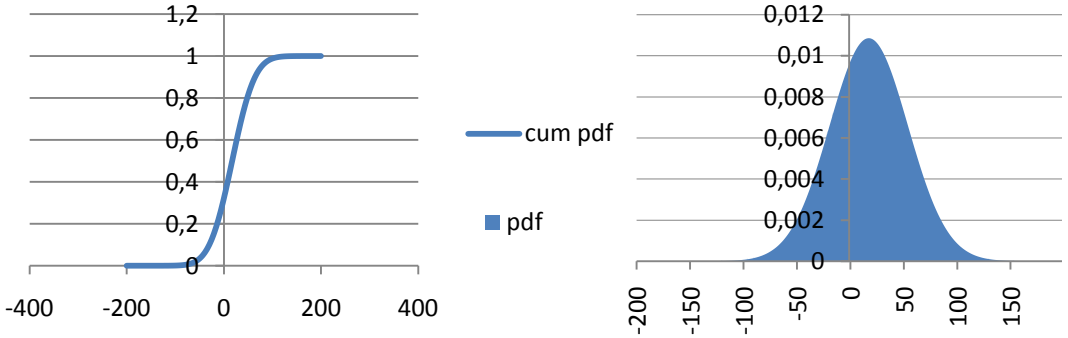

Graph XIII 3a-b: *a) Cumulative probability density function of the observed k_{sat} b) the probability density function of the observed k_{sat}*

k_{sat} within vineyards.

Large heterogeneity was observed within the vineyards (See appendix XIV) and the digital vineyard database). Vineyards were divided into 3 entities (Figure XIII.1):

- the vine bed (A)
- the trampled part(B)
- the tractor path/rills (center of the vine rows, C)

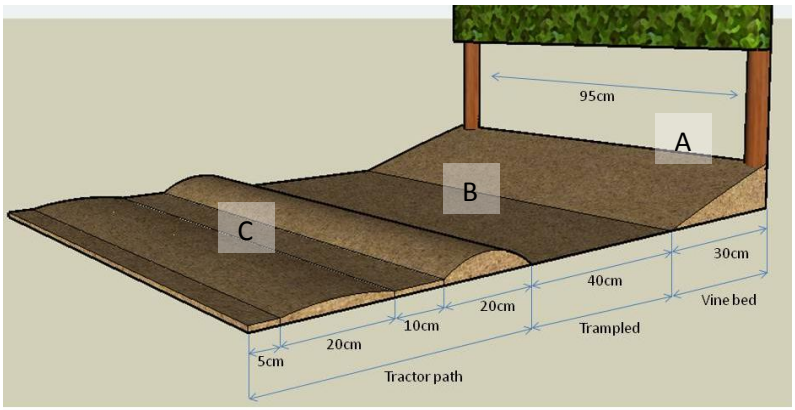

Figure XIII.1: *Schematic representation of the vineyards. Dimensions observed during the fieldwork.*

Crusting within Vineyards.

In total 153 infiltration tests were performed at 50 different vineyard locations randomly spread over the downstream area. Based on the statistics it appears that there is a visible difference in the k_{sat}. On average the mean k_{sat} of a crusted soil is a factor two lower than the observed k_{sat} of a non crusted soil (4,91cm/h versus 10,52cm/h) as can be observed in the following two graphs. It is not yet possible to come to a relation between crusting and the causes. The infield observed crusting is compared with the texture map and the management practices known from literature (Biarnes, *et al.* 2009) and no relation could be found. However the number of samples taken is too small to come to a reliable conclusion.

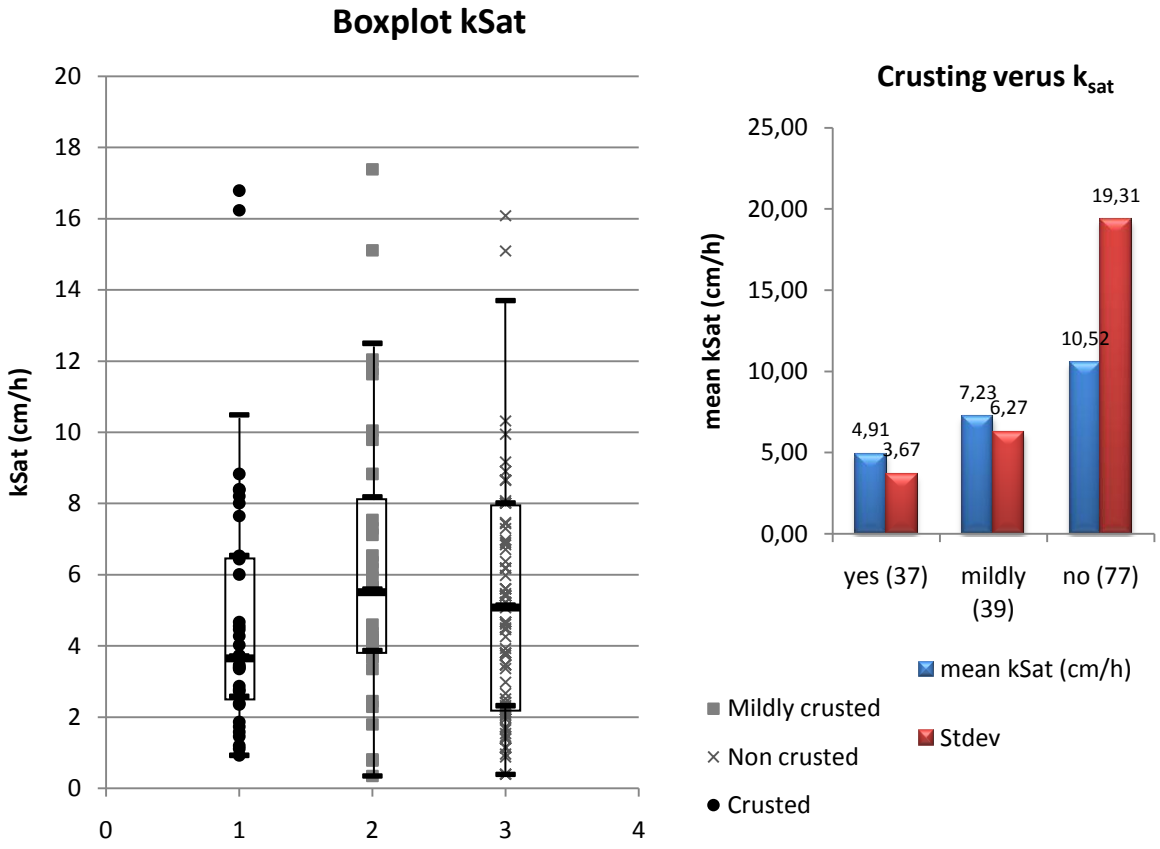

Graph XIII.4a-b: *a) boxplot with the variance in the measured k_{sat} values relative to crusted (1) mildly crusted (2) and non crusted sites (3) b) the measured mean values and the related stdev*

Surface Roughness

To determine surface roughness chain measurements were applied (see appendix 13) 893 times. The following table (table **XIII.2)** shows the number of measurements per land cover type taken during the field campaign. As can be observed there is a variance in taken samples which can bias the final results of the measured surface roughness.

Table XIII.2: The land over types and the number of roughness measurements taken

Landcover	N
bare soil	83
broad leaved forest	50
complex cultivation patterns	60
agriculture and nature	8
mineral extraction site	10
mixed forest	40
natural grasslands	50
natural grasslands/schlerophyllous	10
Pastures	15
schlerophyllous vegetation	20
schlerophyllous/natural grasslands	10
sport and leisure facilities	10
transitional woodland	24
Vineyards	499

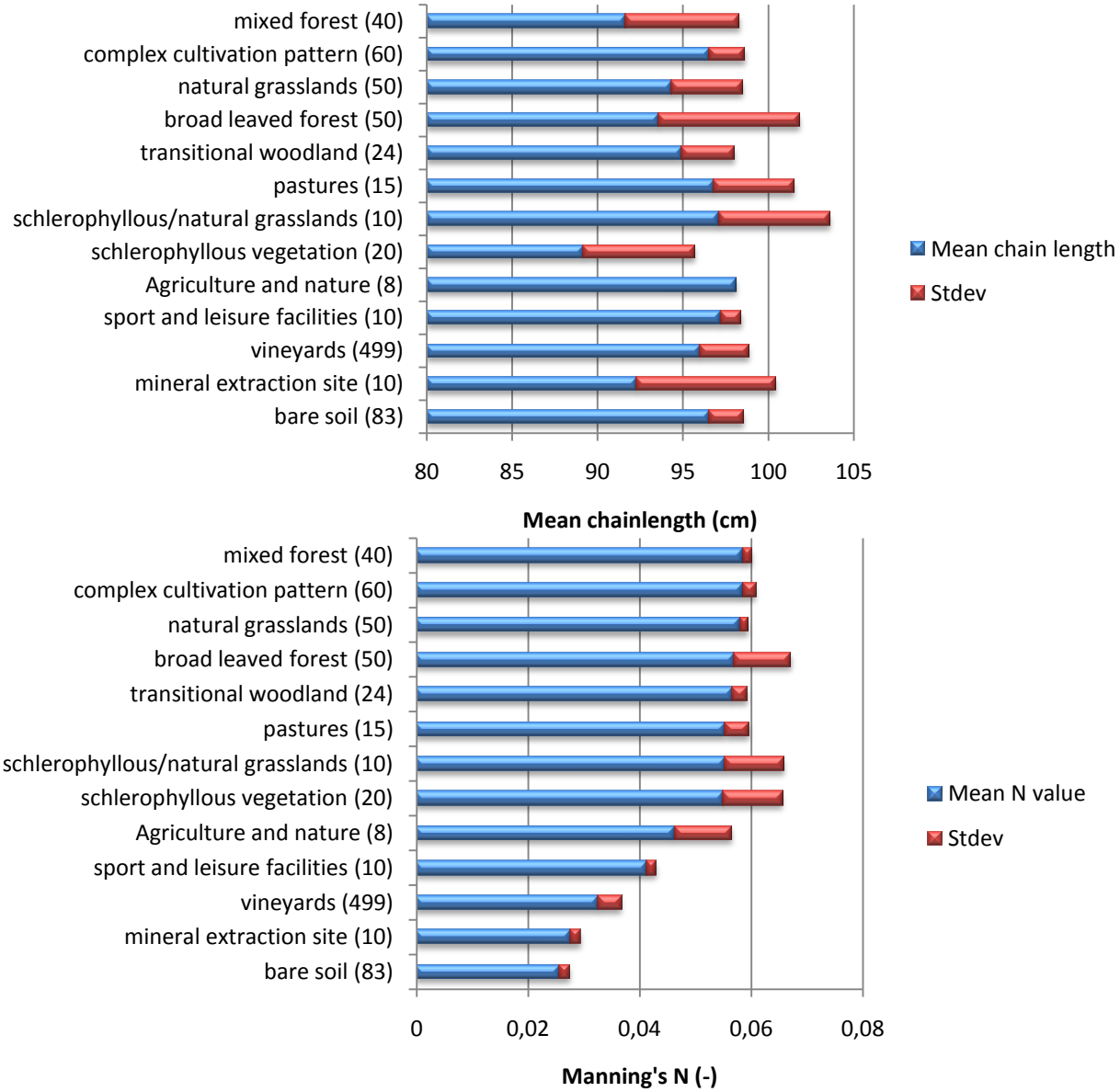

Graph XIII 5a-b : *a) the mean chain length and the related stdev based on the field observations b) the mean Manning's N and the related stdev based on the infield taken measurements*

As can be observed within graph XIII 5a and b the variation within the observations is large, however the differences between the final mean values is relatively low. The resulting N values are in line with the expectations (reference values to compare observations for pastures (0,35), light (0,050) and heavy brush (up to 0,075) were taken from literature: Imnoeng, 2010). The bare soil appears to have the largest roughness which was expected. Highest roughness's where found in forested areas and the complex cultivation patterns (in general dens and low vegetation).

Sorptivity

The Brutsaert formula for 3D infiltration was applied to observed data. The line coefficient (the *Linest* function within Excel) and the RMSE of the calculated and observed cumulative infiltration were used as objective functions. The optimal sorptivity value was then determined by using the Excel Solver function for 6 locations. At these locations, measurements were taken at the vine bed, rill and trampled part. The sorptivity values are displayed in the following table.

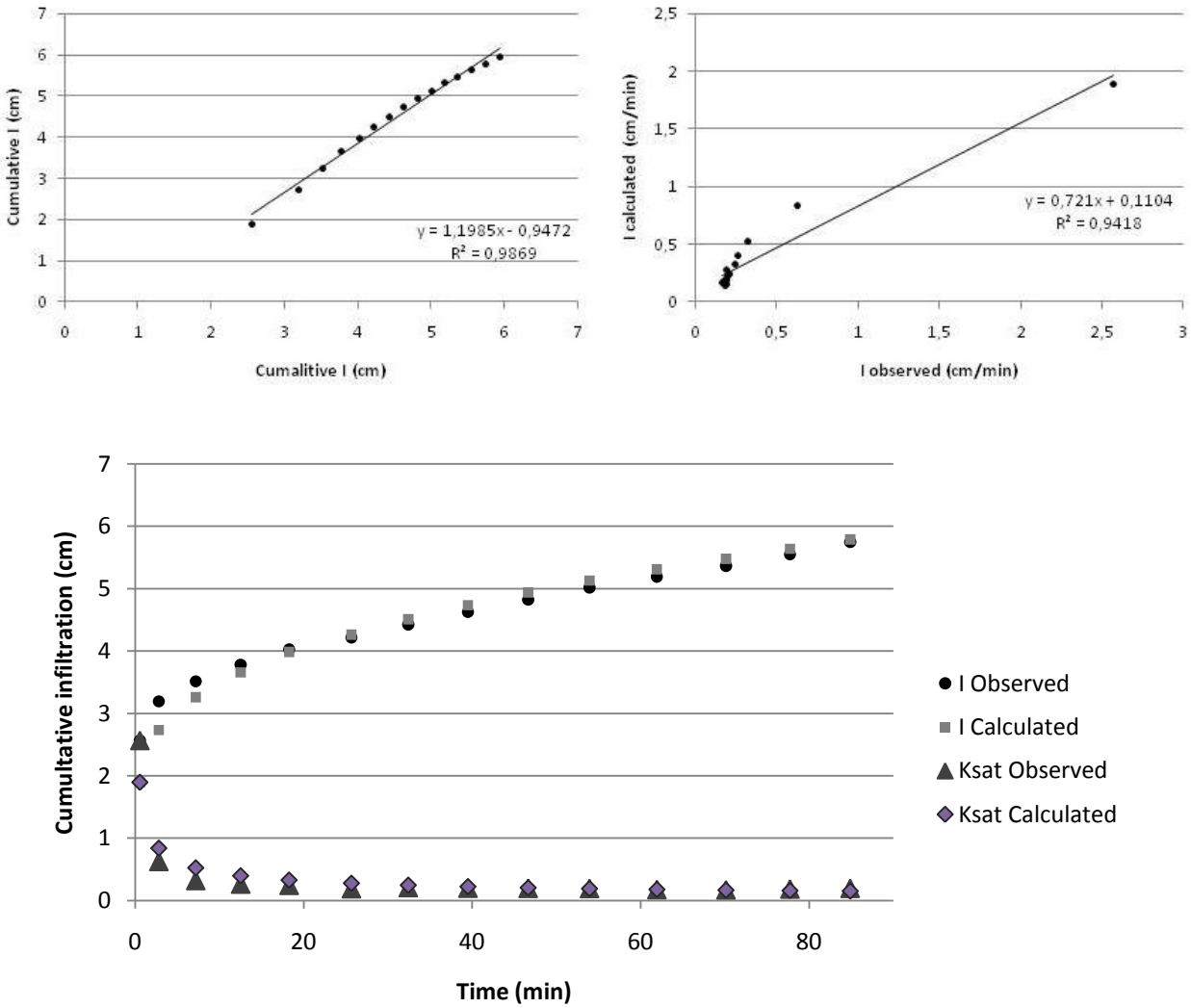

Graph XIII 6a-c *Examples of an applied 'sorptivity fit' a) the correlation between the observed and calculated cumulative infiltration b) the correlation between the observed and calculated infiltration rate c) the observed and calculated cumulative and k_{sat} plotted over time*

	Keff cm/min	Sorptivity	Error I (-)	Error Q (-)	Time to Pond (min)	Initial moisture (TDR) cm3/cm3	Final moisture (TDR) cm3/cm3	Relative to crusted
D 26-okt								
Soil D Vinebed	0,099285	165,817	0,002	0,0393	17,57	0,166	0,349	0,252
Soil D Trampled	0,080504	656,758	0,012	0,002	0	0,227	0,372	1
Soil D Center of row	0,072883	107,535	0,009	0,055	2,94	0,257	0,387	0,164
A 26-okt								
Soil A Trampled	0,082064	108,628	0,004	0,030	3,98	0,210	0,373	1
Soil A Under Vine	0,135722	428,933	0,018	0,047	0	0,183	0,381	3,945
Soil A Centre	0,201644	323,280	0,004	0,038	0	0,177	0,375	2,976
C 26-okt								
Soil C Vinebed	0,384957	559,221	0,013	0,040	0	0,188	0,359	1,305
Soil C Trampled	0,111876	428,360	0,027	0,021	0	0,190	0,372	1
Soil C Rill	0,099285	466,353	0,004	0,019	0	0,265	0,391	1,089
B 26-okt								
Soil B Center of row	0,156544	126,723	0,011	0,069	13,44	0,236	0,369	0,808
Soil B rill	0,345675	339,925	0,035	0,063	0	0,139	0,374	2,169
Soil B Trampled	0,107068	156,754	0,01	0,036	90,60	0,187	0,351	1
32_4 6-okt								
4a Vinebed	0,189889	295,373	0,001	0,046	0	0,069	0,379	1,420
4b Trampled	0,178296	208	0,025	0,040	0	0,100	0,325	1
4c Rill	0,086862	107,535	0,004	0,045	0,77	0,130	0,350	0,517
Sandy 27-okt								
Sandy 3 vinebed	0,227662	307	0,013	0,047	0	0,280	0,399	3,460
Sandy 2 rill	0,18862	199,178	0,013	0,058	0	0,259	0,349	2,245
Sandy 1 trampled	0,067915	88,739	0,017	0,052	6,27	0,232	0,398	1

Appendix XIV. Heterogeneity vineyards

The following photos give an overview of the heterogeneity within the vineyards. Differences are observed in soil properties, (texture and crusting etc.) undergrowth and the management techniques. A complete overview of the observed vineyards is found on the accompanying DVD.

UTM x 529554,359 y 4811138,418

UTM x 529554,359 y 4811138,418

UTM x 527393,443 y 4814044,807

UTM x 527393,443 y 4814044,807

UTM x 527809,401 y 4820339,427

UTM x 527809,401 y 4820339,427

UTM x 533635,608 y 4814598,297

UTM x 533635,608 y 4814598,297

Appendix XV. Crusting and Macropores

The following pictures give an overview of upper soil layer dynamics (crusting, cracks and macro pores from insects and small mammals) which influence the hydrologic behavior of the catchment.

UTM x 527562,023 y 4818461,838

UTM x 525589,154 y4816124,620

UTM x 528459,732 y 4817930,580

UTM x 525589,154 y4816124,620

UTM x 528459,732 y 4817930,580

UTM x 525970,840 y4819722,291

UTM x 528459,732 y 4817930,580

UTM x 525589,154 y4816124,620

Appendix XVI. Precipitation Events

To gain some insight into discharges from the urban area, a small floating device was placed on surface runoff off streams during the precipitation event (35mm in 10h max intensity 12mm/h) of 18 September 2009 in the village of Neffiès. The time to pass a known distance was recorded and interpreted as discharge rates, at two locations.

1) A gutter which ends in a tributary of the Bayelle
2) A concrete floodplain which crosses the village and is one of the tributaries of the Bayelle

Figure XVI.1: *The two locations where discharge of surface runoff was measured location 1: UTM x 526595,158 y 4820040,601 and location 2: UTM x 527021,874 y 4819973,182*

Table XVI.1: *The observed dimensions at the two locations*

	V (m/s)	**A**	**Q (m3/s)**
Location 1	1,58	0,002	0,003
Location 2	0,95	0,014	0,014

The observed values seems small, however these small streams already discharge between 12 and 40m^3/s hour during a 'normal' 35mm event.

During the fieldwork campaign one extreme precipitation event (>100mm/day) occurred on 21 October 2009, during which infield observations gave insight into how the catchment is functioning during such extreme rain. The following pictures give a brief overview of the observed reactions.

Figure XVI.2a-c: *a) runoff from agricultural fields passing the road between Roujan and Vailhan (UTM x 524483,249 y 4821349,510) b) a flooded vineyard (UTM x 525030,671 y 4820712,005) c) runoff flowing from the flooded field into the stream with no water flowing out of the drain pipe*

The two pictures above (Figure XVI.2a & b) show the incapacity of agricultural fields to cope with these amounts of water. The precipitation fell in excess of soil infiltration capacity, causing high runoff fractions. Figure XVI.2c provides strong support to the statement that the majority of water is flowing as surface runoff and not as subsurface flow.

Figure XVI.3ab: *a) The river Peyne inundating the road at the St Majan measuring station (UTM x 524972,811 y 4818902,732) b) the floodplain at Pezenas during the 21st of October (UTM x 534502,123 y 4812056,491)*

Figure x shows the St Majan observation location. The original floodplain could not cope with such high volumes of water. Unfortunately there are no discharge measurements of the event due to malfunctioning of the gauges.
The concrete floodplain in Pézenas was filled with approximately 0,5m of water as a result of the >100mm precipitation event. Only small amounts of debris were observed in the floodplain.

Figure XVI.4ab: *a) the river Peyne flowing into the Herault river showing the large differences in sediment load (UTM x535469,467 y 4810889,579) b) erosion during the crues of the 21st of October 2009 (UTM x535469,467 y 4810889,579)*

At the outlet where the Peyne flows into the Hérault river, heavy erosion of the banks was observed. Figure XVI.4shows the difference in watercolor between the Hérault and Peyne due to the high sediment load as a result of the extreme precipitation event.

Appendix XVII. pF curves

During the fieldwork campaign soil samples were taken at 10 locations (see overview map) representing the most common texture classes of the Peyne catchment. For these soil samples bulk densities and pF curves were determined in the laboratory. The volumetric moisture content between was measured between pF values 0 up to 4,2. To determine the pF curves a sand box, kaolonite box and two pressure pans (3,4 and 4,2) were used. The following graphs show the measured bulk density and pF curves.

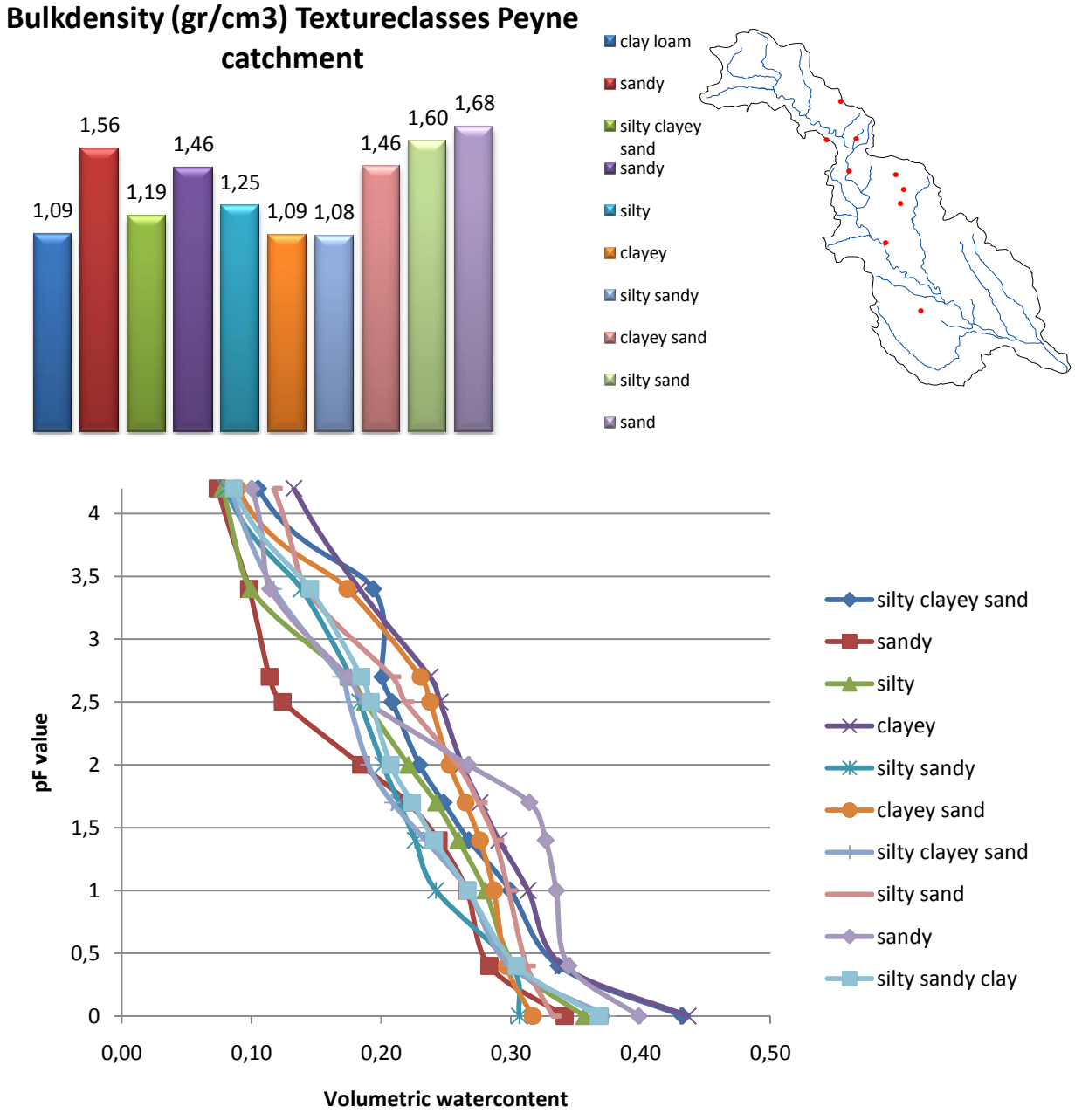

Graph XVII.1a/b a): *Bulk densities of the soil samples taken from the field at locations displayed (right) b) The waterretention curves of the taken soilsamples between saturation and wilting point*

Appendix XVIII. Data preparation ArcGIS and PCraster

Digitizing the stream and the texture map:

Spatial data related to the texture classes and the stream dimensions were only available in analog format. This data was digitized by using ArcGiS to make the data sufficient for model use. Topographic mapping provided by University Utrecht supported the creation of a shapefile illustrating the stream network. Stream ordering according to the Strahler methodology was then carried out by using the ArcGIS spatial analysis 'Stream Order' function. These results were used in combination with the stream ordering derived from Sandre.fr which is entirely based on length. The database related to stream dimensions was finished by using visual interpretation of satellite imagery.

Other important steps in the modeling progress were managed by using the following functions:

- Changing the projection of the meteorological data by using a Python script
- Checking for missing values by using PCraster
- Changing Map attributes using a Python script
- Creating initial maps using a PCraster lookup function
- Defining 18 Subcatchments and the related statistics using ArcGIS, PCraster

Calibration and validation data:

The JRC input meteorological data, available for the period 1990-2009, is course (5km grid) and smoothed due to interpolation between observation points. This data is not suitable for calibration because the due to daily timestep and extreme precipitation events are missing. To calibrate the model more detailed (hourly) data is required. Observations taken during the field campaign for the period of September and October 2009 will be used for the calibration of the model.

Precipitation data

During this period the precipitation was observed in detail with two tipping buckets located in the center of Neffiès (522674; 4820217) and at the other at the banks of Lac des Olivettes (526859; 4823804). This data will be combined with the data downloaded from the internet[1]. The internet provides data for two extra meteorological stations. The first is situated at the village of Vailhan and the other is located at the observation station at St Majan near Roujan. The data is available as point data (tss) and need to be converted to a spatial extend (.map). The two own tipping buckets registered every tip this means that there are several values per hour. These values needed to be summed up to one single value. The summing of these values was done in Excel. The data of the type: *09/18/09 03:36:01,5* was split up in unique columns (day, time). The precipitation per hour was then calculated by using the following *sumifs* function:

sumifs(precipitationrange;date;day;time;hour)

To convert the data to a spatial extend, the catchment was divided into four regions which are then related to one of the four observation points (figure 1). This divide is formed through the following pcrcalc function within a short script:

pcrcalc id.map=nominal(spreadzone(stations.map,0,dem.map))

The applied spread function incorporates the DEM when assigning the area to one of the four observation points. This script resulted in 1464 individual maps (61 days).

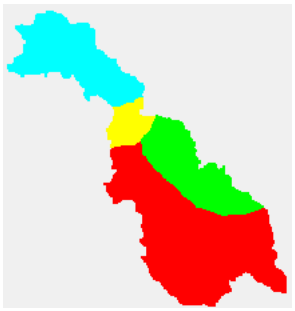

Figure XVIII.1: *Result of the spread function: the four precipitation regions*

Ta, E, Et & Es

Our database does not contain Ta, E, Et and Es data for the calibration period. For this period average values need to be used. An average value will be taken over the period 1990 to 2000. A model run was performed to generate a set of time series at the output locations (the model does not influence these values only uses them as such the can be used to calculate an average). Again these time series need to be converted to a spatial extend. This was done in a more or less similar process as applied to the precipitation data. However in this case an *averageifs* function was used:

=AVERAGEIFS(Tavg;Date1;Month;Date2;Day)

This function results in a value per day. The next step was to assign these values to the hours. To do so a *lookup* function was used:

=LOOKUP(uniqueday;values;dayrange)

The tss which was the result of this process was putted in the same script as the precipitation data with a different id.map (figure 2) and converted to a spatial extend.

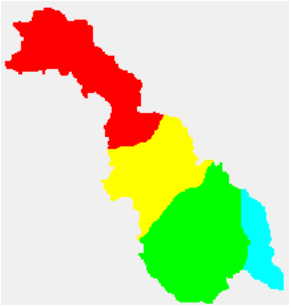

Figure XVIII.2: *Result of the spread function: the four meteorological regions*

Discharge

The discharge data was downloaded from the internet[2] and contains discharges recorded every 15min. However there are quite some missing values in the dataset. To sum the values to hourly data again an *averageifs* function was used.

=AVERAGEIFS(Discharge;Date;Day;Time;hour)

This resulted in an hourly tss. This tss forms an important input for the calibration software.

Appendix XIX. Validation Calibration

Calibration

-Nimbus

To calibrate the LISFLOOD model the NIMBUS calibration software was used. NIMBUS is specifically developed for LISFLOOD and provided by the JRC. Included are several automatic calibration algorithms.

- Shuffled Complex Evolution algorithm

To calibrate the model the Shuffled Complex Evolution Algorithm (SCEUA) was used. Within NIMBUS it is not yet possible to run the alternative algorithms under Windows, (a UNIX platform is required). The shuffled Complex Evolution algorithm is an improved version of the Downhill Simplix algorithm developed by the University of Arizona.

-Nash Sutcliffe and Modified Nash Sutcliffe

Nimbus offers the possibility to use several different objective functions (for instance Nash Sutcliffe, RMSE and Pearson). For this study it was decided after several setup runs to use the Nash Sutcliffe and rRMSE as the objective functions. The Nash Sutcliffe value is calculated by (van Deursen, 2002):

$$NS = (F0^2 - F^2)/F0^2$$

Where:

$F0^2 = \sum (Q \text{ measured at step } t_x - Q \text{ calculated at step } t_x)^2$

$F^2 = \sum (Q \text{ measured at step } t_x - Q \text{ observed mean})^2$

The values should range between -1 and 1, where 1 is a perfect fit between observed and calculated data. Negative values imply that the mean discharge act as a better predictor than the model outcome. NIMBUS also offers the possibility to use the modified Nash Sutcliff. The modified Nash Sutcliffe distinguishes itself from the normal Nash Sutcliffe by using a moving average.

-Choosing the calibration parameters

Nimbus offers by default 8 calibration parameters, including:

- Preferential flow rate multiplier
- Upper and Lower zone time constants
- A empirical b value applied to the VIC/ARNO scheme
- The groundwater percolation rate,
- Power multiplier to correct for the channels Manning's N,
- Snowmelt coefficient

More than 25 calibration runs with varying parameter combinations, were performed (e.g. over 15.000 model runs) to determine the sensitivity of the model and the best calibration set.

- Daily versus Hourly calibration

It was chosen to calibrate the model on a daily and hourly basis due to the properties and behavior of flashfloods (more likely to be an hourly event than a daily). For the daily calibration a 72 days period (14 December 2009 to 23 February 2010) was chosen. The last 10 days of this period (14 to 23 February) were used for the hourly calibration.

Precipitation and discharge data from the Olivette and Roujan observation points was used for this calibration run. The meteorological data (tavg, Es, Ew and Et) was complemented by using an average values based on a 10 year period (1990 to 2000).

-Calibration results

The daily calibration results were discontenting (Nash Sutcliffe values around -0.1 and -3). The main explanation for these low values is found in the peak discharge occurring around timestep 32/33 (graph 1). This peak is simulated by all the calibration runs (values varying between 1,4 and 2,8 m^3/s) but does not show up in the observations (only a slightly discharge rise to 0,02m^3/s). This might seem contradicting because a precipitation event on day 53 with a similar amount of precipitation is causing a major discharge peak on the same day (1,9m^3/s).

The possible cause of this discrepancy is expected to be found in the behavior of the reservoir (appendix 11) and in the properties of the precipitation event. Both days show same order precipitation amounts however the precipitation event of day 32 is spread over the complete day whereas the precipitation event of day 53 occurs within several hours resulting in higher precipitation intensities. The higher precipitation intensities result consequently in higher runoff values and an increased observed discharge. The response of the model supports the idea that an hourly calibration is preferable.

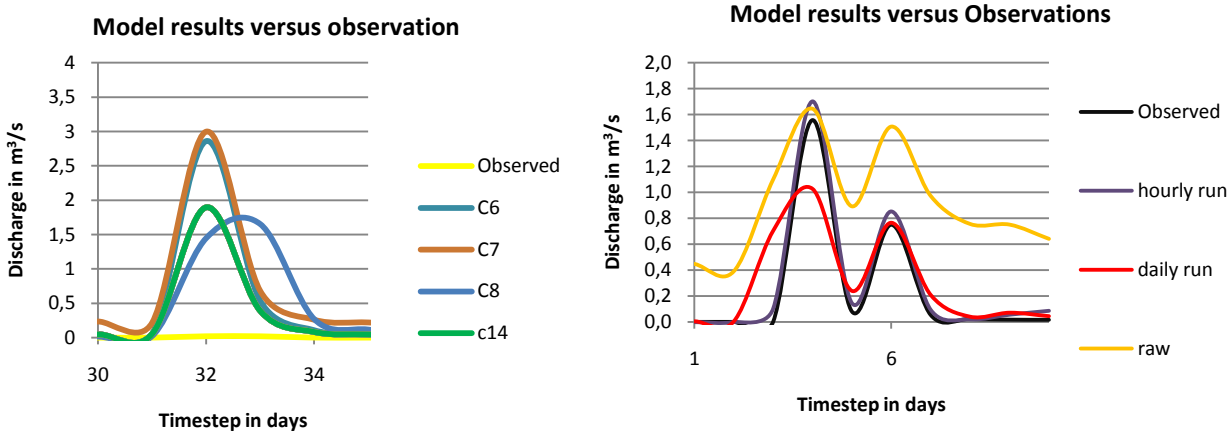

Graph XIX 1 and 2: *graph 1 shows the simulated peaks around timestep 33 which not appear in the observed data. Graph 2 shows the comparison between the hourly and daily calibration results related to the observed data the raw line represents the results of the un calibrated model.*

The hourly calibration was done as stated before on a ten day period (14 to 23 February). The calibration results cover a wide range. However the best results show a far better fit than the daily runs (with a Nash Sutcliffe of 0,86 as best result which is classified as a good fit). To compare the different results (best daily and hourly) the hourly values were averaged to daily values. Graph 2 shows the observed, raw LISFLOOD and calibrated values. It appears that the calibration improves the daily and hourly runs especially related to the base flow. However the difference between the hourly and daily result is clear.
According to the hourly calibration outcome calibrating on CCM, bXinj and the PWPF result in the best fit. For the daily calibration calibrating on bXinj, PWPF and GWPV resulted in the best fit. The calibrated parameters are displayed in table XIX.1:

GWPV (mm/day)	bXInj (-)	PWPF (-)	CCM (-)
0,857	0,184	0,503	x
X	0,316	0,551	4,617

Table XIX.1: *the optimized calibration parameters for the daily and hourly calibration*

Validation

The period from 1 to 8 February was chosen for the validation process. This period contains one major precipitation event. The first validation run is not resulting in the expected Objective Functions values. The best result stranded at a Nash Sutcliffe value between 0,5 and 0,6. To further research this unexpected result a cross calibration was done during which the validation period was used as calibration parameter. In contrast with the validation run the calibration run resulted in a satisfying value of 0,83. After studying the logfiles it appeared that the bXinj and PWPF values were quite similar between the two calibration runs. However the CCM showed a large difference (4,316 vs 10,94). To determine the most suitable CCM value it was decided to further calibrate the model manually. PDF curves were drawn to narrow the range down (graph 3)

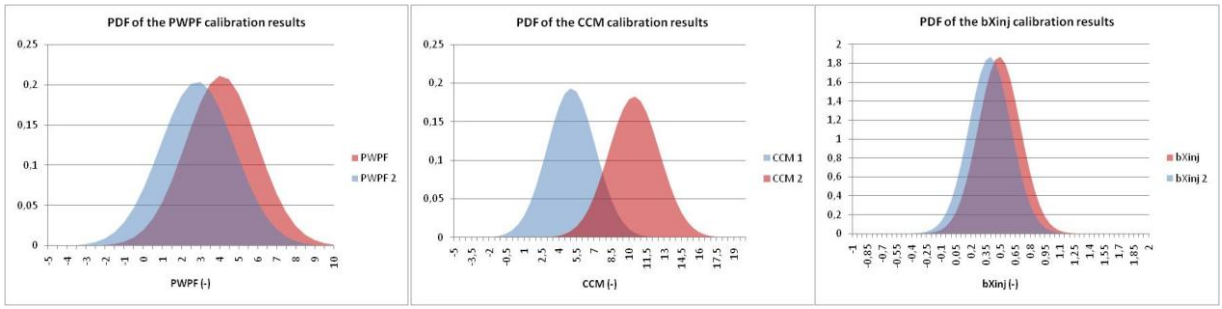

Graph XIX.3: *the three graphs above showing the pdf's of the three calibration parameters. The range of the CCM differs strongly between the two calibration runs*.

As a result of this figure values around 7 to 7,5 were chosen to run the model. These parameters resulted in an objective function lower than the optimal run (0,72 vs 0,86). However the validation Nash Sutcliffe value increased from 0,5 to 0,74 which was a large improvement. Based on these results it was decided to use these parameters rather than the parameters of the optimal calibration run.

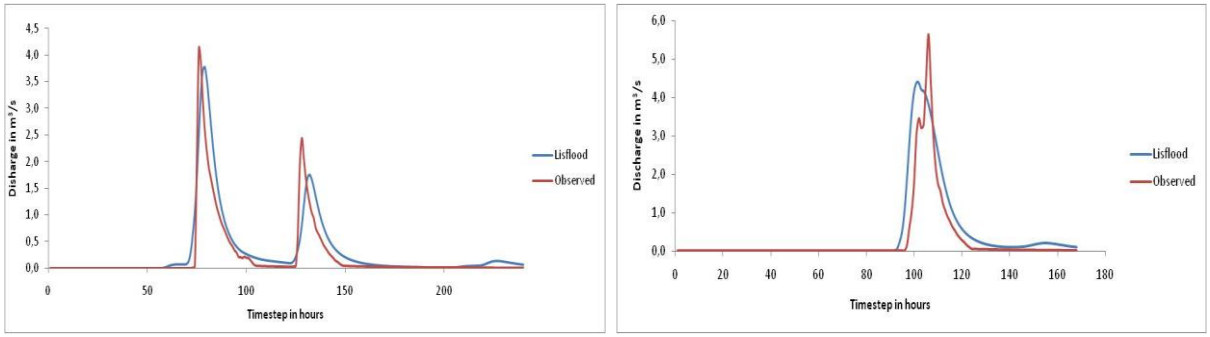

Graph XIX.4: *the results of the calibration and validation run result in reasonable NS values respectively 0,72 and 0,74*

It is known that the catchment properties change over the year due to natural and anthropogenic influences (e.g. crusting, tilling, crop growth, precipitation properties and the influence of the reservoir). It is thus highly unlikely that the parameters for the February set will perform well in for example September. The different response of the catchment can be seen in the following table (RDBMC 2010 & Vigicrues 2010).

Event	Date	Mm	Discharge
2	18-sept	30	0,04
3	8-okt	40	1,4
4	21-okt	100	nodata
5	22-okt	18	1,5
6	14-jan	30	0,2
7	5-feb	23,5	5,7
8	9-feb	21	1,5
9	17-feb	30	4,2
0	19-feb	15	2,25

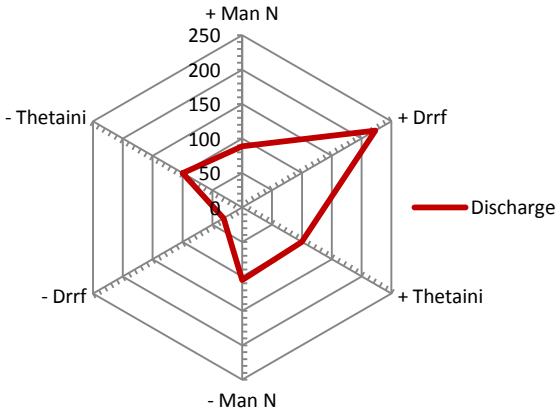

Table XIX.2: *shows the precipitation events and the resulting discharges.*

Graph XIX.5: *shows the sensitivity of the LISFLOOD model to (initial) parameters which are none to change over the seasons*

To compensate for these differences a monthly sub calibration is needed. However this is difficult if not impossible due to an inconsistent dataset. The calibrated parameters should be kept the same and the sub calibration is aiming at changing the season sensitive parameters. The model was tested on sensitivity to these parameters (graph 5) after which the most sensitive parameters were chosen to perform the monthly calibration (direct runoff fraction, Manning's N and theta initial). However as can be seen in chapter 3 it is likely that flashflood events will happen in the winter period, the period for which the model is calibrated successfully. It is therefore decided that the monthly calibration for the summer period is beyond the scope of this thesis.

Calibration results:

The following tables give in-depth information (nr of calibration steps, objective function parameter values etc.) on the different calibration results. The first two tables show the results for the daily calibration. The third and fourth table contains data related to the hourly calibration runs.

TableXIX.3 a & b: *Results of daily calibration*

	nr	Period	Nr of Para	Steps	RMSE	rRMSE	NS
1	62	14dec-13feb	4	487	0,28	90,05	-0,09
2	62	14dec-13feb	4	516	0,28	94,38	-0,08
3	62	14dec-13feb	2	457	0,35	176,65	-0,67
4	62	14dec-13feb	2	502	0,64	298,14	-4,54
5	62	14dec-13feb	2	531	0,35	176,65	-0,67
6	72	14dec-23feb	3	709	0,59	268,35	-2,36
7	72	14dec-23feb	2	532	0,67	336,97	-3,24
8	72	14dec-23feb	6	1002	0,41	124,44	-0,59
9	72	14dec-23feb	2	474	0,34	184,74	-0,10
10	72	14dec-23feb	2	497	0,34	184,74	-0,10
11	72	14dec-23feb	2	503	0,34	184,74	-0,10
12	72	14dec-23feb	2	470	0,34	184,74	-0,10
13	72	14dec-23feb	3	492	0,34	184,74	-0,10
14	72	14dec-23feb	3	505	0,34	184,74	-0,10
15	72	14dec-23feb	3	472	0,34	184,74	-0,10
16	72	14dec-23feb	3	488	0,34	184,74	-0,10
17	72	14dec-23feb	3	482	0,33	0,64	-0,06
18	72	14dec-23feb	3	466	0,33	0,64	-0,06
19	72	14dec-23feb	3	766	0,54	291,33	-1,75
20	72	14dec-23feb	3	833	0,54	291,28	-1,75

	Modfied NS	GWPV	bXinj	PWPF	CCM	UPZC	LZC
1	0,264	1,350	0,336	0,607	14,950	x	x
2	0,270	1,140	0,140	0,570	13,550	x	x
3	-0,124	x	0,180	0,500	x	x	x
4	-2,710	x	0,012	2,570	x	x	x
5	-0,124	x	0,319	0,505	x	x	x
6	0,301	0,014	0,026	7,936	x	x	x
7	0,122	x	0,015	6,770	x	x	x
8	0,669	0,012	0,025	7,294	14,921	49,796	106,615
9	0,771	x	0,086	0,502	x	x	x
10	0,771	x	0,150	0,504	x	x	x
11	0,771	x	0,103	0,500	x	x	x
12	0,771	x	0,141	0,501	x	x	x
13	0,771	0,857	0,184	0,503	x	x	x
14	0,771	0,287	0,326	0,506	x	x	x
15	0,771	0,312	0,141	0,500	x	x	x
16	0,771	1,179	0,017	0,501	x	x	x
17	0,779	x	X	X	x	1,008	2345,122
18	0,779	x	X	X	x	1,006	1554,915
19	0,429	x	X	X	x	49,811	50,036
20	0,430	x	X	X	x	49,811	50,036

Tables XIX.4 a & b: Results of hourly calibration.

Hourly	NR	UPZTC	LTZC	GWPV	bxinj	PWPF
1	1002	2	257	0,670696	0,54	0,52
2	478	11	106	0,010057	0,71	6,03
3	455	X	x	1	1	0,50073
4	509	X	x	1	x	1
5	411	X	x	0	x	8
6	473	40	50	x	x	x
7	485	50	1.875	x	x	X
8	496	34	2.490	x	x	X
9	470	X	x	1	x	1
10	524	X	x	0,316	x	0,551
11	670	26,400	52,824	0,758	x	7,188
12	480	X	x	0,186487	x	0,552332

Hourly	CCM	NASHSUTCLIFFE	MODIFIED NS	RMSE	RRMSE
1	X	0,076672	-2	0,589143	122
2	X	-0,08982	-2	0,640059	98
3	X	-0,08	-2,40	1	95
4	X	-0,08429	-2,40	0,64	95
5	X	-0,10577	-2,47	0,64	0,867783
6	X	-0,31277	-3,12	0,70	166
7	6	-0,08	-2,25	1	339
8	X	0,054814	-1,96	0,60	92
9	X	0	-2,40	0,64	95
10	4,617	0,838	0,492	0,247	40,417
11	5,056	0,642	-0,038	0,367	178,869
12	11	0,839415	0,147808	0,361025	22

From the above tables it can be concluded that the RMSE and rRMSE show high values which seem to point out large model errors. The RMSE and hence the rRMSE are based on the mass balance function within NIMBUS. This mass balance (Figure XIX.1) is configured on daily timesteps. This daily timestep mainly explains the large values of the RMSE and rRMSE.

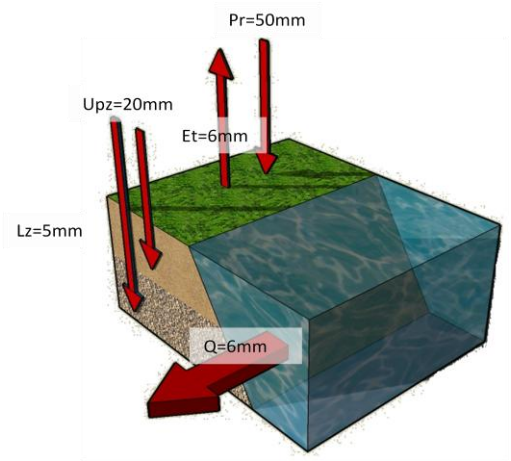

Figure XIX.1: *Mass Balance of a calibration session*

Appendix XX. Scenarios

The model was used to gain insight in the response of the catchment. To confirm or reject the formulated hypotheses an extensive set of scenarios was run with LISFLOOD. The following scenarios where ran during this research:

- Changing all the land cover classes in a uniform class
  Aim of this scenario was to determine the most hazardous land cover class.

- Changing all the soil texture classes in a single uniform class
  Aim of this scenario was to determine the most hazardous soil texture class.

- Changing the direct runoff fraction (to increasing simulate crusting) of the vineyards
  Aim of this scenario was to research the effect of crusting on total discharge in Pézenas and the shape of the hydrograph.

- Running the model under extreme precipitation conditions (February 1996)
  Aim of this scenario was to study the catchment response (peak flow propagation, time to peak) during an extreme event.

- Running the model under extreme conditions with observation points at the outlet of each tributary
  Aim of this scenario was to determine the contribution of each single tributary to the hydrograph in Pézenas and to determine the most important source areas.

Scenario 1: Land Cover Change

It was chosen to use spider diagrams to show the modeled influence of land cover changes. The following shows merely a *fictional example* of a spider diagram. In this example, each diagram displays 5 land cover change scenarios (during these model runs, the entire catchment, except the urban areas and lake, are transformed into a single land cover type i.e. forest, vineyards etc.). The diagram shows the influence of these changes (in percentage compared to the original run) on the total discharge measured at Pézenas. A calculated discharge of 24m^3/s versus the observed of 4,2m^3/s will result in a spider value of ((24/4,2)*100) 571,43 m^3/s. Each diagram has the same axis values ranging between 0 and 700% as displayed in the following example:

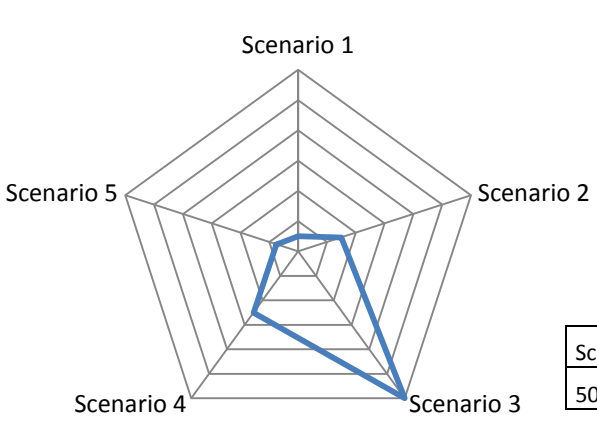

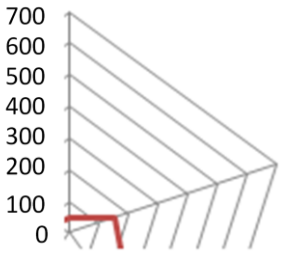

Scenario 1	Scenario 2	Scenario 3	Scenario 4	Scenario 5
50,00	150,00	600,00	250,00	75,00

Graph XX.1 *An example spider diagram, indicating changes in discharge due to changes in land cover.*

Graph XX.2 a, b, & c shows changes in discharges relative to complete coverage of the catchment by singular land covers. Those with a high direct runoff fraction within the model produced the highest surface runoff discharges. Urban area (direct runoff fraction 0.8) and crusted vineyards (direct runoff fraction 0.4) produce the highest discharges within our model. Each level in the spider diagram is 100% of the discharge produced in the original scenario. LAI, Forest fraction, Direct runoff fraction are the parameters changed for each of the following scenarios.

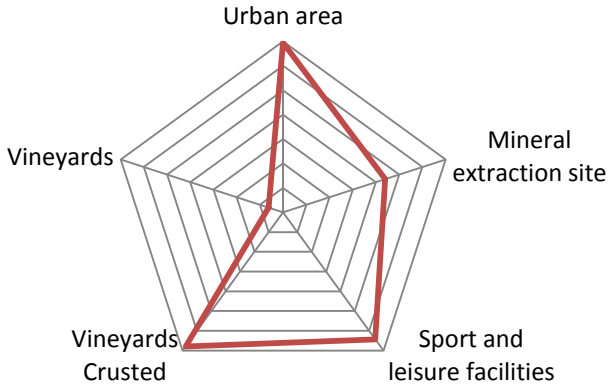

Graph XX.2 a): *Land covers generating relatively high discharges.*

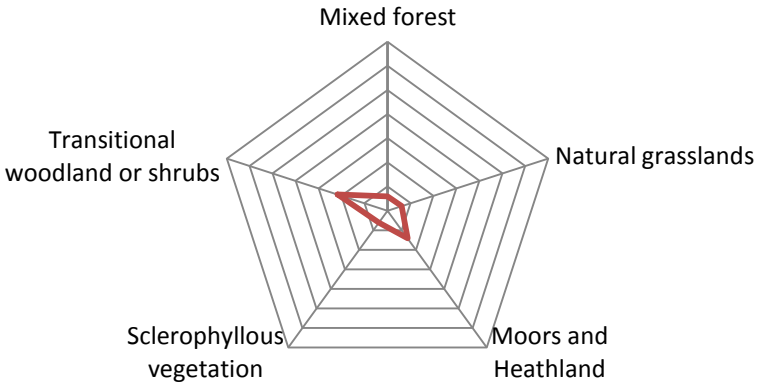

Graph XX.2. b): *Land covers generating relatively medium discharges.*

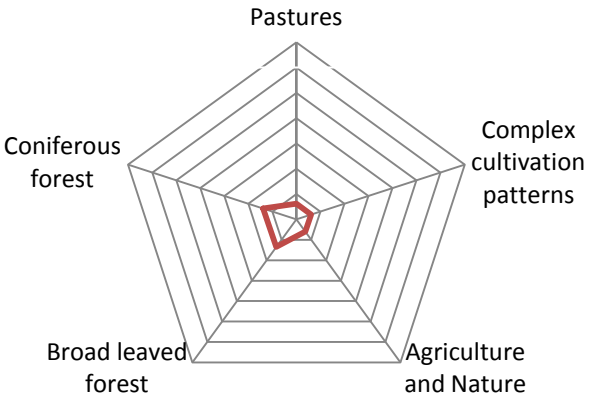

Graph XX.2. c): *Land covers generating relatively small discharges.*

Scenario 2: Soil Type Change

To research the influence of the soil types the whole catchment was transformed into one uniform soil type. The first graph seems to imply that the differences are reasonably significant however the second graph which shows change in fractions relative to discharge from soil 1 forces a different conclusion as the change relative to the scenario of soil type 1 is 0.01% or less for all.

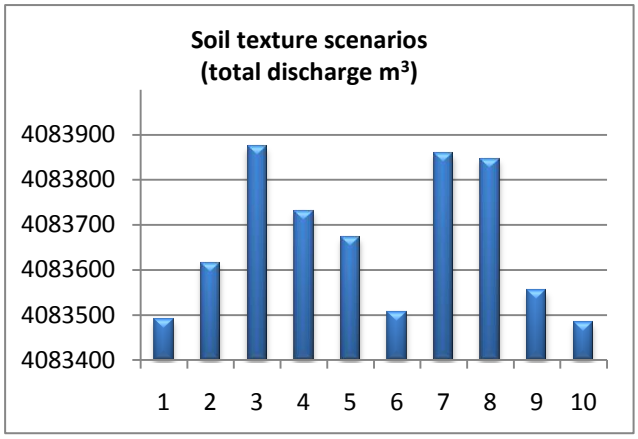

Graph XX.3: *Shows the total discharges of scenarios with a complete catchment coverage of one singular soil texture class.*

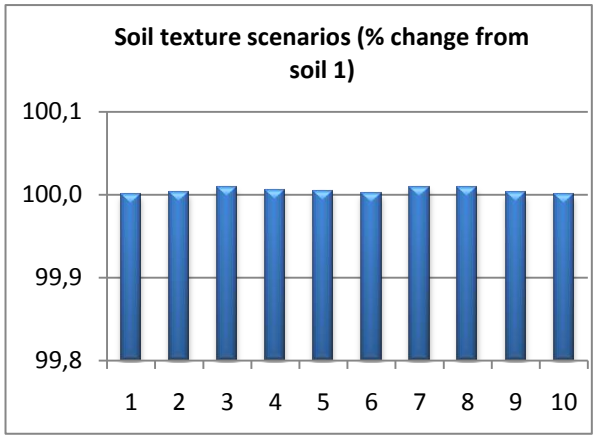

Graph XX.4: *Shows the percentage change of each scenario relative to the original scenario (1).*

Scenario 3: The 1996 Extreme Event

The extreme 1996 event was used to determine the influence of each single tributary. The following graph shows the hydrographs for each tributary relative to the Peyne.

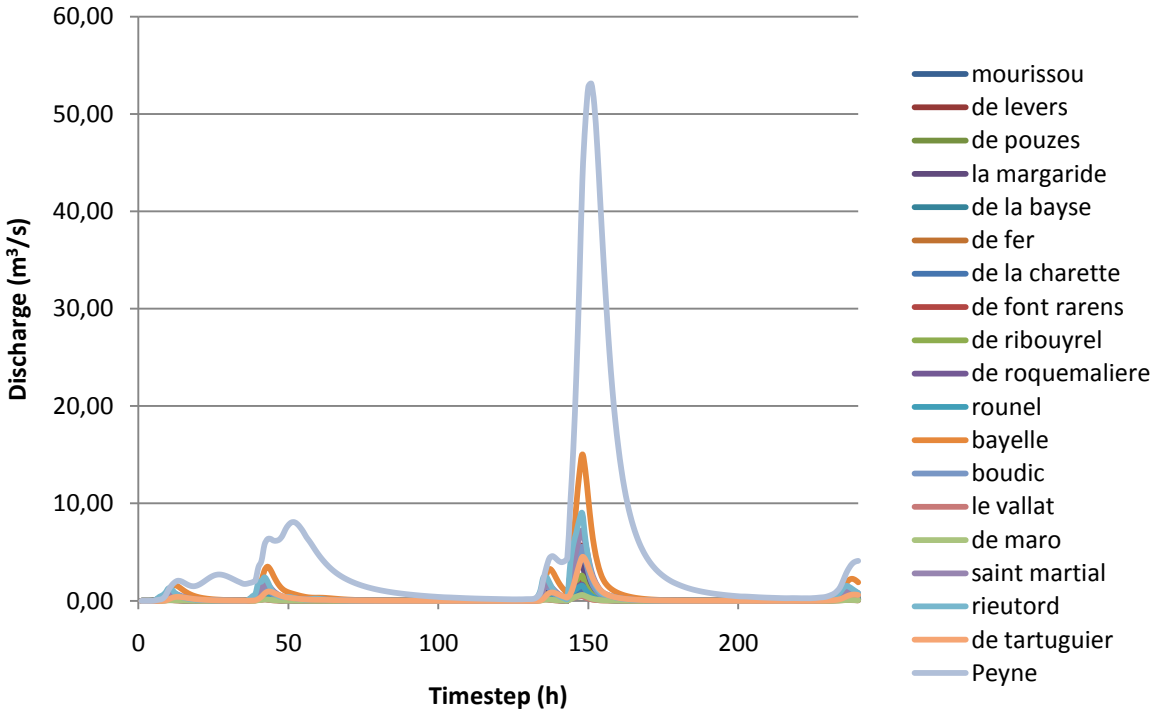

Graph XX.5: *The peyne and its tributaries.*

The three most contributing tributaries are:

Graph XX.6:
The Bayelle

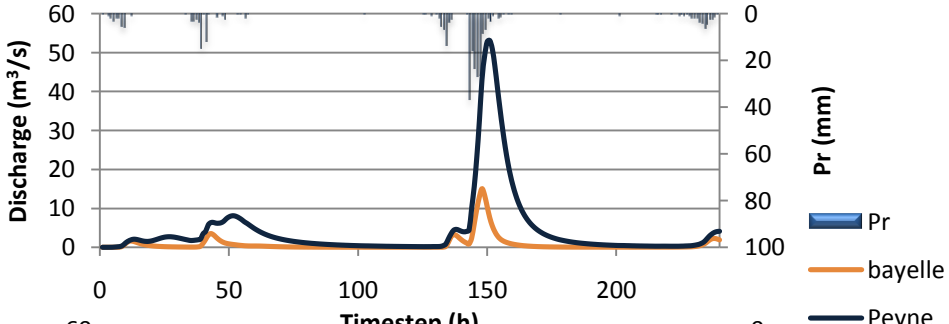

Graph XX.7:
The Rieutord

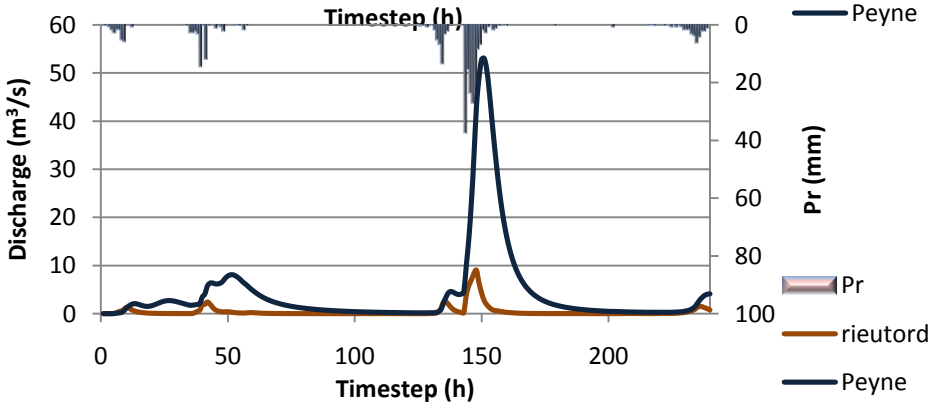

Graph XX.8:
The Saint Martial

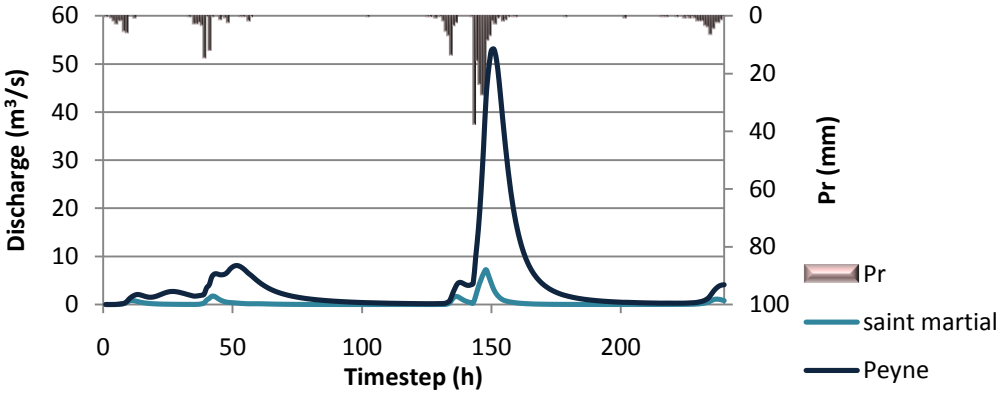

The following tables order tributaries based on modeled total discharge and the order based on the cubic meters of discharge relative to the stream length.

Table XX.1: *tributaries based on modeled total discharge.*

Order	Name	Length in km	m3/100m	Order	Name	Length (km)	m3/100m
1	Peyne	32,9	11167,09	11	de ribouyrel	3	3494,44
2	Bayelle	8,4	7775,87	12	saint martial	10,5	2947,94
3	Rieutord	6,7	5569,14	13	mourissou	3,7	2833,59
4	Boudic	4,2	5522,82	14	de tartuguier	7,6	2696,88
5	de roquemaliere	1,2	5509,59	15	Rounel	2,7	2381,17
6	de font rarens	1,8	5312,65	16	de fer	1,3	2066,32
7	de levers	4,7	4919,75	17	de la charette	2,1	2002,90
8	de pouzes	4,4	4089,89	18	de maro	1,5	1714,63
9	la margaride	4,2	3633,86	19	le vallat	2,1	910,22
10	de la bayse	1,8	3624,14				

Table XX.2: *meters of discharge relative to the stream length.*

Order	Name	Length (km)	Total m3	Order	Name	Length (km)	Total m3
1	Peyne	32,9	3673972,56	11	de ribouyrel	3	104833,32
2	Bayelle	8,4	653173,08	12	de font rarens	1,8	95627,75
3	Rieutord	6,7	373132,19	13	de roquemaliere	1,2	66115,13
4	saint martial	10,5	309534,10	14	de la bayse	1,8	65234,52
5	Boudic	4,2	231958,60	15	rounel	2,7	64291,52
6	de levers	4,7	231228,16	16	de la charette	2,1	42060,82
7	de tartuguier	7,6	204962,87	17	de fer	1,3	26862,12
8	de pouzes	4,4	179955,25	18	de maro	1,5	25719,52
9	la margaride	4,2	152622,14	19	le vallat	2,1	19114,63
10	Mourissou	3,7	104843,01				

Appendix XXI. Curve Number vs. LISFLOOD

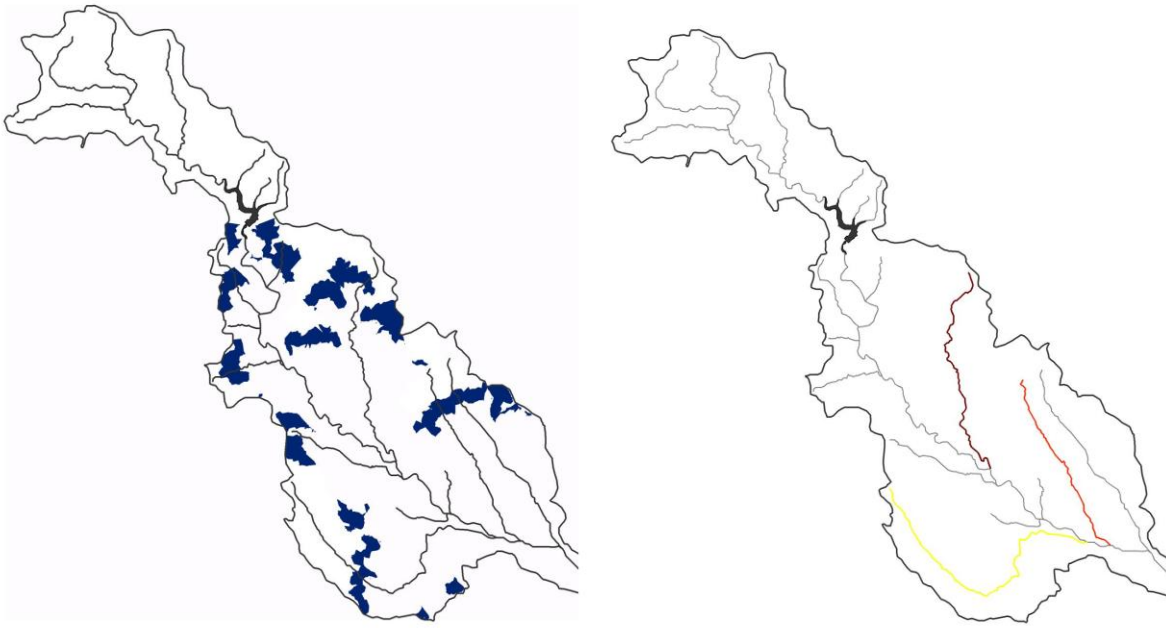

Figures XXI.1a and XXI.1b: *Peak discharges from curve number method (left) compared to peak discharges from LISFLOOD (right)*

According to the Curve Number method the peak flow in Pézenas will take place approximately 4,5 hours after the precipitation event (Backwell and Bijkerk, 2009). The above maps show the most important source areas based on the applied curve number method and the most important tributaries based on the LISFLOOD model. The blue shaded regions release their water within 4,5 hours to the outlet at Pézenas according to the curve number which is comparable to LISFLOOD's predicted time to peak of 5 hours. Furthermore, the areas pointed out by LISFLOOD show high similarities with the regions predicted by the Curve Number method. However the predicted discharges are a certain magnitude out of order. The curve number method predicts discharge values which are not consistent with the LISFLOOD Model predict values which are in accordance with observed data (Backwell and Bijkerk 2009).

One can conclude from this that the Curve Number method is suitable for a quick scan to determine the source areas and the time to peak. Meanwhile the LISFLOOD model is more suitable to research in-depth analysis of land cover changes, absolute discharge values and hence threshold breaching.

Appendix XXII. A non technical glossary of the annual scenario

Temporal changes in a basin's response to precipitation are related strongly to seasonal shifts and length of rain season. The dry summer reduces soil moisture to minimum values. Upon arrival of the first rain event, soil moisture increases across the catchment and in the case of crust prone areas (typically vineyards) the first sign of crusting appears.

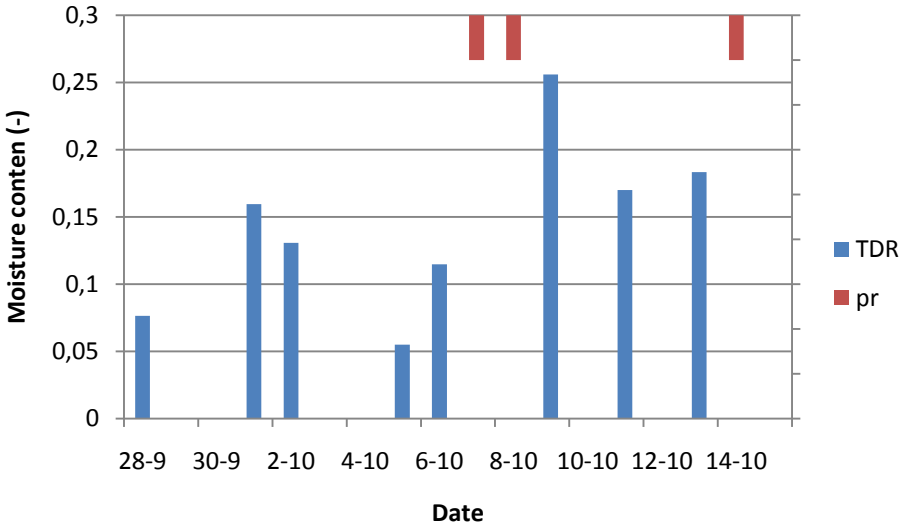

Graph XXII.1: *The behavior of the soil moisture as function of time before and after precipitation events*

All non crusted soils will increase the degree of saturation and decrease in hydraulic conductivity (due to lower top layer sorptivity values) as precipitation becomes more frequent throughout the rain season. The exceptions are crusted vineyard soils which for the commencing phase of the rain season remain considerably dry, due to the crusted layer acting as a barrier to moisture infiltration. However over time the crusts degrade under the wetter conditions and consequently they become saturated toward the latter phase of the rain season. Simultaneously Lac des Olivettes is not at full capacity during summer and begins to fill due to subsurface flow and saturation excess overland flow of soils north of the lake. Some time into the rain season the lake reaches maximum storage capacity at the base flow output threshold. Until now no flashfloods have occurred however the precipitation has been at its annual highest. Toward the latter half of the rain season in winter, the precipitation becomes less intense however the risk of flooding is higher at Pézenas due to cessation of lake buffering (as it is at full capacity) and lack of available soil storage capacity.